

การปรับปรุงค่าการนำไฟฟ้าของฟิล์มพีดอท-พีเอสเอส และพีดอท-เอสพีไอ โดยการเติมสารลดแรงตึงผิวและการใช้พอลิอิมิดที่มีหมู่ซัลโฟเนตหลายหมู่เป็นเทมเพลตสำหรับการประยุกต์ใช้ทางอิเล็กทรอนิกส์

นางสาวกุลธิดา สุขชล

วิทยานิพนธ์นี้เป็นส่วนหนึ่งของการศึกษาตามหลักสูตรปริญญาวิทยาศาสตรดุษฎีบัณฑิต

สาขาวิชาวิศวกรรมเคมี ภาควิชาวิศวกรรมเคมี

คณะวิศวกรรมศาสตร์ จุฬาลงกรณ์มหาวิทยาลัย

ปีการศึกษา 2556

ลิขสิทธิ์ของจุฬาลงกรณ์มหาวิทยาลัย

บทคัดย่อและแฟ้มข้อมูลฉบับเต็มของวิทยานิพนธ์ตั้งแต่ปีการศึกษา 2554 ที่ให้บริการในคลังปัญญาจุฬาฯ (CUIR)

เป็นแฟ้มข้อมูลของนิสิตเจ้าของวิทยานิพนธ์ที่ส่งผ่านทางบัณฑิตวิทยาลัย

The abstract and full text of theses from the academic year 2011 in Chulalongkorn University Intellectual Repository (CUIR) are the thesis authors' files submitted through the Graduate School.

IMPROVING CONDUCTIVITY OF PEDOT-PSS AND PEDOT-SPI BY ADDITION OF
SURFACTANT AND USING THE NOVEL SYNTHESIZED MULTI-SULFONATED
DIAMINE AS A NEW TEMPLATE FOR ELECTRONIC APPLICATION

Miss Kulthida Sukchol

A Dissertation Submitted in Partial Fulfillment of the Requirements
for the Degree of Doctor of Engineering Program in Chemical Engineering

Department of Chemical Engineering

Faculty of Chemical Engineering

Chulalongkorn University

Academic Year 2013

Copyright of Chulalongkorn University

กุลธิดา สุขชล: การปรับปรุงค่าการนำไฟฟ้าของฟิล์มพีคอต-พีเอสเอส และพีคอต-เอสพีไอ โดยการเติมสารลดแรงตึงผิวและการใช้พอลิอิมิดที่มีหมู่ซัลโฟเนตหลายหมู่เป็นเทมเพลตสำหรับการประยุกต์ใช้ทางอิเล็กทรอนิกส์ (IMPROVING CONDUCTIVITY OF PEDOT-PSS AND PEDOT-SPI BY ADDITION OF SURFACTANT AND USING THE NOVEL SYNTHESIZED MULTI-SULFONATED DIAMINE AS A NEW TEMPLATE FOR ELECTRONIC APPLICATION)

อ. ที่ปรึกษาวิทยานิพนธ์หลัก: รศ.ดร.มล. ศุกกนก ทองใหญ่, 147 หน้า.

พอลิเมอร์นำไฟฟ้าที่มีพีคอตเป็นองค์ประกอบหลักได้รับความสนใจมากขึ้นในปัจจุบันในฐานะที่เป็นวัสดุชนิดใหม่ที่สามารถไปประยุกต์ใช้ได้หลายประเภท โดยเฉพาะอย่างยิ่งการใช้งานด้านอุปกรณ์อิเล็กทรอนิกส์ การเตรียมพอลิเมอร์นำไฟฟ้านาโนสามารถปรับปรุงคุณสมบัติการนำไฟฟ้าและคงความเสถียรทางความร้อน อย่างไรก็ตามจากอดีตถึงปัจจุบัน ยังไม่พบรายงานการศึกษาผลของการกวนผสมเชิงกลที่ความเร็วรอบต่าง ๆ รวมถึงการเติมสารลดแรงตึงผิวที่มีต่อคุณสมบัติต่าง ๆ ของพอลิเมอร์นำไฟฟ้าประเภทพีคอต ดังนั้นงานวิจัยนี้ศึกษาผลของการเตรียมพอลิเมอร์นำไฟฟ้าโดยใช้เครื่องกวนผสมเชิงกลที่ความเร็วรอบต่าง ๆ และการเติมสารลดแรงตึงผิวประจุบวกที่มีผลต่อคุณสมบัติการนำไฟฟ้า และความเสถียรทางความร้อน นอกจากนี้ยังศึกษาการสังเคราะห์และคุณสมบัติพอลิอิมิดเทมเพลตชนิดใหม่ที่มีหมู่ซัลโฟเนตหลายหมู่ในโมเลกุล โดยแบ่งการทดลองออกเป็น 3 ส่วน ดังนี้ ส่วนแรกเป็นการกล่าวถึงการศึกษาผลของระบบกวนผสมเชิงกลที่ความเร็วรอบต่าง ๆ ที่ใช้ร่วมกับใบกวนที่ออกแบบขึ้นและการเติมสารลดแรงตึงผิวประจุบวก พบว่าพีคอต -พีเอสเอสสามารถถูกปรับปรุงค่าการนำไฟฟ้าเมื่อเตรียมด้วยเครื่องผสมเชิงกลที่ความเร็วรอบ 4000 รอบต่อนาที โดยสามารถปรับปรุงค่าการนำไฟฟ้าให้สูงขึ้น 346 เท่า และมีค่าการนำไฟฟ้ามากที่สุดเมื่อมีการเติมสารลดแรงตึงผิว 1 เปอร์เซ็นต์โดยน้ำหนักนอกจากนี้ คุณสมบัติการนำไฟฟ้า ความเสถียรทางความร้อน และสัญญาณวิทยาสามารถปรับปรุงได้โดยการเติมสารลดแรงตึงผิวประจุบวกในระหว่างกระบวนการเตรียมพอลิเมอร์ในระบบของ พีคอต-เอสพีไอ และพีคอต-พีเอสเอส ซึ่งพอลิเมอร์นำไฟฟ้าที่สังเคราะห์ได้เป็นทรงกลมและมีขนาดอนุภาคระดับนาโน งานวิจัยในส่วนสุดท้าย ศึกษาการสังเคราะห์พีคอต /ซัลโฟเนตพอลิอิมิดที่มีหมู่ซัลโฟเนตหลายหมู่ซึ่งเป็นพอลิเมอร์นำไฟฟ้าชนิดใหม่พบว่าพอลิเมอร์นำไฟฟ้าที่มีซัลโฟเนตพอลิอิมิดที่มีหมู่ซัลโฟเนตหลายหมู่มีคุณสมบัติการนำไฟฟ้าและการเสถียรทางความร้อนที่ดีขึ้น

ภาควิชา...วิศวกรรมเคมี.....ลายมือชื่อนิสิต.....

สาขาวิชา...วิศวกรรมเคมี.....ลายมือชื่อที่ปรึกษาวิทยานิพนธ์หลัก.....

ปีการศึกษา 2556.....

5271802221: MAJOR CHEMICAL ENGINEERING

KEYWORDS: CONDUCTING POLYMERS/ SURFACTANT/ THERMAL STABILITY/ POLYIMIDE
TEMPLATE/ WATER-DISPERSIBLE

KULTHIDA SUKCHOL: IMPROVING CONDUCTIVITY OF PEDOT-PSS AND PEDOT-SPI BY
ADDITION OF SURFACTANT AND USING THE NOVEL SYNTHESIZED MULTI-
SULFONATED DIAMINE AS A NEW TEMPLATE FOR ELECTRONIC APPLICATION.

ADVISOR: ASSOC. PROF. ML. SUPAKANOK THONGYAI, Ph.D., 147 pp.

PEDOT-based conductive polymers are electrically conductive polymers that have attracted much attention recently as novel functional materials in many applications, especially in areas electronic devices. The preparation of nanosized particles of PEDOT-based conductive polymers could present advantages for the improvement of the electrical and thermal properties. However, up to date, no reports about the impacts of agitation effect at different stirring speeds including addition of surfactant on the template polymerization of PEDOT-based conducting polymer. Therefore, we had paid attention of study for agitated template polymerization with various amounts of surfactants under different stirring speeds. In addition, the novel template, multi-sulfonated polyimide had been studied in this research. The experiment consisted of 3 parts. The first part involved experimental observation on the mixing systems and ways to significantly enhance the conductivity of PEDOT-sulfonatedpoly(imide)s aqueous dispersion. By varying the mixing system (magnetic stirring at 1000 rpm, mechanical at 1000 rpm and mechanical at 4000 rpm), we observed significant conductivity and thermal stability enhancement of the obtained PEDOT-SPI films by using designed stir shaft with high-speed mechanical mixing systems allowing for smaller particle sizes of PEDOT:SPI about 43 nm averaging. The maximum conductivity of 2.04 was observed for using the 4000-rpm mechanical mixing system, which were higher than those of magnetic and 1000 rpm-mechanical mixing systems by factor of 346 and 3.1. The highest conductivity, 9.5 S/cm, was achieved at 1 wt% SDS, which increased by a factor of 5 from the PEDOT-SPI without addition of SDS. We had further improved the conductivity, thermal stability and morphology of PEDOT-based conductive polymers by addition of anionic surfactant during template polymerization in the second part.

Department Chemical Engineering Student's signature

Field of study Chemical Engineering Advisor's signature

Academic Year 2013

Acknowledgements

“The only thing that stands between you and your dream is the will to try and the belief that it is actually possible.”

– Joel Brown

My deepest gratitude goes to Associate Professor Dr. ML. SupakanokThongyai for his guidance, motivation and support. His creativity and ingenuity have motivated me to come up with and explore my own ideas, which helped me grow as an independent engineer. Getting his students involved in meetings and intellectual properties have better prepared us for life after graduate school. In my moments of doubts, I am truly grateful for the confidence and encouragement he has given me. I also would like to thank my associate advisor, Prof. Gregory Sotzing at the Institute of Materials Science and the Polymer program, University of Connecticut, USA, for always being supportive and for showing me how to handle things gracefully.

Sincere thanks are made to the Thailand Research Fund through the Royal Golden Jubilee Ph.D. Program (Grant No. PHD/0203/2552) and Chulalongkorn University for financial support during my study. This work was supported by Integrated Innovation Academic Center:IIACChulalongkorn University Centenary Academic Development Project (CU56-EN04) and partially supported by the Higher Education Research Promotion and National Research University Project of Thailand, Office of the Higher Education Commission (EN283A-56). I also would like to thank MEKTEC Manufacturing Corporation (Thailand) Ltd. for supporting the materials and the characterize equipment.

I thank my family for their love and support, for always cheering me on, especially my mother. I am truly blessed to be your daughter. Sincerest thanks to my uncles: Mongkol Sukchol and NiponThongnoke who generous supported and encouraged me through the year spent on this study.

Lastly, my sincerest and deepest gratitude to my patience, my effort, my strength and the great I am, all the glory goes back to you.

CONTENTS

	Page
ABSTRACT (THAI)	iv
ABSTRACT (ENGLISH)	v
ACKNOWLEDGEMENTS	vi
CONTENTS	vii
LIST OF TABLES	ix
LIST OF FIGURES	x
CHAPTER	
I INTRODUCTION	1
1.1 Objectives of the research.....	5
1.2 Scope of the research.....	6
II THEORY	
2.1 Conducting polymer	8
2.2 Poly (3,4-ethylenedioxythiophene)	12
2.3 Poly (3,4-ethylenedioxythiophene):poly(styrenesulfonate acid)	17
2.4 Template polymerization.....	21
2.5 Polyimides	24
2.6 SulfonatedPolyimides.....	27
2.7 Basic concept of shear treatment by using high speed mechanical mixer	30
2.8 Surfactants	32
III LITERATURE REVIEWS	40
3.1 Poly(3,4-ethylene dioxythiophene) with poly(styrene sulfate) template	40

	Page
3.2 Sulfonated poly (imide).....	44
3.3 Conductivity enhancement of conducting polymers	52
IV EXPERIMENT	65
4.1 Materials and Chemicals	65
4.2 Equipments.....	69
4.3Experiment Procedures.....	74
4.4 Characterization instruments.....	83
V RESULTS AND DISCUSSION	89
5.1 Experimental observation on the mixing systems and ways to significantly enhance the conductivity of PEDOT:SPI aqueousdispersion.....	89
5.2 Effects of the addition of anionic surfactant during template polymerization of conducting polymers containing PEDOT with SPI or PSS templates for nano-thin film applications	105
5.3 Synthesis and characterization of PEDOT/multi-sulfonated poly(imide) viatemplate polymerization	118
VI CONCLUSIONS AND RECOMMENDATIONS	134
6.1 Conclusions	134
6.2 Recommendations	136
REFERENCES	138
VITA.....	147

LIST OF TABLES

	Page
Table 2.1 Selected physical properties of EDOT.....	13
Table 2.2 Commercial PEDOT:PSS dispersion in water and their properties	20
Table 2.3 Examples of interaction between monomer and template	22
Table 2.4 Sulfonateddiamines.....	29
Table 3.1 Conductivities of PEDOT-PSS(in house) and PEDOT-SPAA. Upon annealing, PEDOT-SPAA imidizes to PEDOT-SPI	45
Table 3.2 Conductivities of secondary-doped PEDOT-SPAA at various processingtemperatures. Upon annealing, PEDOT-SPA imidizesto PEDOT-SPI.....	45
Table 3.3 Polymerization yield, powder size distribution, and conductivity ofPPysynthesis with or without each surfactant	54
Table 3.4 Conductivity of original PPy-sulfate and PPy-DBSNa sample	62
Table 5.1 Conductivities of PEDOT-SPI systems from each mechanical and magnetic stirring process	96
Table 5.2 Conductivities of PEDOT-SPI(SDS) systems from mechanical stirringprocess	97
Table 5.3 Conductivities of PEDOT-SPI andPEDOT-PSS (in house) with various different method of addition of anionic surfactant.....	117
Table 5.4 Elemental analysis of multi-sulfonateddiamine.....	123
Table 5.5 Elemental analysis of multi-sulfonated poly(imide).....	126
Table 5.6 Conductivities of PEDOT/multi-sulfonated poly(imide) at various processing temperature.....	129

LIST OF FIGURES

		Page
Figure 2.1	Electric conductivity of isolators, semiconductors, and conductive materials	9
Figure 2.2	Chemical structure of few π -conjugated polymers and their bandgapenergy	10
Figure 2.3	Binding in conducting conjugate polymers	11
Figure 2.4	Energy band in solid.	12
Figure 2.5	^1H -NMR spectrum of EDOT	14
Figure 2.6	^{13}C -NMR spectrum of EDOT	14
Figure 2.7	IR-spectrum of EDOT	15
Figure 2.8	Synthesis of EDOT from oxalic acid ester and thiodiacetic acid ester	16
Figure 2.9	Transetherification as a synthetic route to EDOT derivatives.....	16
Figure 2.10	Left: representation the top view of the morphology of a thin film of PEDOT:PSS particles, surrounded by a thin PSS-rich surface layer PEDOT chains are displayed as short bars. Right: chemical structure of the species present in the film.....	17
Figure 2.11	PEC arrangement: (left) ladder-type and (right) scrambled eggtype	18
Figure 2.12	Particles size distribution of a PEDOT:PSS before and after a shear treatment	21
Figure 2.13	Polycomplex creation from high molecular weight polymer and oligomer molecules, “Host-guest” model	23

	Page
Figure 2.14 Polycomplex from two high molecular weight polymers, “Scrambledeggs” model.....	23
Figure 2.15 Two-step condensation polyimide synthesis, shown here for PMDA/ODA	25
Figure 2.16 A general overview of mixers	31
Figure 2.17 Illustration of flow situations in mixers	32
Figure 2.18 Representation of surfactant.....	32
Figure 2.19 Surfactant classification according to the composition of their head:nonionic, anionic, cationic, and amphoteric.....	34
Figure 2.20 Chemical structure of sodium dodecyl sulfate	35
Figure 2.21 Electrostatic and steric stabilization of an emulsion by surfactants	39
Figure 3.1 Structure of poly(styrene sulfonic acid) (PSSA).....	41
Figure 3.2 Representation of water-dispersible PEDOT-SPAA undergoing conversion to the thermally stable PEDOT-SPI.....	44
Figure 3.3 Synthesis of BAPSBPS	46
Figure 3.4 Synthesis procedure of sulfonated polyimides (SPIs).....	47
Figure 3.5 Synthesis of a novel sulfonated aromatic diamine monomer (DSBAPB).....	48
Figure 3.6 Synthesis of sulfonated polyimides (SPIs).....	48
Figure 3.7 Synthesis of a sulfonated monomer, ODADS.....	49
Figure 3.8 Synthesis of sulfonated polyimide	50
Figure 3.9 Synthesis of sulfonated perylenedianhydride compound: (a) n- butylamine, propanol/water; (b) ArOH, K ₂ CO ₃ ; (c) KOH,t-BuOH.....	51

Figure 3.10	Chemical structures of surfactants	53
Figure 3.11	Powder size distribution of the PPy with SDBS, CTAC and Triton X-100 of a) 0.2 mmol, b) 2 mmol c) 5 mmol d) 20 mmol and e) 40 mmol at 650 rpm.....	55
Figure 3.12	Agitation speed of polymerization and power size distribution of the PPy prepared a) without surfactant and with b) SDBS c) SDS d) CTAC and f) Triton X-100 by 20 mmol feed.....	56
Figure 3.13	TEM images of the PPy without surfactant synthesized at a) 6,500 and b) 13,500 rpm and with c) SDBS, d) CTAC, and e) Triton X-100. Each surfactant was 20 mmol for the emulsion polymerization at 13,500 rpm	57
Figure 3.14	Variation of the conductivity of the PEDOT:PSS (surfactant) film. The additives are a) SDS, b) TsNa and c) dodecylbenzenesulfonic acid sodium salt	58
Figure 3.15	Schematic structure of a PEDOT segment and a PSS segment in water a) without and b) with the addition of anionic surfactant.....	59
Figure 3.16	Chemical structure of surfactants a) sodium dodecyl sulfate (SDS), b) tosylate sodium (TsONa), c) sodium dodecylbenzenesulfonic acid (SDBA), d) polyoxyethylene(12) tridecyl ether (POETE), and e) (tetra-n-octylammonium bromide)(TOAB)	60
Figure 3.17	Variations of the conductivity of PEDOT:PSS with the weight ratio of added surfactants to PEDOT:PSS	60
Figure 3.18	Variations of the conductivity of treated PEDOT:PSS films with InCl_3 , CuCl_3 , and NaCl concentrations in aqueous solutions.....	61

	Page
Figure 3.19 Chemical structures of sodium dodecylbenzenesulfonated (DBSNa).....	62
Figure 3.20 TGA curves of PPy-sulfate, PPy-chloride, PPy-DBSNa and curve of neat anionic surfactant DBSNa.....	63
Figure 3.21 SEM micrograph of PPy-sulfate (a and b) and PPy prepared in the presence of anionice surfactant, DBSNa.....	64
Figure 4.1 Schlenk line	69
Figure 4.2 Inert gas supply system.....	70
Figure 4.3 Vacuum pump.....	70
Figure 4.4 Magnetic stirrers and hot plate	71
Figure 4.5 A high-speed mechanical mixer	72
Figure 4.6 A stir shaft used with the mechanical stirrer	72
Figure 4.7 Reactor.....	73
Figure 4.8 Rotary evaporator.	74
Figure 4.9 Scheme for the 4,4'-ODADS reaction.	75
Figure 4.10 Chemical structure of PEDOT:SPI.....	76
Figure 4.11 Synthesis of diamine.....	81
Figure 4.12 Synthesis of multi-sulfonateddiamine	81
Figure 4.13 Synthesis of sulfonated polyimide using a novel synthesized diamine	82
Figure 4.14 Chemical structure of PEDOT-SPI.....	83
Figure 4.15 Fourier transform infrared spectroscopy (FT-IR) equipment.....	84
Figure 4.16 Thermogravimetric analysis (TGA) equipment.....	84
Figure 4.17 Nuclear magnetic resonance spectrometers.....	85

	Page
Figure 4.18	A four-point-probe conductivity cell 86
Figure 4.19	Current generator and multimeter (left), four-point-probe (gold wires) (right)..... 86
Figure 4.20	Current generator and nanovoltmeter equipped with four-point-probe (platinum wires) 87
Figure 4.21	Transmission electron microscope (TEM) 88
Figure 4.22	Elemental analysis 88
Figure 5.1	FTIR spectrum of 4,4'-ODADS 90
Figure 5.2	¹ H NMR spectrum of 4,4'-ODADS..... 91
Figure 5.3	Chemical structure of SPI 92
Figure 5.4	FTIR spectrum of SPI(6FDA) and SPI(O-DPDA) 93
Figure 5.5	FTIR spectrum of PEDOT-SPI 94
Figure 5.6	Variation of the conductivity of the PEDOT-SPI(SDS) film mechanical stirring system with the weight fraction of the anion surfactant..... 98
Figure 5.7	TGA of PEDOT-SPI with varied mixing systems 100
Figure 5.8	TGA of PEDOT-SPI with various %wt of SDS 101
Figure 5.9	TEM of various mixing systems (A-B1=magnetic bar, A-B2=mechanical at 1000 rpm, and A-B3=mechanical at 4000 rpm 102
Figure 5.10	TEM of PEDOT-SPI with various %wt of SDS 104
Figure 5.11	Chemical structure of SDS, PEDOT, sulfonated polyimide (SPI)and PSS 106
Figure 5.12	FTIR results of PEDOT-SPI system 107
Figure 5.13	FTIR results of PEDOT-PSS system 107
Figure 5.14	TGA results of PEDOT-SPI system..... 111

	Page
Figure 5.15 TGA results of PEDOT-PSS system	112
Figure 5.16 TEM of PEDOT-SPI system	114
Figure 5.17 TEM of PEDOT-PSS system	115
Figure 5.18 Chemical structure of a novel multi-sulfonated polyimide	118
Figure 5.19 Scheme of synthesis of diamine monomer	119
Figure 5.20 FTIR spectrum of synthesized diamine	120
Figure 5.21 ¹ H NMR spectrum of synthesized diamine	120
Figure 5.22 Scheme of synthesis of multi-sulfonateddiamine monomer	121
Figure 5.23 FTIR spectrum of multi-sulfonateddiamine	122
Figure 5.24 ¹ H NMR spectrum of multi-sulfonateddiamine.....	122
Figure 5.25 Scheme of synthesis of multi-sulfonatedpoly(imide).....	124
Figure 5.26 FTIR spectrum of sulfonatedpoly(imide).....	125
Figure 5.27 Overlaid FTIR spectrum of synthesized diamine, multi-sulfonateddiamine and sulfonated poly(imide).....	125
Figure 5.28 FTIR spectrum of PEDOT/multi-sulfonatedpoly(imide)	127
Figure 5.29 Overlaid FTIR spectrum of multi-sulfonateddiamine, sulfonatedpoly(imide) and PEDOT-SPI	127
Figure 5.30 TGA synthesized diamine	130
Figure 5.31 TGA of multi-sulfonatedpoly(imide)	131
Figure 5.32 TGA of PEDOT/multi-sulfonatedpoly(imide)	131
Figure 5.33 TGA of PEDOT/multi-SPI and PEDOT/SPI(4,4'-ODADS).....	132
Figure 5.34 TEM of PEDOT/multi-sulfonatedpoly(imide)	133

CHAPTER I

INTRODUCTION

Organic electronics is a relatively new multidisciplinary field of research that encompasses a series of conceptual, experimental, and modeling challenges regarding electronic devices made with organic-based materials. It is different from conventional electronics that use inorganic materials, like gallium arsenide or silicon. In the scientific and technological revolution of the last few years the study of high-performance materials has been steadily enlarged to include organic-based materials. The exploration for more powerful, smaller, thinner, and flexible electronic devices require materials with new and improved characteristics and new fabrication processes.

Alan J. Heeger, Alan G. MacDiarmid and Hideki Shirakawa established the basis of the field of organic electronics field back in the 1970s with the discovery of electrically conducting polymers. For their breakthrough work in this area, Alan J. Heeger, Alan G. MacDiarmid and Hideki Shirakawa were awarded the Noble Prize in Chemistry in the year 2000 [1-3].

Conducting polymers have combined the advantageous characteristics of conventional polymers, such as low density [4], flexibility, good processability, and low cost [5], with the functional physical properties of conventional semiconductors, such as light absorption/emission and a tunable conductivity. These characteristic lead to novel materials for optoelectronic devices such as solar cells [6], light emitting diodes [7], electrochromic devices [8], and sensors [9]. In a large majority of devices, this role is played by poly(3,4-ethylenedioxythiophene):poly(styenesulfonate) (PEDOT:PSS).

PEDOT is a relatively new material in the conducting-polymer family. It shows attractive properties, including relatively good electrochemical, low HOMO-LUMO band gap, and ambient and thermal stability of its electrical properties as compared with that of other polythiophenes

[10]. PEDOT is obtained from the polymerization of ethylenedioxythiophene (EDOT) monomers. PEDOT, which combines a fairly high electrical conductivity ($10^2 - 10^3 \text{ S cm}^{-1}$ in the doped state) with unsurpassed stability, is probably the single most industrially important organic conductor with use in a wide range of applications. PEDOT itself is insoluble in many common solvents and unstable in its neutral state, as it rapidly oxidizes in air. To solve the processability problem, a polyanion, such as PSS, can be used as a template, resulting in a colloidal aqueous dispersion of PEDOT:PSS, where PEDOT is its oxidized state. Each phenyl ring of the PSS monomer has one acidic SO_3H (sulfonate group). PEDOT:PSS is industrially synthesized from the EDOT monomer oxidizing agent and PSS as a template polymer. The role of PSS is to act as the counter ion and to keep PEDOT chain segments dispersed in the aqueous medium. Aqueous dispersion of PEDOT:PSS are commercially available, for example, under the trade name Baytron P from H. C. Stark. In general PEDOT:PSS gel particles are formed and thin, highly transparent, and conducting films can be prepared on almost any hydrophilic surface by drop-casting or spin-casting. The film properties depend on solid content, doping concentration, and particle size. However, the thermal stability of commercialized PEDOT:PSS has hindered its usage for high-temperature processing. PEDOT:PSS is only stable up to $200 \text{ }^\circ\text{C}$ [11], annealing beyond this temperature results in a significant decrease in conductivity [12]. For certain high-temperature applications, a different template is needed.

Sulfonated poly(imide)s (SPIs) are well-known high performance polymers, especially in the proton exchange membrane (PEM) fields because of their excellent properties, including thermal stability [13], mechanical properties [14], good film forming ability, superior chemical resistance, and especially high solubility in organic solvents, which are enable for solution processing [15]. Therefore, the SPI templates could possibly be used for high-temperature processing while still being compatible with electronic devices.

A common feature of conducting polymers, the electrical and optical properties, is the strong influence of morphology, chemical, and physical structure. Research and development

efforts over the past ten years have quickly brought PEDOT to the forefront in the field of conducting polymers. Its properties, being its high conductivity in combination with excellent stability, a relative high transparency to visible light, and aqueous processability, have allowed the material to now become industrially useful. Research area has been focused on improving the conductivity, through the addition of surfactants and non-ionic additives (so called secondary dopants), such as high-boiling-point polar organic compounds [16], treatment of the conducting film with a polar solvent, such as ethylene glycol or dimethyl sulfoxide [17], and thermal annealing [18-20]. In addition, some research has been centered around improving the solubility of the colloidal dispersion, particle size distribution, and morphology of the conducting films. Therefore, this research aims to compare synthesized PEDOT:SPI aqueous dispersions using a mechanical stirring system to a conventional magnetic stirring system. The mechanical stirring system was subjected to improve particle size, thermal stability, and dispersion stability. In addition, an anionic surfactant, sodium dodecyl sulfonate (SDS), was utilized as an additive to improve the dispersion stability, conductivity and thermal stability. Furthermore, a novel multi-sulfonated group in a single molecule of sulfonated polyimides, which obtained from 2 symmetrical aromatic synthesized sulfonated bulky diamines, was proposed. The comparison effects of conductivity of PEDOT using the different sulfonated polyimide templates were also investigated.

Basically, the subjects studied in this thesis can be split into three main topics:

- (i) Experimental observation on the mixing systems and ways to significantly enhance the conductivity of PEDOT:SPI aqueous dispersion;
- (ii) Effects of the addition of anionic surfactant during template polymerization of conducting polymers containing PEDOT with SPI or PSS templates for nano-thin film applications;
- (iii) Synthesis and characterization of PEDOT/multi-sulfonated polyimide via template polymerization

The first topic discussion concerns the study of comparative synthesized PEDOT:SPI aqueous dispersions using mechanical stirring or conventional magnetic stirring system. The mechanical stirring system was subjected to improve particle size, thermal stability, and dispersion stability due to the shear force from the stirrer. In addition, an anionic surfactant, sodium dodecyl sulfonate (SDS), was utilized as an additive to improve the dispersion stability, conductivity and thermal stability. Due to the combination of those concepts, superior dispersion stability, high conductivity and thermally stable PEDOT:SPI films were achieved. The effects of different polyimide structures in PEDOT:SPI on the film properties was also investigated.

The second topic further explains the study of a novel approach to synthesize nanoparticle suspensions (PEDOT-PSS, PEDOT-SPI) through addition of the anionic surfactant, SDS, during template polymerization while using a mechanical shear stirrer to disperse the particles. The surfactant could be incorporated into synthesized particles during polymerization as well as effectively functioning as a dopant, resulting in an increasing dispersion of nanoparticles, improved thermal stability, and inducing smaller nanoparticles dimensions. In this study, we have divided this topic into three systems: (1) surfactant added during template polymerization of nanoparticle suspensions (PEDOT-PSS, PEDOT-SPI); (2) surfactant added after template polymerization of nanoparticle suspensions; (3) surfactant added both during and after polymerization. Also, we have evaluated the effect of SDS on the chemical structure of the colloid particles, their thermal stability, morphological dispersion, and their conductivity.

The last topic deals with a novel multi-sulfonated group in a single molecule of sulfonated polyimides, which obtained from a symmetrical aromatic synthesized sulfonated bulky diamines, was proposed. The new symmetrical aromatic diamine was synthesized by the aromatic nucleophilic substitution reaction. Furthermore, a comparison effects of conductivity of PEDOT using the different sulfonated polyimide templates was investigated. The sulfonated polyimides were characterized by Nuclear Magnetic Resonance (NMR), Fourier Transform Infrared Spectroscopy (FT-IR), Thermal Gravimetric Analysis (TGA) and conductivity measurement.

1.1 Objectives of the Research

The aims of this study are fourfold as follows:

- 1.1.1 To synthesize conducting polymers namely poly(3,4-ethylenedioxy- thiophene) (PEDOT) using sulfonated polyimide template via template polymerization.
- 1.1.2 To compare the conductivity, thermal properties, and morphological properties of conducting polymers using two different mixing systems for dispersing the polymer into a suspending medium.
- 1.1.3 To study the effect of anionic surfactant on chemical structure, dispersion stability, conductivity, thermal stability, and morphology of conducting polymers.
- 1.1.4 To synthesize and characterize a novel PEDOT/multi-sulfonated polyimide

1.2 Scope of the Research

- 1.2.1 Synthesis of sulfonated polyimide from 4,4'-diaminodiphenyl ether-2,2'-disulfonic acid (4,4'-ODADS) and 4,4'-oxydiphthalic anhydride (O-DPDA), in case PEDOT:SPI(OPDA) or 4,4'-Hexafluoroisopropylideneoxydiphthalic anhydride (6FDA), in case PEDOT:SPI(6FDA).
- 1.2.2 Synthesis of PEDOT:SPI aqueous dispersions using high-speed mechanical stirring system at 2 different speeds (1,000 and 4,000 rpm) and comparison of the obtained conducting polymer properties with a conventional magnetic stirring system.
- 1.2.3 Evaluation of the effect of addition of anionic surfactant, sodium dodecyl sulfonate (SDS) to PEDOT:SPI aqueous dispersion at various SDS contents (0.1, 0.5, 1, 3, 5 wt%) on the dispersion stability, conductivity, and thermal stability.
- 1.2.4 Studying three different systems of addition of SDS based on when the SDS was added to the dispersion: (1) surfactant added during template polymerization of nanoparticle suspensions (PEDOT-PSS, PEDOT-SPI) (2) surfactant added after template polymerization of nanoparticle suspensions (3) surfactant added both during and after polymerization.
- 1.2.5 Synthesis and characterization of the novel PEDOT/multi-sulfonated polyimide using 4,4'-diaminodiphenyl ether-2,2'-disulfonic acid (4,4'-ODADS) and a novel symmetrical aromatic synthesized sulfonated bulky diamines

This thesis is divided into six chapters as follows:

Chapter I provides an overview of the history of the conducting polymers and the objectives and scope of this research.

Chapter II explains the basic theory about this work such as synthesis of conducting polymer, enhancement of conductivity, including the basic of sulfonated poly(imide), template polymerization, the basic of surfactants and polymer in aqueous solution, and colloidal polymer.

Chapter III presents literature reviews of the previous works related to this research such as the conventional template (PSSA), the modern template, and improving the conductivity of conducting polymer by addition of surfactants.

Chapter IV shows the experimental equipment and experimental procedures to synthesis sulfonated diamine monomer, sulfonated (polyimide), template polymerization, the addition of surfactants studies, including the preparation of films, also instruments and techniques used in characterizing the resulting polymers.

Chapter V exhibits the experimental results, which are divided into three parts.

- (i) Experimental observation on the mixing systems and ways to significantly enhance the conductivity of PEDOT:SPI aqueous dispersion;
- (ii) Effects of the addition of anionic surfactant during template polymerization of conducting polymers containing PEDOT with SPI and PSS a template for nano-thin film applications;
- (iii) Synthesis and characterization of PEDOT/multi-sulfonated polyimide via template polymerization.

Chapter VI, the last chapter, shows overall conclusions of this research and recommendations for future research.

CHAPTER II

THEORIES

This chapter introduces the basic concept of the discovery and development of conducting polymers with an emphasis on the conducting polymer poly (3,4-ethylenedioxythiophene) (PEDOT). Moreover, the basic concept of sulfonated poly(imides) is also discussed. A short overview of polymer mixing systems in which shear treatment a high speed mechanical mixer is imparted as well as varying surfactants with emphasis on electrical conductivity, thermal properties, and the morphology of the conducting polymers is discussed. Lastly, the motivations of this thesis are presented.

2.1 Conducting Polymers

Conductivity borderlines between electrically isolating, semiconducting, and conductive materials are fluent and cannot precisely defined. An overview of typical, widely accepted ranges of conductivity for these three, not very sharply separated material classes is given in Figure 2.1. Conducting polymers/conjugated polymers and their conductivity range is diagrammed in Figure 2.1. The conductivity range of these polymers has been extensively widened in the last few decades. It is obvious that adjusting the desired conductivity for a polymeric material is a very difficult challenge; some sort of “molecular engineering” is required.

Since their discovery in the mid-1970s, conducting polymers have been a hot research area for many academic institutions. This research has supported the industrial development of conducting polymer products and provided the fundamental understanding of the chemistry, physics and materials science of these materials. In 2000, the Noble Prize for Chemistry was awarded to Alan J. Heeger, Alan G. MacDiarmid, and Hideki Shirakawa “for their discovery and development of conducting polymer”. Since then, conductive polymers have won growing

attention in the scientific world, and the public now has more benefits from innovations due to the increasing technical usage of conductive polymers.

Conducting polymers combine the advantageous characteristics of conventional polymers, such as low weight, processability, and flexibility, with the tunable conductivity inherent semiconductors, to provide innovative materials for optoelectronic devices.

	Conductivity (S/cm)	Materials
Metallic conductors	10^6	Copper
	10^4	Iron Graphite
	10^2	Bismuth
Semi-conductors	10^0	Indium/Antimony
	10^{-2}	Gallium/Arsenic Germanium
	10^{-4}	Silicon
	10^{-6}	
	10^{-8}	
Isolators	10^{-10}	Glass
	10^{-12}	
	10^{-14}	Diamond
	10^{-16}	Sulfur Polyethylene
	10^{-18}	Polystyrene Teflon®
	10^{-20}	Quartz

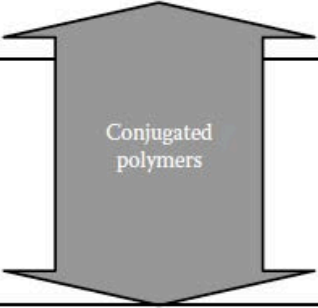


Figure 2.1 Electric conductivity of isolators, semiconductors, and conductive Materials. [21]

Nowadays conducting organic materials, both electron (n-type) and hole transport (p-type) materials, can be made. Many innovative materials for the use in electronic applications have been developed and characterized. The particular bonding arrangement of the carbon atoms in the polymer backbone is the reason for the characteristic electronic properties of tunable conductivity, electrochromism, electroluminescence and electroactivity [22].

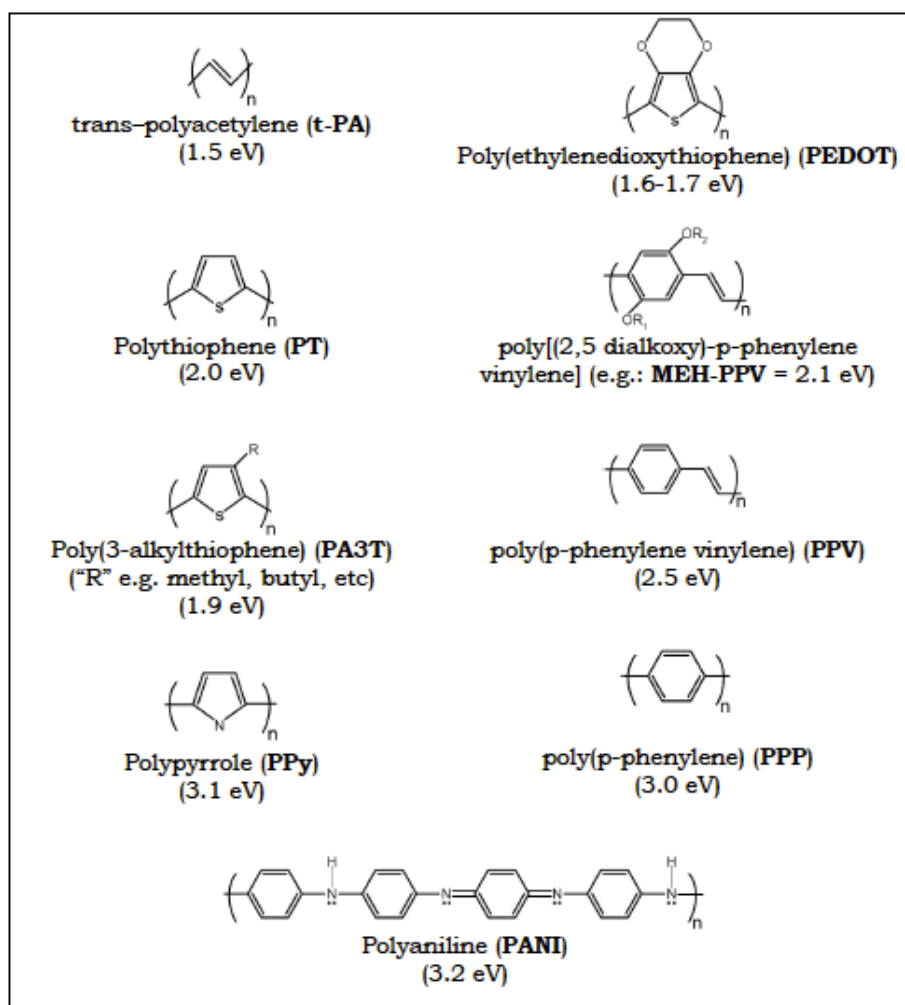


Figure 2.2 Chemical structure of few π -conjugated polymers and their bandgap energy

[23].

In Figure 2.2, a general characteristic of conducting polymers is the presence of double bonds alternating with single bonds along the polymer chain, i.e. conjugated bonds. The electron configuration of the six electrons in a carbon atom (in its ground state) is $1s^2 2s^2 2p^2$. Two of the sp^2 -orbitals on each carbon atom form covalent bonds with neighboring carbons, the third generally forms a covalent bond with a hydrogen or side group. This is called a σ -bond, which is any bond with cylindrical symmetry around the internuclear axis [22]. The unhybridized p_z -orbital overlaps with the unhybridized p_z -orbital on the neighboring carbon. This is called a π -

bond, as is any bond, which arises from electrons approaching side by side, off the internuclear axis. Figure 2.3 summarizes the preceding explanation.

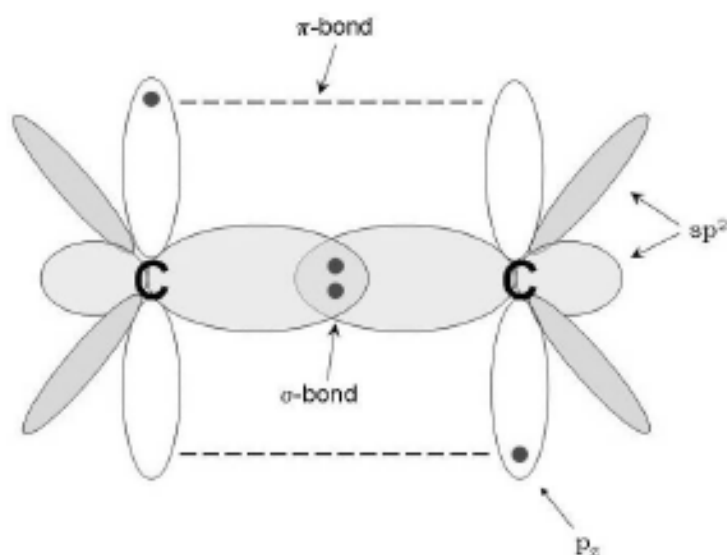


Figure 2.3 Binding in conducting conjugated polymers. [23]

The electrons in the π -bonds are weakly bound, and thus they are relatively easily delocalized. These delocalized π electrons are what make conjugated polymers conductive. In summary, the sp^2 hybridization in conducting polymers is important because this leaves one p-electron per atom to form its own band. Under the assumption that the single and double bonds have the same length, However, the length of the single and double bonds are not identical and the Peierls instability (i.e., C–C bonds are longer than C=C bonds) [24] splits this simple band into 2 sub-bands, a completely filled valence band (highest occupied molecular orbital or HOMO level) and an empty conduction band (lowest unoccupied molecular orbital or LUMO level), separated by an energy gap as shown in Figure 2.4. Hence the material is a semiconductor.

Through the process of doping, the conductivity of pristine π -conjugated polymers can be changed from insulating to conducting, with the conductivity increasing as the doping level increases. The conductivity of these systems can be increased by more than 10 orders of

magnitude upon doping the pristine polymer [22]. With these improvements in electrical conductivities, many traditional signatures of metallic conductivity have been demonstrated.

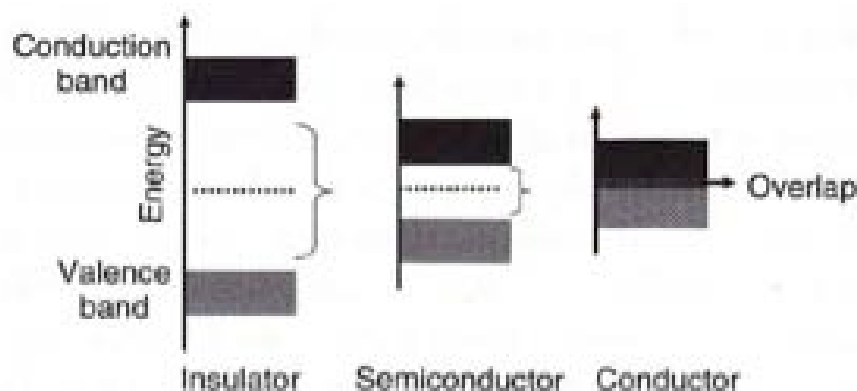


Figure 2.4 Energy band in solid [21]

2.2 Poly (3,4-ethylenedioxythiophene) (PEDOT)

PEDOT is synthesized from ethylenedioxythiophene (EDOT) monomers. It shows interesting properties, including great electrochemical, and thermal stability of its electrical properties as compared with that of other polythiophenes.

Physical Properties

Pure, freshly distilled EDOT is a nearly colorless liquid with an unpleasant odor. A small change in color to pale yellow is possible after extended storage, especially in the daylight, without significantly affecting the analytical purity. The purification procedure of choice is vacuum distillation. Some physical data, including flash point and ignition temperature, are given in Table 2.1 [25].

Table 2.1 Selected physical properties of EDOT

Viscosity (20°C)	11 mPa·s
Density (20°C)	1.34 g/cm ³
Melting point	10.5°C
Boiling point (1013 mbar)	225°C
Vapor pressure (20°C)	0.05 mbar
Vapor pressure (90°C)	10 mbar
Solubility in water (20°C)	2.1 g/l
Flash point	104°C
Ignition temperature	360°C

The ¹H-NMR spectrum of EDOT (solvent: CDCl₃; 400 MHz) consists of two singlets at 4.17 ppm (4H, $\text{—OCH}_2\text{CH}_2\text{O—}$) and 6.30 ppm (2H, CH -2,5) (Figure 2.5). The ¹³C-NMR spectrum in CDCl₃ (Figure 2.6) exhibits three signals at 141.8 ppm (C -3,4), 99.5 ppm (C -2,5), and 64.6 ppm ($\text{—OCH}_2\text{CH}_2\text{O—}$). Using infrared (IR) spectroscopy (Figure 2.7), the typical strong absorption of the C=C-stretching vibration in the thiophene heteroaromatic ring and the ether C—O-stretching band are observed besides the common aromatic and aliphatic C—H vibrations close to 3000 cm⁻¹.

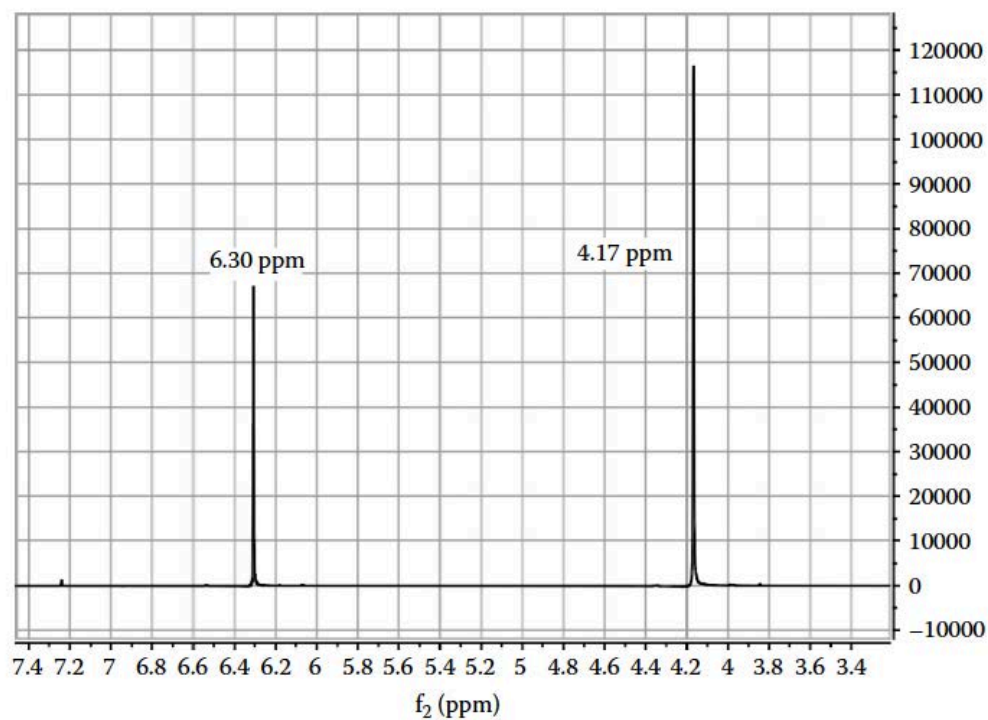


Figure 2.5 $^1\text{H-NMR}$ spectrum of EDOT (400 MHz; solvent: CDCl_3 ; δ/TMS) [21]

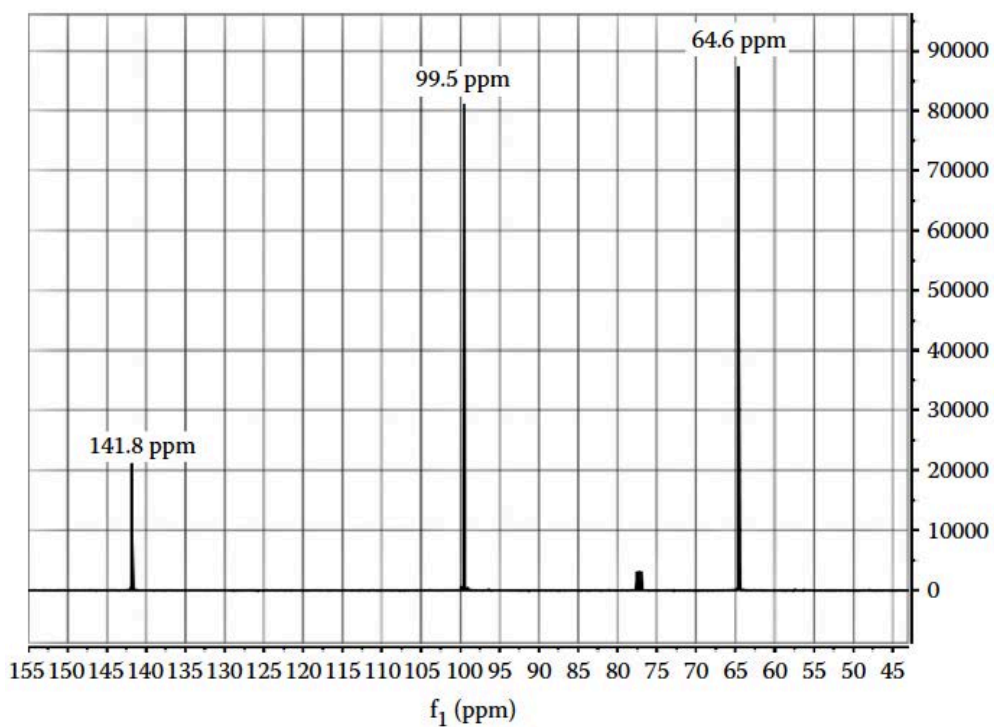


Figure 2.6 $^{13}\text{C-NMR}$ spectrum of EDOT (CDCl_3 ; 400 MHz) [21]

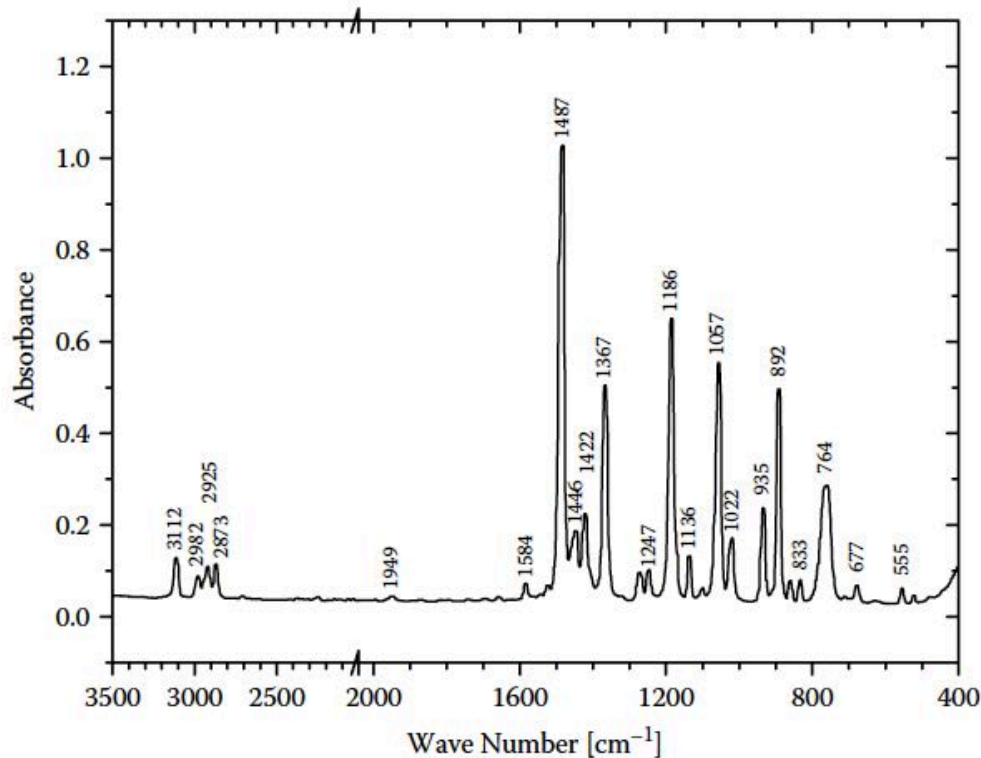


Figure 2.7 IR-spectrum of EDOT (neat film between KBr windows) [21] EDOT Synthesis

EDOT chemistry started as early as the 1930s, when corresponding 2,5-dicarboxylic acid esters were first described [25,26]. A detailed synthesis description for 3,4-ethylenedioxythiophene-2,5-dicarboxylic acid was given by Gogte et al. in 1967 [27]. Decarboxylation of this intermediate led to EDOT [28] and since its introduction into the chemistry of ICPs its industrial manufacture has been based on the Gogte pathway with minor changes, utilizing a copper-catalyzed decarboxylation in the last step [29] as shown in Figure 2.8.

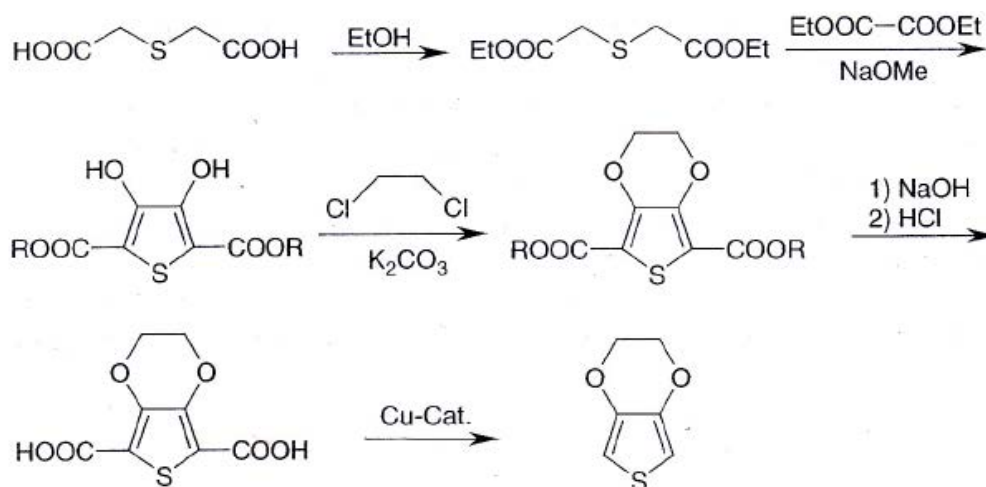


Figure 2.8 Synthesis of EDOT from oxalic acid ester and thiodiacetic acid ester [21].

Several alternative routes have been suggested, which in some cases are especially useful for preparing derivatives of EDOT. One of the highest preparative values of these other pathways seems to be associated with the transesterification of 3,4-dimethoxythiophene (or other lower alkoxythiophenes) with vicinal diols [30-31]. The Williamson ether synthesis step sometimes suffers from low yields with long-chain 1,2-dibromoalkanes due to competing elimination reactions, making transesterification the synthetic strategy of choice. For several EDOT derivatives, for example benzo-EDOT the transesterification reaction provides the best synthetic access. Transesterification proved to be especially useful in synthesizing enantiomerically pure chiral disubstituted EDOTs as shown in Figure 2.9.

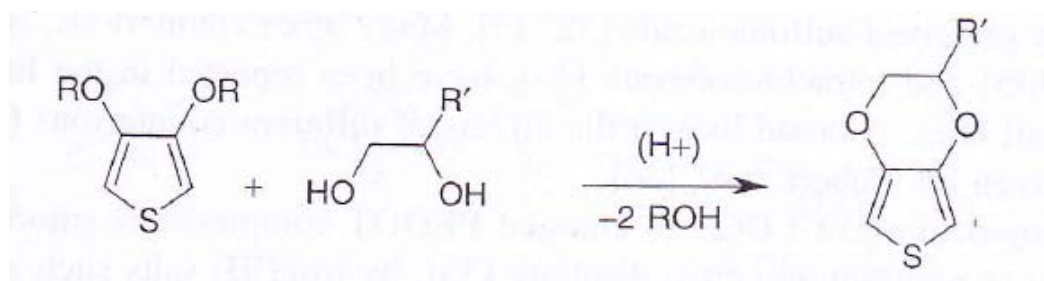


Figure 2.9 Transesterification as a synthetic route to EDOT derivatives [21]

2.3 Poly (3,4-ethylenedioxythiophene):poly(styrenesulfonate acid) (PEDOT:PSS)

One of the reasons why PEDOT has become a successful conductive polymer is because of its availability as polymer dispersion. In combination with PSS, acting as a counterion, a polyelectrolyte complex (PEC) can be prepared that forms a stable dispersion, which is producible on an industrial scale and can be used in many deposition techniques. Industrially, PEDOT:PSS (see Figure 2.10) is synthesized from the EDOT monomer, PSS as the template polymer, and sodium peroxydisulfate as the oxidizing agent. This affords PEDOT in its highly conducting, cationic form. The degree of polymerization of PEDOT is limited and it is assumed that PEDOT is a collection of oligomers with lengths up to ~20 repeating units. The role of PSS, which has a much higher molecular weight, is to act as the counter ion and to keep the PEDOT chain segments dispersed in the aqueous medium. In general, PEDOT:PSS gel particles are formed that possess excellent processing characteristics allowing for the production of thin, transparent, conducting films.

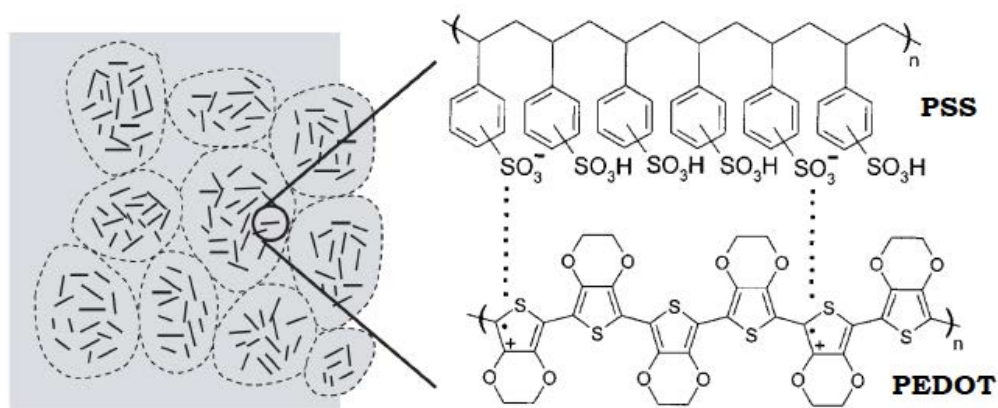


Figure 2.10 Left: representation the top view of the morphology of a thin film of PEDOT:PSS particles, surrounded by a thin PSS-rich surface layer PEDOT chains are displayed as short bars. Right: chemical structure of the species present in the film [32].

2.3.1 Polyelectrolyte Complexes

Polyelectrolyte complexes are typically formed by mixing aqueous solutions of polyanions and polycations. On a molecular level, two arrangements of PECs have been discussed in literature [33]. The ladder type (Figure 2.11) shows a pairing of most of the polar groups from one macromolecule with those of the opposite charge of another macromolecule. The ladder type is found particularly in dilute solutions and in cases where the spacing of the charged groups along the chain is similar for both polyelectrolytes. Furthermore, the ladder type is found when polyelectrolytes with very different molecular weights are used [34]. The so-called scrambled egg type is based on random interactions between polar groups of one macromolecule and various other polar groups of many other polymer chains with no order on the molecular or supermolecular level. Of course, many gradual variations from the ordered ladder type toward the disordered scrambled egg type are also possible. It is worthwhile noting that the degree of order for both cases is far lower than that in natural polyelectrolytes, such as the double helix in DNA with its precise spacing between the nucleic acids. The solvent used for most PECs described in literature is water, since it dissolves polyelectrolytes well due to its high dielectric constant; furthermore, it is easily accessible, nontoxic, and therefore the “natural” solvent for polyelectrolyte [35].

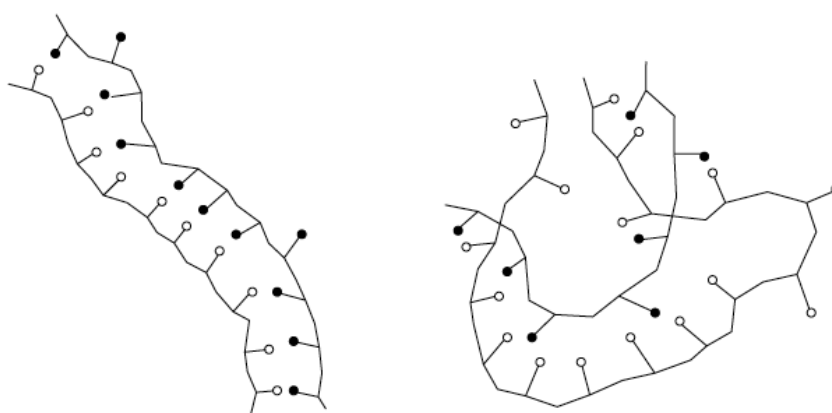


Figure 2.11 PEC arrangements: (left) ladder-type and (right) scrambled egg type [35].

The mixing of solutions containing stoichiometric amounts of polyanions and polycations generally leads to the precipitation of both species. This is due to the fact that the polar groups screen each other and the overall solubility is lost. However, when polyanions and polycations are mixed in nonstoichiometric ratios, soluble complexes can be formed. These polyelectrolyte complexes are found in the form of discrete soluble gel particles in the aqueous medium. For nonstoichiometric polyelectrolyte complexes the major component can also be described as the host polyelectrolyte (HPE), whereas the oppositely charged minor component can be described as the guest polyelectrolyte (GPE). The latter joins the repeat units of the HPE via electrostatic interactions, so that a network is formed. For the formation of soluble particles, it is beneficial if the HPE consists of high molecular weight, whereas the GPE has a low molecular weight. Furthermore, it is beneficial for a stable PEC if at least one of the polyelectrolytes has weak ionic groups.

Synthesis of a PEDOT:PSS Complex

PSS was the first polyelectrolyte used for a PEC with PEDOT in 1990 and has remained the industrial standard ever since [36, 37]. PSS is commercially available in a large range of molecular weights with different polydispersities. Besides commercial availability and its solubility in water, PSS forms durable films and shows no absorption in the visible range of light, resulting in transparent films. PSS as a counterion for PEDOT is always used in excess, that is, as the host polyelectrolyte (HPE). The molar ratio of thiophene groups to sulfonic acid groups in standard PEDOT:PSS dispersions is in the range of 1:1.9 to 1:15.2, which corresponds to a weight ratio range of 1:2.5 up to 1:20. Since only one charge is found for every three to four thiophene rings, the charge excess of PSS is between 6-fold and 46-fold. More details on standard commercial PEDOT:PSS dispersions are given in Table 2.2. Due to the delocalization of positive charges in PEDOT, the resulting weak polar groups and the different spacing of charges in PEDOT compared to PSS, it is reasonable to assume that the structure of PEDOT:PSS shows

the form of a scrambled egg type. A pairing of charges as required in the ladder type is not possible.

Table 2.2 Commercial PEDOT:PSS Dispersion in Water and Their Properties [21].

Trade Name	Solids Content in Water (w/w) (%) ^a	PEDOT:PSS Ratio (w/w)	Viscosity at 20°C (mPas) ^a	Particle Size d ₅₀ (nm) ^a	Conductivity (S/cm) ^a
Clevios P	1.3	1:2.5	80	80	<10
Clevios PH	1.3	1:2.5	20	30	<10
Clevios P VP AI 4083	1.5	1:6	10	40	10 ⁻³
Clevios P VP CH 8000	2.8	1:20	15	25	10 ⁻⁵
Clevios PH 500	1.1	1:2.5	25	30	500 ^b
Clevios PH 750	1.1	1:2.5	25	30	750 ^b
Clevios PH 1000	1.1	1:2.5	30	30	1000 ^b

^a Typical values for solids content, viscosity, particle size, and conductivity are given; no specification.

^b Conductivities for Clevios PH 500, PH 750, and PH 1000 are measured for dispersions containing 5% dimethyl sulfoxide.

An important parameter for the EDOT polymerization is the pH value. The presence of PSS leads to a low pH of less than 3. This is beneficial since the reaction is catalyzed. In the absence of acid, the oxidation of EDOT can result in keto-functionalized side products. A range of oxidizing agents is available for the polymerization of EDOT in water. Iron(III) salts such as iron(III) nitrate and iron(III) chloride can be used. The average particle size of PEDOT:PSS dispersions is in the range of 10 nm to 1 μ m. The gel particles of PEC dispersions can be altered after the synthesis using shear energy. Figure 2.12 shows the particle size distribution of a PEDOT:PSS dispersion before and after a shearing process. In this case, the average particle size is reduced from 380 nm to 23 nm.

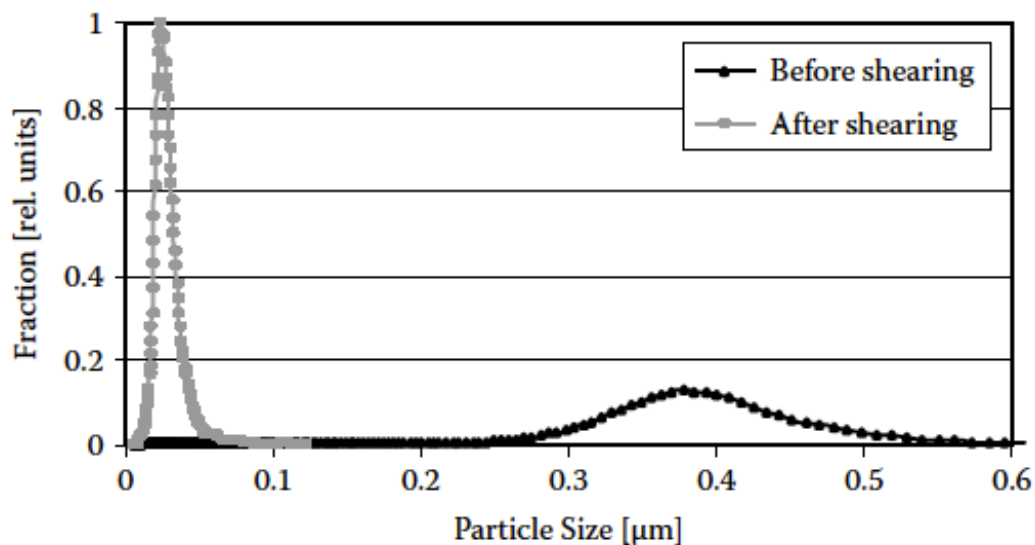


Figure 2.12 Particle size distribution of a PEDOT:PSS PEC before and after a shear treatment (data from W. LÖvenich 2007. Unpublished results.) [21]

2.4 Template Polymerization [38]

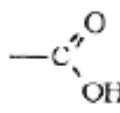
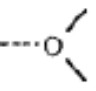
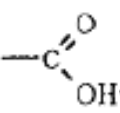
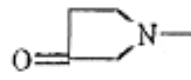
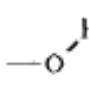
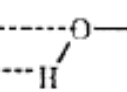
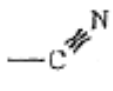
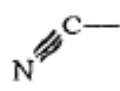
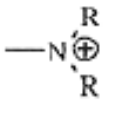
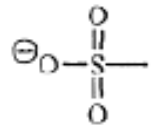
Template polymerization has been used to polymerize PEDOT with the poly(styrene sulfonic acid) or poly(amic acid)/poly(imide) templates. Template or matrix polymerization can be defined as a method of polymer synthesis in which specific interactions between preformed macromolecules (template) and a growing chain are utilized. These interactions affect the structure of the polymerization product (daughter polymer) and the kinetics of the process. The term “template polymerization” usually refers to one-phase systems in which monomer, template, and the reaction product are soluble in the same solvent.

The growth of living organisms is associated with very complicated processes of template polymerization. Low molecular weight substrates, such as sugars, amino acids, fats, and water in animals and carbon dioxide in plants are precursors of polymers (polypeptides, polynucleic acids, polysaccharides, etc.). They are organized in tissues and can be reproduced. In many biological reactions such as DNA replication or polypeptide creation, low molecular weight

substrates and polymeric products are present in the reaction medium together with the macromolecular compounds called matrices or templates controlling the process.

A few examples illustrate the interaction between monomer and template groups and the nature of forces operating in the system template-monomer (see table 2.3). In conducting polymerization systems, the interaction between monomer (PEDOT) and template (PSS or SPI) is an electrostatic one.

Table 2.3 Examples of interaction between monomer and template [39]

Monomer	Template	Nature of forces
		Hydrogen bonds
		Hydrogen bonds
		Hydrogen bonds
		Dipole-dipole
		Electrostatic

Polymerization of monomers interacting with templates by ionic, transferring interactions, or by hydrogen bonding leads to polycomplexes. Formation of polymeric complexes from two mutually interacting polymers is well known. By mixing two solutions of polyelectrolytes having

opposite charges, one can obtain the polymeric complex usually in the form of a precipitate or liquid phase containing a high concentration of the two polymeric components and a second liquid phase containing much lower concentration of the polymeres. Methods of synthesis, properties and characteristic of polyelectrolyte complexes have been described in many papers [39, 40]. A structure of typical polycomplexes is illustrated in Figure 2.13 and 2.14.

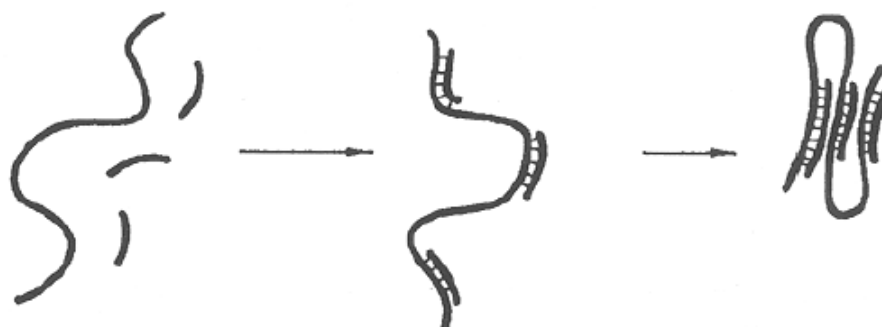


Figure 2.13 Polycomplex creation from high molecular weight polymer and oligomer molecules, “Host-guest” model [21]



Figure 2.14 Polycomplex from two high molecular weight polymers, “Scrambled eggs” model [21]

If one polymer has much higher molecular weight than the other, a model “host-guest” is commonly applied. Smaller “guest” molecules are absorbed on the “host” molecule. Because hydrophobic interactions take place between created blocks, the molecule of the complex becomes more compact. Similar intermolecular interactions can lead to precipitation. It seems probable that a similar process takes place at the very beginning of the template polymerization proceeding according to a “pick-up mechanism”. Interacting molecules are bonded at random. Short “ladder” parts of the polycomplex as well as “loops” created from unconnected parts of the components are present in the product. Such structure is sometimes called “scrambled eggs” model. Similar polycomplexes can be obtained by template polymerization of complementary monomer on the proper template. The template and the daughter polymer in this case form polymer complexes. The structure of such polycomplexes is in many cases different from the analogous complexes obtained by mixing two complementary polymers.

2.5 Polyimides

Most of the developments in modern polyimide chemistry can be traced to pioneering work at DuPont in the 1950s and 1960s. Polyimides are step or condensation polymers that have heterocyclic imide functionalities in their repeat units. They are generally derived from the reaction of organic diamines and organic tetracarboxylic acids or derivatives. The structure of a general polyimide is shown in Figure 2.15.

Polyimides are both scientifically and commercially important, because of their excellent thermal stability and mechanical strength. Proper design of polyimides has led to their use in aerospace, microelectronics, automotive, and packaging industries.

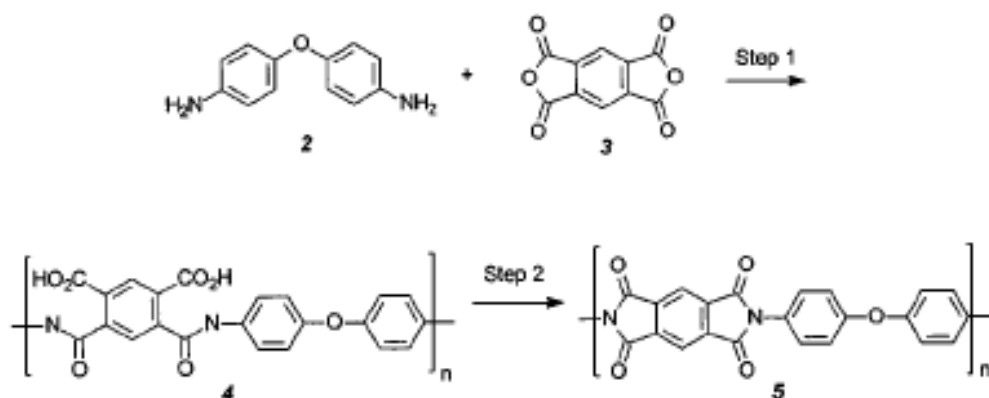


Figure 2.15 Two-step condensation polyimide synthesis, shown here for PMDA/ODA.

Synthesis of Polyimides

Classical Two-Step Route

The most common method of preparing aromatic polyimides involves the reaction of an aromatic tetracarboxylic acid anhydride with an aromatic diamine. The initial step consists of preparing a solution of the aromatic diamine in a polar aprotic solvent, such as *N*-methylpyrrolidone (NMP), dimethylacetamide (DMAc) or dimethylsulfoxide (DMSO), to which is added a tetracarboxylic dianhydride, which forms a soluble, processable poly(amic) acid intermediate at ambient temperature.

The high molecular weight isomeric poly(amic)acid formation is completed within 24 hours or less, depending on monomer reactivity. Since it is fully soluble in the reaction solvent, the solution may be cast into a film on a suitable substrate. The second step in this synthetic method is the cyclodehydration reaction (imidization) that is accomplished by thermal (heating to elevated temperatures), chemical (incorporating a chemical dehydration agent) or by azeotropic solution imidization.

This method is representative of the initial work on aromatic polyimides and remains the most practical way to synthesize high performance polyimides. The reason for this two-step

method is that many of the resulting polyimides (e.g., Kapton®) are insoluble and infusible due to their rigid aromatic repeat unit. On the other hand, the soluble and processable poly(amic acid) intermediates that are heated to elevated temperatures also facilitate the generation of fully cyclized films via spin casting coating procedures.

One-Step Polymerization

A single-stage homogeneous solution polymerization technique can be employed for polyimides, which are soluble in organic solvents at polymerization temperatures. In this process, a stoichiometric mixture of monomers is heated in a high boiling point solvent or a mixture of solvents at a temperature range of 140-250°C where the imidization reaction proceeds rapidly. Commonly used solvents are nitrobenzene, benzonitrile, α -chloronaphthalene, *o*-dichlorobenzene, trichlorobenzenes, or phenolic solvents such as *m*-cresol and chlorophenols in addition to dipolar aprotic amide solvents. Toluene is often used as a cosolvent to facilitate the removal of the water from the condensation reactions. During polymerization, water is distilled off continually as an azeotrope along with the solvent. Preparation of high-molecular-weight poly(amic acid) is not necessary in this procedure. Imidization still proceeds via amic acid intermediate. However, the concentration of amic acid group is very small at any time during the polymerization because it is unstable at high temperature and rapidly imidizes, or reverts to amine and anhydride. Because water is formed as the result of the imide formation, some of the anhydride groups are rapidly hydrolyzed to *o*-dicarboxylic acid. When a mixture composed of diamine, dianhydride, and a solvent is heated, a viscous solution is formed at intermediate temperature of 30-100°C. The composition of the product is mainly poly(amic acid). At this stage, phase separation is usually observed in nonpolar solvents such as chlorinated aromatic hydrocarbons. However, on raising the temperature to 120-160°C, a vigorous evolution of water occurs and the reaction mixture suddenly becomes homogeneous. At this stage the product is essentially a low-molecular-weight

polyimide having *o*-dicarboxy and amino end groups. Thereafter, a slow stepwise polycondensation takes place according to the reaction between the end groups.

Formation of Polyamic Acids

When a diamine and a dianhydride are added into a dipolar aprotic solvent such as *N,N*-dimethylacetamide, polyamic acid is rapidly formed at ambient temperatures. The reaction mechanism involves the nucleophilic attack of the amino group on the carbonyl carbon of the anhydride group, followed by the opening of the anhydride ring to form amic acid group.

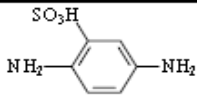
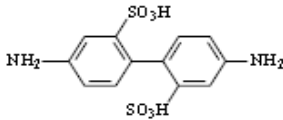
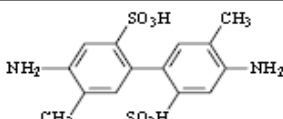
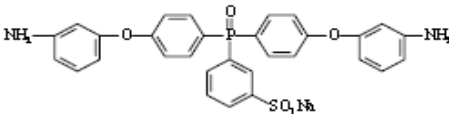
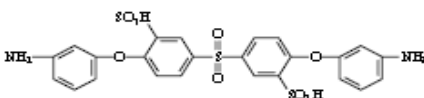
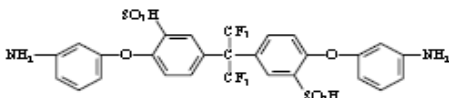
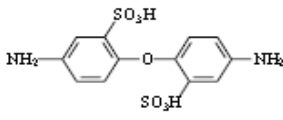
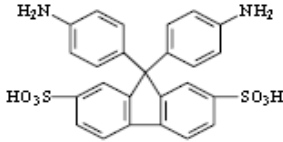
The most important aspect of this process is that it is an equilibrium reaction. Often it appears to be an irreversible reaction because a high-molecular-weight poly(amic acid) is readily formed in most cases as long as pure reagents are used. This is because the forward reaction is much faster than the reverse reaction, often by several orders of magnitude. If the large reaction rate difference is not met, the high-molecular-weight poly(amic acid) is not formed. Therefore, it is important to examine the driving forces that favor the forward reaction over the reverse reaction. It should also be noted that acylation reaction of amines is an exothermic reaction and that the equilibrium is favored at lower temperatures. The forward reaction in dipolar solvents is a second-order reaction and the reverse reaction is a first-order reaction. Therefore, the equilibrium is favored at high monomer concentrations to form high-molecular-weight poly(amic acid)s.

2.6 Sulfonated Polyimide [39]

Presently, the synthesis of sulfonated polyimide copolymers has been by a direct copolymerization procedure. This approach requires that sulfonated monomers are used in the copolymerization, as opposed to sulfonation of the parent polymer. Stoichiometric amounts of sulfonated diamine relative to nonsulfonated diamine, and naphthalenic dianhydride (NDA) as the dianhydride, have been used for sulfonated copolyimide synthesis. A 1:1 stoichiometric ratio of total diamine to dianhydride was used to obtain high molecular weight polymer. The degree of

sulfonation could be varied by changing the ratio of sulfonated to nonsulfonated diamine. The copolymerizations were always a one-step high temperature polycondensation in *m*-cresol; however, the catalysts employed have been varied. In all cases, the triethylammonium salt form of the sulfonated diamine is used to synthesize high molecular weight polyimides. The acid and sodium sulfonate forms of most diamines are insoluble in *m*-cresol. By adding triethylamine to a sulfonated diamine in *m*-cresol at room temperature for about 4 hours, the triethylammonium salt form of the sulfonated diamine was formed which was soluble in the reaction media. Also, the free uncomplexed aromatic amine will be more reactive. Benzoic acid or isoquinoline are used as catalysts for imide formation.

Table 2.4 Sulfonated diamines [39].

Structure	Name	Abbreviation
	2,5-Diaminobenzenesulfonic acid	DAB
	4,4'-Diamino-2,2'-biphenyl disulfonic acid	BDA
	4,4'-Diamino-5,5'-dimethyl-2,2'-biphenyl disulfonic acid	6TS
	3-Sulfo-4',4''-bis(3-aminophenoxy)triphenyl phosphine oxide sodium salt	SBAPPO
	3,3'-Disulfonate-bis[4-(3-aminophenoxy)phenyl]sulfone	SA-DADPS
	2,2-Bis[4-(4-aminophenoxy)phenyl]hexafluoropropane disulfonic acid	BAHFDS
	4,4'-Diaminodiphenylether-2,2'-disulfonic acid	ODADS
	9,9'-Bis(4-aminophenyl)fluorene-2,7-disulfonic acid	BAPFDS

Direct sulfonation of polymer

Perhaps the most simple and widely used method to prepare sulfonated polysulfones or polyimide is through the direct sulfonation of the main chain using *chlorosulfonic acid* or *fuming sulphuric acid* in chlorinated solvents. Since this is an electrophilic substitution reaction, positions *ortho* to the ether groups are favored. As mentioned earlier, these positions are electrophilically activated by the oxygen atoms giving an electron-rich character to the arylene ether segments, which in turn make them the most favorable sites for substitution. However, because the sulfonation reaction is a reversible reaction, the ease of sulfonation also implies that these positions are activated for desulfonation under acidic aqueous conditions. This might prove detrimental for the successful use of such polymers in PEMFCs. Of particular concern to the polymer chemists are the harsh conditions needed for the sulfonation of the polymer main chain, which can lead to partial cleavage of the polymeric main chain. Another complication is that directly sulfonated polymers characteristically exhibit extensive swelling and lose their mechanical stability when a certain critical degree of sulfonation, or temperature, is exceeded under immersed conditions. For example, directly sulfonated polysulfones with a degree of sulfonation of 80% have been found to be water-soluble at room temperature, therefore limiting the *IEC* of the polymers that can be used as membranes in fuel cells.

2.7 Basic concept of shear treatment by using high speed mechanical mixer

Mixers or blenders work by shearing, which is created by a tangential force being applied to the sample. There are several tools that disrupt by shearing, including blenders, roto-stators, and some of the homogenizers.

High-speed mechanical mixer using shear force is usually produced by spinning blades, thus, homogenizing the sample. The vast majority of mechanical shear homogenizers are probe-style instruments, which contain a motor-driven blade at the end of a roto shaft (see Figure 2.16).

The knife creates a shear force to disrupt the samples. These types of instrument are far more powerful than a magnetic stirrer. Various models of varying probe size and power are designed to handle different sizes, and toughness of the sample. Due to the rapid mechanical shearing action inside the samples, a significant amount of heat can build up with extended use. Since the heat is generated within the sample itself, it is not well by cooling method.

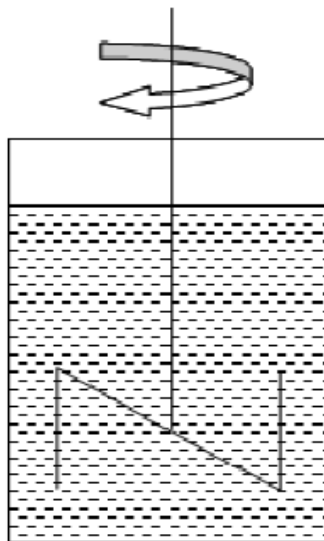


Figure 2.16 A general overview of mixers [41]

How samples are disrupted: Flow Situations in Mixers

- Flow profiles are complex based on geometry of mixers
- Flow maybe laminar or turbulent (turbulent flows preferred)
- It can create vortexes which cause foaming so the absence of air is critical
- Fairly inexpensive

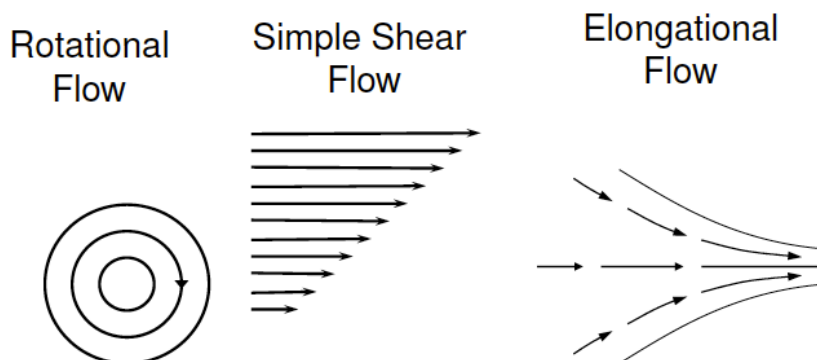


Figure 2.17 Illustration of flow situations in mixers [41]

2.8 Surfactants

Surfactants are amphipathic molecules that consists of a non-polar hydrophobic portion, usually a linear or branched hydrocarbon or fluorocarbon chain containing 8-18 carbon atoms (hydrophobic), which is attached to a polar or ionic portion (hydrophilic). Before discussing specific details of surfactant types, it may be useful to introduce some basics of surfactant science. Chemical structures having suitable solubility properties for surface activity vary with the nature of the solvent system to be employed and the conditions of use. In “standard” surfactant terminology, the “head” refers to the solubilizing groups-the lyophilic or hydrophilic group, in aqueous systems-and the “tail” refers to the lyophilic or hydrophobic group in water (see the example shown in Figure: 2.18):

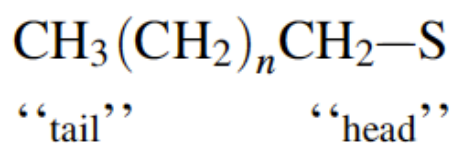


Figure 2.18 Representation of surfactant [42]

In water, the hydrophobic group may be, for example, a hydrocarbon, fluorocarbon, short polymeric chain, or siloxane chain of sufficient size to produce the desired solubility characteristics when bound to a suitable hydrophilic group. In aqueous systems, the hydrophilic group (the “head”) will be ionic or highly polar, so that it can act as a solubilizing functionality.

The systematic classification of surfactants

In aqueous systems, by far the most important of surfactant applications in volume and economic impact, the hydrophobic group is generally a long-chain hydrocarbon group, although there are examples using fluorinated or oxygenated hydrocarbon or siloxane chains. The hydrophile or head will be an ionic or highly polar group that can impart some water solubility to the molecule. The most useful chemical classification of surface-active agents is based on the nature of the hydrophile, with subgroups based on the nature of the hydrophobe or tail. With such a wide variety of structures available, it is not surprising that the selection of a suitable surfactant can become a significant problem in terms of making the best choice of material for a given application. The following discussion briefly provides the basic concept of classification of surfactants.

A simple classification of surfactants based on the nature of the hydrophobic group is commonly used. Their main classes may be distinguished as anionic, cationic and amphoteric. The four basic classes of surfactants are defined according to the composition of their head as follows (see Figure 2.19):

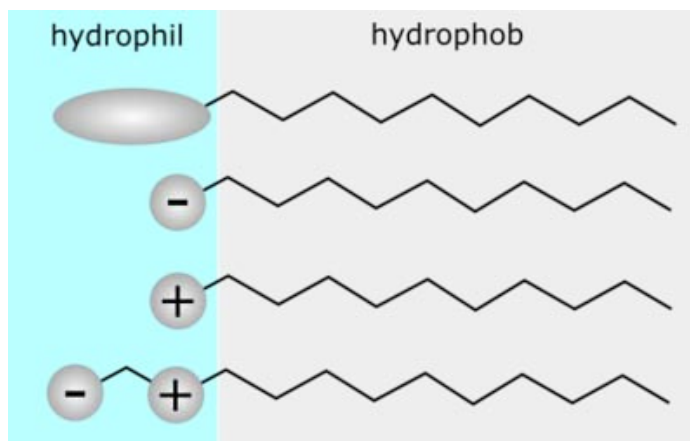


Figure 2.19 Surfactant classification according to the composition of their head:nonionic, anionic, cationic, and amphoteric [43].

1. Anionic Surfactants

The largest class of surface-active materials in general use today fall in the anionic classification, constituting 70–75% of total worldwide surfactant consumption. The major subgroups of this class are the alkali carboxylates or soaps, sulfates, sulfonates, and to a lesser degree, phosphates. The variety of anionic materials available arises primarily from the many types of hydrophobic groups that can be modified by addition of the proper anionic species.

Anionic surfactants are the most widely used class of surfactants due to their relatively low cost and they are practically used [44]. Some research groups have investigated the role of the surfactant, and show that these materials affect the conductivity, thermal stability, and morphology of conducting polymers such as polyanilines, polypyrroles, polythiophenes, and PEDOT [45-47]. Kudoh et al. investigated the role of anionic surfactants in the synthesis of PEDOT [48] and found that PEDOT with good thermal stability was obtained in the presence of a bulky anionic surfactant because this anion was incorporated into PEDOT as a dopant. The conductivity was increased with higher concentrations of anionic surfactant because of the increasing in a degree of polymerization. Gök et al. [47] had published the details of an investigation into the effects of anionic, cationic, and nonionic surfactants on the properties of

polythiophenes (PTs). It had been shown that PTs prepared in the presence of cationic and non-ionic surfactants produce smooth surfaces, while PTs synthesized with cationic surfactants have the highest thermal stability of all samples. Surfactants were often used for controlling the morphology of the PEDOT film by electrochemical methods [48]. The morphologies of the conducting polymers and sizes of their nanocomposites had profound effects on their physical and chemical properties, which could improve their performance in many of important application fields [49–50].

Anionic surfactants contain anionic functional groups at their head, such as sulfate, sulfonate, phosphate, and carboxylates. Prominent alkyl sulfates include ammonium lauryl sulfate, sodium lauryl sulfate (SDS, sodium dodecyl sulfate, another name for the compound) and the related alkyl-ether sulfates sodium laureth sulfate, also known as sodium lauryl ether sulfate (SLES), and sodium myreth sulfate. Docusates: dioctyl sodium sulfosuccinate, perfluorooctanesulfonate (PFOS), perfluorobutanesulfonate, linear alkylbenzene sulfonates (LABs).

In this thesis, an anionic surfactant, sodium dodecyl sulfonate (SDS), was utilized as an additive to improve the dispersion stability, conductivity and thermal stability.

Sodium dodecyl sulfate (SDS)

Sodium dodecyl sulfate (SDS), is an organic compound with the formula $\text{CH}_3(\text{CH}_2)_{11}\text{OSO}_3\text{Na}$ (see Figure 2.20). The salt is of an organosulfate consisting of a 12-carbon tail attached to a sulfate group, giving the material amphiphilic properties.

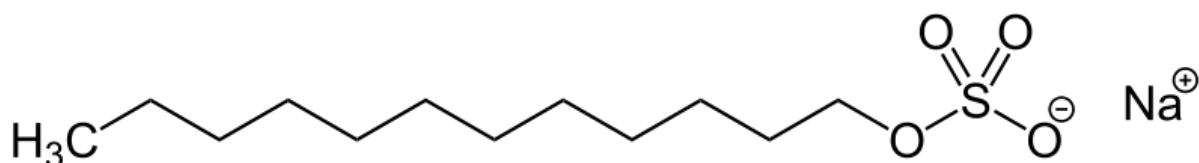


Figure 2.20 Chemical structure of sodium dodecyl sulfate (SDS) [42]

2. Cationic Surfactants

Cationic surfactants first became important when the commercial potential of their bacteriostatic properties was recognized in 1938. Since then, the materials have been introduced into hundreds of commercial products, although their importance does not approach that of the anionic materials in sheer quantity or dollar value.

Cationic surfactants are basically soaps or detergents, in which the hydrophilic, or water-loving, end contains a positively-charged ion, or *cation*. Typical examples are trimethylalkylammonium chlorides, and the chlorides or bromides of benzalkonium and alkylpyridinium ions. All are examples of *quats*, so named because they all contain a quaternary ammonium ion.

3. Non-ionic Surfactant

Many long chain alcohols exhibit some surfactant properties. Prominent among these are the fatty alcohols such as cetyl alcohol, stearyl alcohol, and cetostearyl alcohol (consisting predominantly of cetyl and stearyl alcohols), and oleyl alcohol.

- Polyoxyethylene glycol alkyl ethers (Brij): $\text{CH}_3-(\text{CH}_2)_{10-16}-(\text{O}-\text{C}_2\text{H}_4)_{1-25}-\text{OH}$:

Octaethylene glycol monododecyl ether

Pentaethylene glycol monododecyl ether

- Polyoxypropylene glycol alkyl ethers: $\text{CH}_3-(\text{CH}_2)_{10-16}-(\text{O}-\text{C}_3\text{H}_6)_{1-25}-\text{O}$
- Glucoside alkyl ethers: $\text{CH}_3-(\text{CH}_2)_{10-16}-(\text{O}-\text{Glucoside})_{1-3}-\text{OH}$:

Decyl glucoside,

Lauryl glucoside

Octyl glucoside

- Polyoxyethylene glycol octylphenol ethers: $C_8H_{17}-(C_6H_4)-(O-C_2H_4)_{1-25}-OH$:

Triton X-100

- Polyoxyethylene glycol alkylphenol ethers: $C_9H_{19}-(C_6H_4)-(O-C_2H_4)_{1-25}-OH$:

Nonoxynol-9

- Glycerol alkyl esters:

Glyceryl laurate

- Polyoxyethylene glycol sorbitan alkyl esters: Polysorbate
- Sorbitan alkyl esters: Spans
- Cocamide MEA, cocamide DEA
- Dodecyldimethylamine oxide
- Block copolymers of polyethylene glycol and polypropylene glycol: Poloxamers
Polyethoxylated tallow amine (POEA).

4. Zwitterionic Surfactants

Zwitterionic (amphoteric) surfactants have both cationic and anionic centers attached to the same molecule. The cationic part is based on primary, secondary, or tertiary amines or quaternary ammonium cations. The anionic part can be more variable and include sulfonates, as in CHAPS (3-[(3-Cholamidopropyl)dimethylammonio]-1-propanesulfonate). Other anionic groups are sultaines illustrated by cocamidopropyl hydroxysultaine. Betaines, e.g., cocamidopropyl betaine. Phosphates: lecithin.

Modes of Stabilization of an Emulsion by Surfactants

Electrostatic Stabilization

Electrostatic stabilization by ionic (in particular anionic) surfactants is very common. In addition, polyelectrolytes can be used for this purpose. Electrostatic stabilization is based on the repulsive interaction that results when the diffuse double layers around the particles start to overlap. The overlapping gives an increase in ion concentration, which results in a loss in entropy.

Steric Stabilization (Polymer Stabilization)

Steric stabilization can be achieved by non-ionic surfactants having long polyoxyethylene chains as the polar head groups. Non-ionic polymers are also frequently employed to provide steric stabilization. A necessary requirement for steric stabilization to be effective is that the continuous phase is a good solvent for the polymer chains, which protrude into the surrounding medium.

Particle Stabilization

Solid particles can be used to stabilize an emulsion. The particle should be small in comparison to the emulsion droplets and they should be relatively hydrophobic.

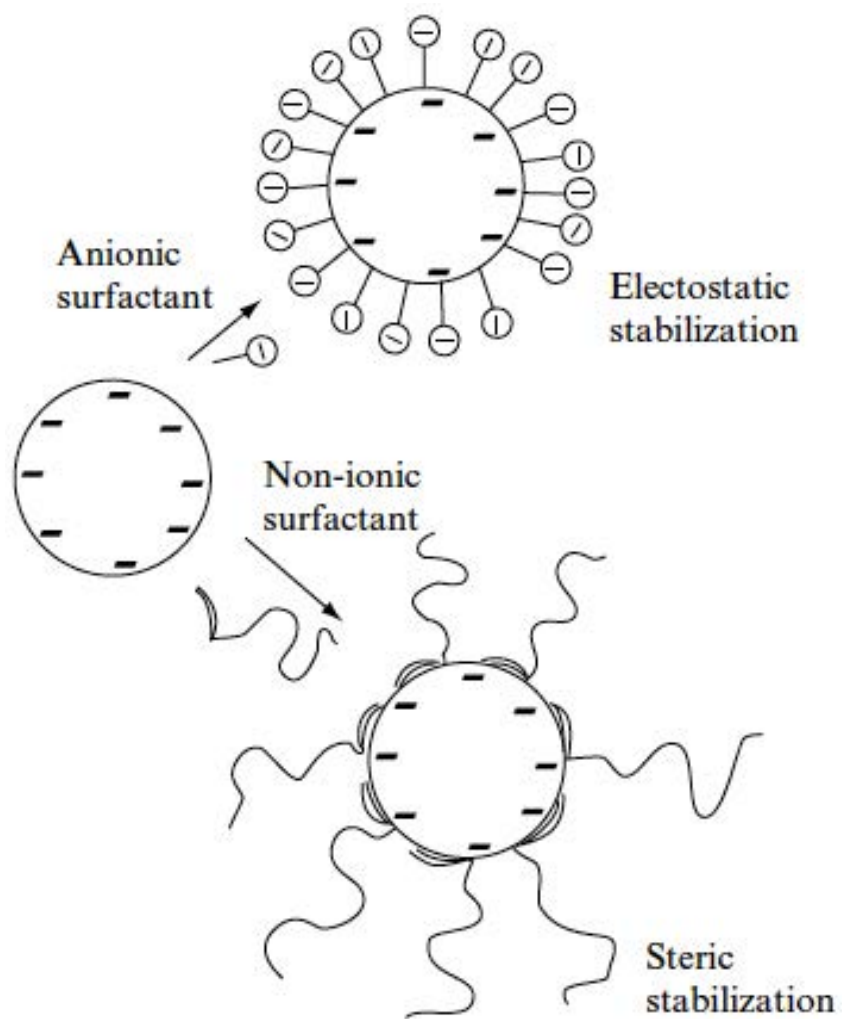


Figure 2.21 Electrostatic and steric stabilization of an emulsion by surfactants [42]

CHAPTER III

LITERATURE REVIEWS

Conducting polymers have attracted extensive scientific activities because they have been shown to provide many practical possibilities as electrochromic displays, chemical sensors, electromagnetic shutters, rechargeable batteries, photo- and electroluminescent materials in optical device and photovoltaic application including Printed Electronics. Efforts have been made in the synthesis and the processing of novel conducting polymers in order to enhance their electrical properties. This chapter describes the literature reviews of the previous works related to the conducting polymer field, including its application and also the method to improve the conductivity.

3.1 Poly (3,4 ethylene dioxythiophene) with Poly (styrene sulfonate)

Template

There are many researches about using poly(styrene sulfonic acid), PSSA as a template of various conducting polymer polymerization. PSSA is a charge - balancing dopant during polymerization in water, which allows for the formation of a colloidal dispersion. The structure of PSSA was shown in Figure 3.1. The literature reviews of this template can be shown as below.

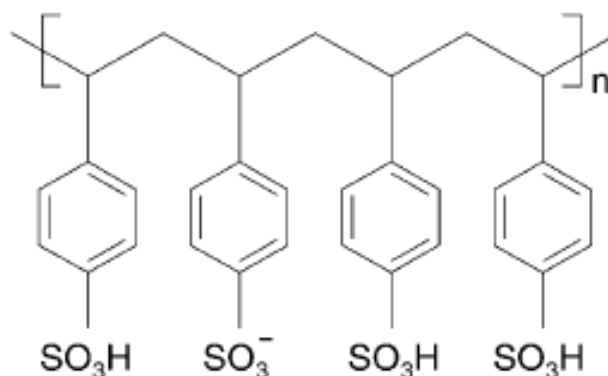


Figure 3.1 Structure of poly(styrene sulfonic acid) (PSSA).

Kim J.Y. et al. [39] observed the increase in conductivity of the PEDOT-PSS systems through the change of solvent from ~ 0.8 to 80 S/cm. The temperature dependence of the reduced activation energy showed that the PEDOT-PSS system approached the critical regime when organic solvents (THF, DMF, and DMSO) were used. From XRD and the absorbance experiments, the polymer chain conformation of the samples did not change by the solvents used. The doping concentration of the systems with various solvents was almost the same, which was observed by EPR and XPS experiments. The screening effect due to the polar solvent between the dopant and the polymer main chain played an important role for charge transport properties such as conductivity and its temperature dependence.

Ouyang J. et al. [53] studied on the conductivity enhancement of PEDOT-PSS films which resulted from adding organic compounds to PEDOT-PSS aqueous solution or treating the PEDOT-PSS film with organic solvents, such as Ethylene glycol, DMSO, NMP, DMAc, 4-methoxyphenol, acetonitrile, cyclohexane, nitromethane, methyl alcohol, and pyridine. The PEDOT-PSS film, which was soluble in water, became insoluble after treatment with EG. This strongly suggested an increased interchain interaction among the PEDOT chains. Raman spectroscopy indicated that this increased interchain interaction resulted from conformational change of the PEDOT chains, which change from a coil to linear or expanded-coil structure.

Conductivity enhancement was observed only when organic compounds with two or more polar groups in a molecule were used. They proposed that the driving force for the conformational changes in the PEDOT chains was the interaction between the dipole of one polar group of the organic compound and the dipoles or the charges on the PEDOT chains.

Ouyang J. et al. [16] investigated the conductivity of a PEDOT-PSS film, which could be enhanced by more than two orders of magnitude by adding a compound with two or more polar groups, such as ethylene glycol (EG), meso-erythritol (1,2,3,4-tetrahydroxybutane), 2-nitroethanol into an aqueous solution of PEDOT-PSS. Their study indicated that the conductivity enhancement strongly depended on the chemical structure of the additive. When an alcohol with only one OH group, such as methanol, ethanol, or heptanol was used, no conductivity enhancement was observed. Also, no conductivity enhancement of the film was observed when nitromethane or acetonitrile was added to an aqueous solution of PEDOT-PSS. Raman spectroscopy indicated that the additive induces a conformational change in the PEDOT chain in the PEDOT-PSS film. Both coil and linear or expanded-coil conformations existed in untreated PEDOT-PSS films, whereas the linear or expanded-coil conformation became dominant in high-conductivity PEDOT-PSS films. This conformational change resulted in an increase in the intrachain and interchain charge-carrier mobilities.

Huang J. et al. [18] investigated the influence of annealing conditions on the physical properties of thin films of PEDOT-PSS. In particular, they described how annealing temperature, the ambient gas, and the choice of dopant affect the conductivity, morphology, and work function of the films. Two specific dopants, sorbitol and glycerol were used. The presence of water and O₂ in the ambient gas reduces the conductivity and work function of the undoped PEDOT-PSS films. Inert gases such as N₂ were therefore recommended for the treatment of PEDOT-PSS films. The improvements in conductivity after annealing were attributed to morphology changes that led to

larger grain sizes and lower inter-grain hopping barriers. The introduction of dopants led to substantial increased in conductivity, by up to a factor of about 500, depending on the exact doping ratio. The surface roughness was also found to increase, with the degree of roughness at a given annealing temperature, apparently were depended on the rate of evaporation of the dopant molecules.

Nardes A.M. et al. [59] studied and further clarified the role of sorbitol as a typical high-boiling processing additive on the conductivity of PEDOT-PSS thin films under thermal annealing and exposure to humidity. The well-established conductivity enhancement of thin PEDOT-PSS films caused by adding sorbitol to the aqueous dispersion occurs during thermal annealing and coincided with the evaporation of sorbitol from the films. The increased conductivity after annealing was accompanied by a lowering of the work function and by a remarkable increase in environmental stability after thermal annealing, as evidenced from a reduced water uptake, which we attributed to a denser packing of the PEDOT: PSS material.

Kang K.S. et al. [60] found that the conductivity of PEDOT-PSS film enhanced nearly three orders of magnitude after HCl-methanol treatment. As duration of treatment in acidic methanol increased, FTIR results showed that the peaks characteristic to PSS decreased and that the PSS was gradually transferred to the solvent. The conductivity of PEDOT-PSS film increased by approximately two orders of magnitude after soaking PEDOT-PSS into the HCl-methanol solution for 10 min. The conductivity gradually increased up to 30 min but slightly decreased thereafter. The surface of PEDOT-PSS was extremely smooth before the solvent treatment. However, various sizes of humps appeared on the surface of the film after treatment for 10 min. The size and number of the humps increased up to 20 min of treatment but gradually decreased thereafter. Most of the humps disappeared from the surface of the film after soaking the film in HCl-methanol solution for 70 min. Removal of PSS from PEDOT-PSS film was beneficial for increasing the conductivity and protecting the electrode corrosion.

Dimitriev O.P. et al. [61] showed results on conductivity of PEDOT-PSS films, which contained different amounts of organic solvents, i.e., dimethyl sulfoxide (DMSO) or ethylene glycol (EG), and annealed at different temperatures. The maximum of conductivity of the resulting films was reached at about 5 wt.% of DMSO or EG in the solution. At the same time, the presence of the solvent residue in the film also resulted in the poor control of the film morphology and conductivity. The author used an alternative method of the films exposure to the solvent vapors. The latter method had more advantages, because it preserved film morphology, and allowed one to control conductivity as a function of the exposure time.

3.2 Sulfonated Poly(imide)

Somboonsub et al. [51] studied the template polymerization of EDOT with sulfonated poly(amic acid) (SPAA) (shown in Figure 3.2), resulting in a conducting polymer, with 10-fold conductivity enhancement after underwent the imidization within 10 min at temperature greater than 150 °C. This material had high thermal stability as compared to PEDOT-PSS because PEDOT-SPAA had a smaller degradation slope.

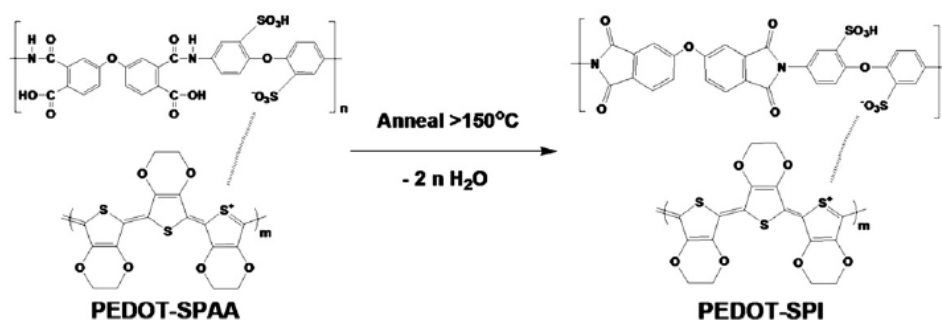


Figure 3.2 Representation of water-dispersible PEDOT-SPAA undergoing conversion to the thermally stable PEDOT-SPI [51]

The films of PEDOT-SPAA showed 6-fold increase in conductivity after annealing at 300 °C for 10 min, but PEDOT-PSS films showed unmeasurable conductivity ($< 1 \times 10^{-5}$ S/cm) after annealed (Table 3.1).

Table 3.1. Conductivities of PEDOT-PSS (in-house) and PEDOT-SPAA. Upon annealing, PEDOT-SPAA imidizes to PEDOT-SPI [51]

Processing temperature		PEDOT-PSS	PEDOT-SPAA
20 °C	Conductivity (S/cm)	3.15×10^{-4}	1.12×10^{-4}
	Std. Dev.	4.03×10^{-5}	8.69×10^{-6}
180 °C (90 min)	Conductivity (S/cm)	2.65×10^{-4}	2.96×10^{-4}
	Std. Dev.	3.32×10^{-5}	5.49×10^{-6}
300 °C (10 min)	Conductivity (S/cm)	$< 1 \times 10^{-5}$	6.06×10^{-4}
	Std. Dev.	$< 1 \times 10^{-5}$	4.84×10^{-5}

The secondary dopants on the PEDOT-SPAA/PEDOT-SPI system could, upon annealing, increase 100-fold conductivity when doped with D-sorbitol or DMF (Table3.2).

Table 3.2. Conductivities of secondary-doped PEDOT-SPAA at various processing temperatures. Upon annealing, PEDOT-SPAA imidizes to PEDOT-SPI [51]

Processing temperature		PEDOT-SPAA	DMF 0.1 wt.%
20 °C	Conductivity (S/cm)	2.04×10^{-4}	5.76×10^{-4}
	Std. Dev.	3.42×10^{-3}	6.09×10^{-5}
180 °C (10 min)	Conductivity (S/cm)	5.83×10^{-3}	8.99×10^{-2}
	Std. Dev.	1.18×10^{-3}	8.28×10^{-2}
300 °C (10 min)	Conductivity (S/cm)	6.47×10^{-4}	4.25×10^{-2}
	Std. Dev.	3.73×10^{-5}	2.03×10^{-2}

Processing temperature		Surfynol 0.1 wt.%	D-sorbitol 5 wt.%	Combination
20 °C	Conductivity (S/cm)	1.82×10^{-4}	4.22×10^{-2}	3.78×10^{-4}
	Std. Dev.	2.51×10^{-5}	5.84×10^{-3}	9.33×10^{-5}
180 °C (10 min)	Conductivity (S/cm)	3.33×10^{-4}	2.00×10^{-2}	4.34×10^{-3}
	Std. Dev.	3.59×10^{-5}	3.51×10^{-3}	8.54×10^{-4}
300 °C (10 min)	Conductivity (S/cm)	5.68×10^{-3}	6.56×10^{-3}	3.74×10^{-3}
	Std. Dev.	1.48×10^{-3}	1.50×10^{-3}	1.13×10^{-3}

Shouwen Chen *et al.* [62] successfully synthesized and characterized the properties of novel side-chain-sulfonated polyimides, comprised random and sequence block copolymerization of bis[4-(4-aminophenoxy)-2-(3-sulfobenzoyl)]phenyl sulfone (BAPSBPS) (shown in Figure 3.3), 1,4,5,8-naphthalene tetracarboxylic dianhydride, and nonsulfonated diamine. The synthesized polymers had good solubility in common aprotic solvents, high stability of sulfonic acid groups and high mechanical strength. In addition, they showed high proton conductivity, regardless of their lower ion exchanging capacity (IEC).

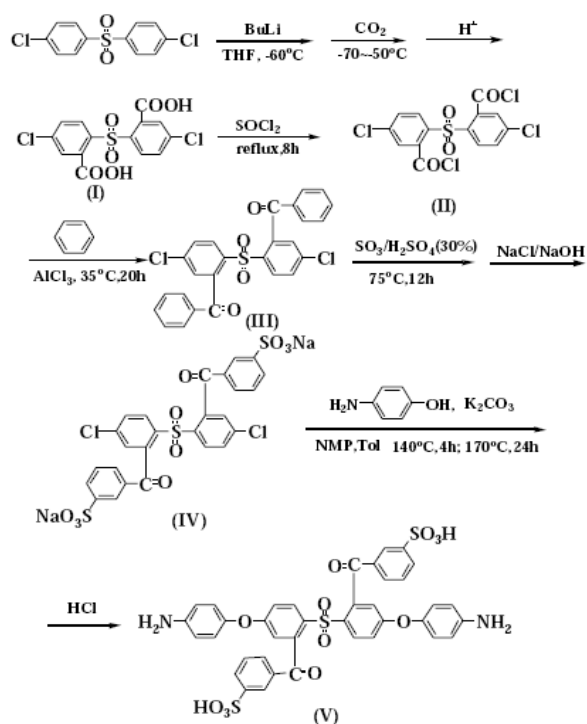


Figure 3.3 Synthesis of BAPSBPS [62]

Xiuling Zhu *et al.* [63] successfully synthesized and characterized the two series of six-membered sulfonated polyimides from 1,4,5,8-naphthalenetetracarboxylic dianhydride (NTDA), S-DHPZDA and nonsulfonated diamines DHPZDA or 4,4'-diaminodiphenyl ether (ODA) (shown in Figure 3.4).

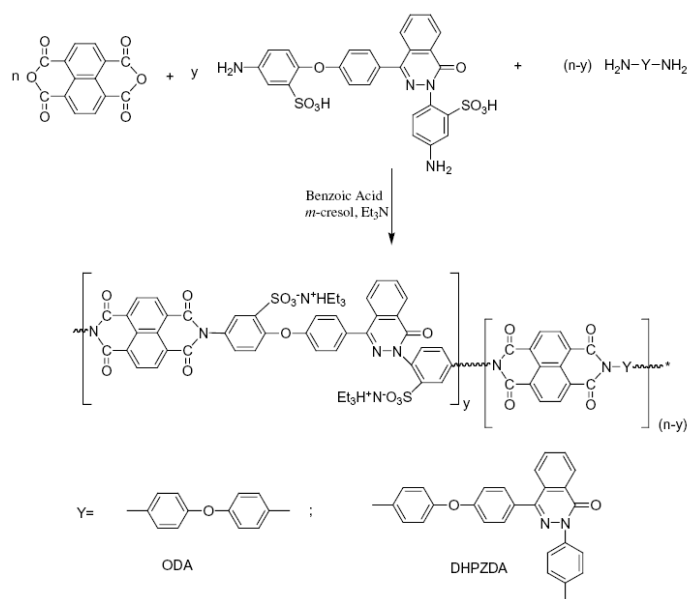


Figure 3.4 Synthesis procedure of sulfonated polyimides (SPIs) [63]

The sulfonated polyimides (SPIs) displayed good solubility in polar aprotic organic solvents such as *m*-cresol, NMP, DMSO, DMF etc. because of the improvement in phthalazinone moieties. Furthermore, the membranes from casting SPIs' solution in NMP were tough, brownish and transparent.

Yuming Shang *et al.* [64] successfully synthesized a novel sulfonated aromatic diamine monomer, 1,4-bis(4-amino-2-sulfonic acid-phenoxy)-benzene (DSBAPB), (show in Figure 3.5) and prepared a series of sulfonated polyimides (SPIs) from DSBAPB with 1,4,5,8-naphthalene tetracarboxylic dianhydride (NTDA) and a non-sulfonated diamine, 4,4'-oxydianiline (ODA) via one-step high-temperature polymerization method (shown in Figure 3.6).

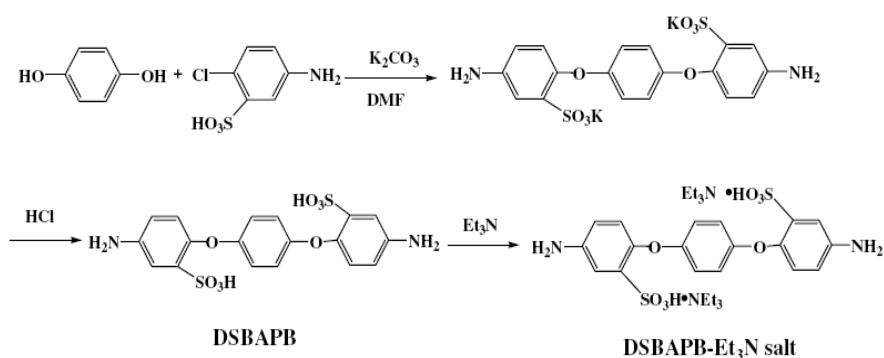


Figure 3.5 Synthesis of a novel sulfonated aromatic diamine monomer

(DSBAPB) [64]

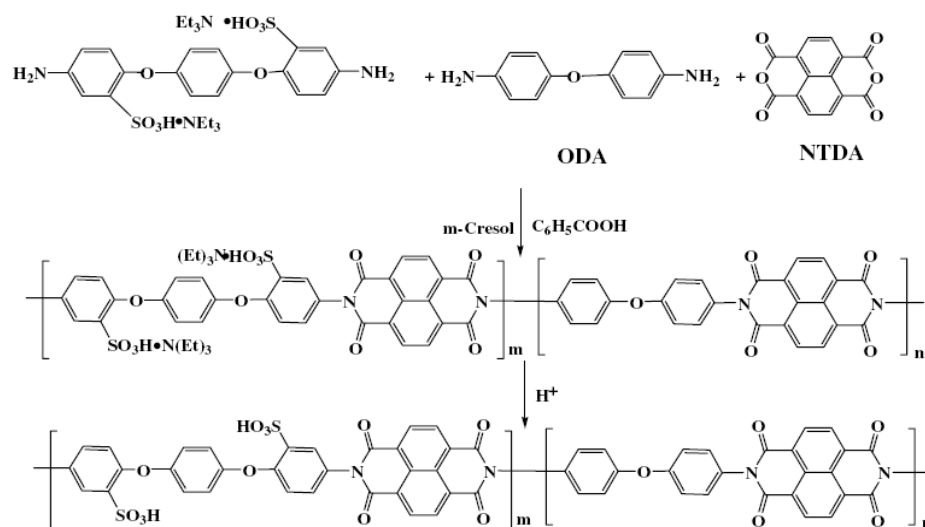


Figure 3.6 Synthesis of sulfonated polyimides (SPIs) [64]

The proton conductivity of the SPI membranes ranged from 7.9×10^{-3} to 7.2×10^{-2} S/cm. The methanol permeability was less than 2.85×10^{-7} cm²/s, which was considerably lower compared with Nafion. The obtained SPIs exhibited much better hydrolysis stability than the BDSA based ones attributed to their flexible chain structure.

Jianhua Fang *et al.* [65] successfully prepared a series of sulfonated polyimides from 1,4,5,8-naphthalenetetracarboxylic dianhydride (NTDA), ODADS, and common nonsulfonated diamines. A sulfonated diamine monomer, 4,4'-diaminodiphenyl ether-2,2'-disulfonic acid (ODADS), was synthesized by direct sulfonation of a commercially available diamine, ODA, using fuming sulfuric acid as the sulfonating reagent (shown in Figure 3.7).

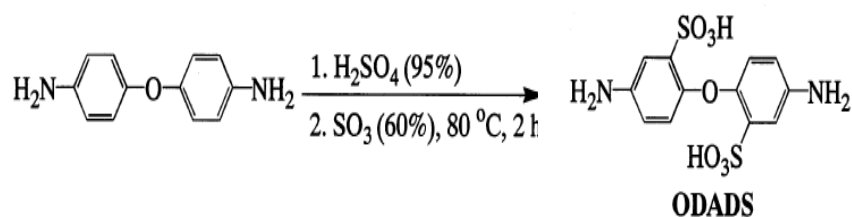


Figure 3.7 Synthesis of a sulfonated monomer, ODADS [65]

Proton conductivities of these polyimide membranes were strongly dependent on their IEC values and the relative humidities, i.e., membranes with higher IEC tended to have higher proton conductivity, and for the same polyimide membrane the proton conductivity increased with increasing the relative humidity. Furthermore, the ODADS-based polyimide membranes displayed similar proton conductivities but much better water stability than the corresponding BDSA-based ones, 2,2'-benzidinedisulfonic acid. This was because ODADS-based polyimide membranes had a more flexible structure than the BDSA-based ones.

Yan Yin *et al.* [66] successfully synthesized a novel sulfonated diamine monomer, 3-(2',4'-diaminophenoxy)propane sulfonic acid (DAPPS), and prepared the sulfonated polyimide (SPI) from 1,4,5,8-naphthalenetetracarboxylic dianhydride (NTDA) and DAPPS (shown in Figure 3.8). The resulting SPI, NTDA–DAPPS, was soluble in common organic solvents.

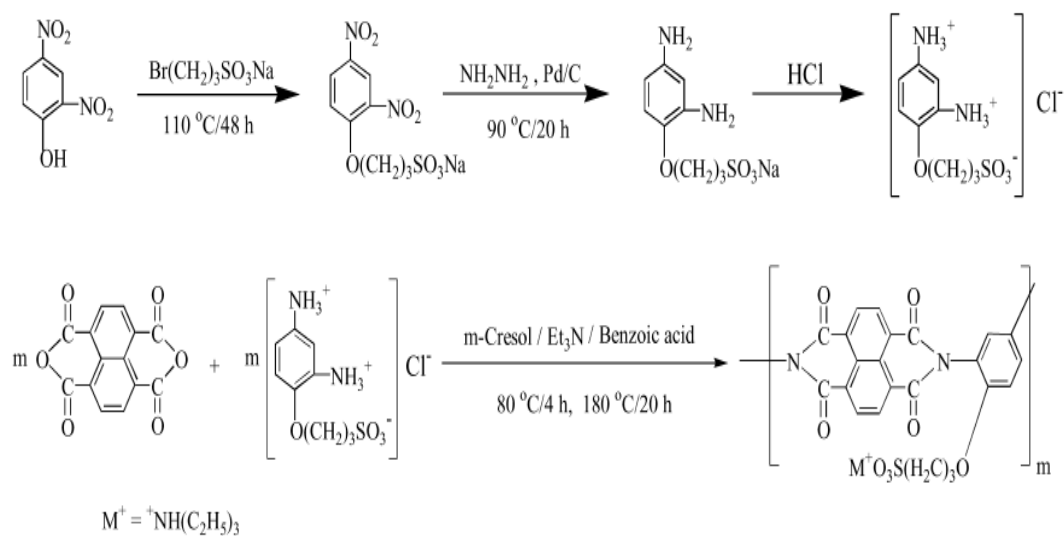


Figure 3.8 Synthesis of a sulfonated polyimide

The SPI membrane displayed proton conductivity σ values of 0.12–0.35 S/cm at temperatures ranging from 35 to 90 °C in liquid water. NTDA–DAPPS membrane displayed higher proton conductivities at higher WU levels. In the fully hydrated state, it displayed higher proton conductivities than Nafion 117, whereas in the range of lower WU it displayed much lower conductivities than Nafion 117 but larger ones than NTDA–ODADS/ODA (3/1). Furthermore, NTDA–DAPPS membrane exhibited much better water stability compared with ODADS and BAPFDS-based ones due to the high basicity of DAPPS resulting from the electron-donation effect of alkoxy group.

Feng Zhang *et al.* [67] successfully synthesized a novel locally and densely sulfonated dianhydride with four sulfonic acid groups, 1,6,7,12-tetra[4-(sulfonic acid)phenoxy]perylene-3,4,9,10-tetracarboxylic dianhydride (SPTDA), by direct sulfonation of the parent dianhydride, 1,6,7,12-tetraphenoxyperylene-3,4,9,10-tetracarboxylic dianhydride (PTDA) (shown in Figure 3.9).

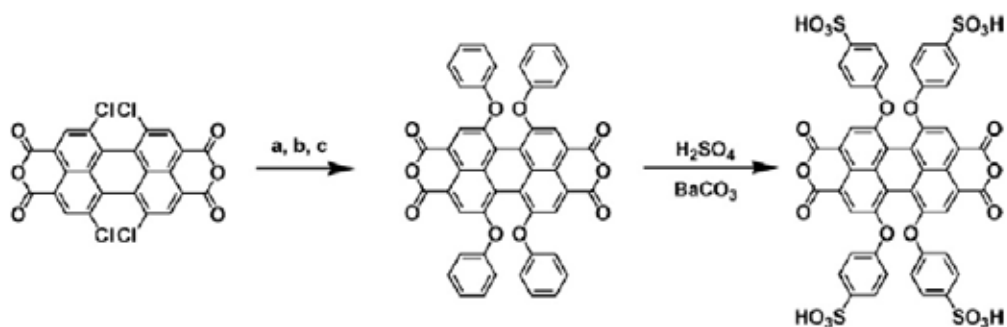


Figure 3.9 Synthesis of sulfonated perylene dianhydride compounds: (a) *n*-butylamine, propanol/water; (b) ArOH , K_2CO_3 ; (c) KOH , *t*-BuOH [67]

The synthesized copolymers, with the $-\text{SO}_3\text{H}$ group on the polymer side chain, possessed high molecular weights and high viscosities, and they formed tough, flexible membranes. The sulfonated polymers membranes in the dry state had tensile stresses of 41.2–112.1 MPa, Young's moduli of 0.46–1.10 GPa, and elongation-at-break values of 30.1–43.4%. In the wet state, the SPI membranes showed tensile stresses of 26.9–72.2 MPa, Young's moduli of 0.28–0.69 GPa, and elongation-at-break values of 32.6–56.2%. The SPI membranes exhibited proton conductivities in the range of 0.035–0.126 S/cm at 20°C. Moreover, the SPI membranes also exhibited excellent hydrolytic stability due to the introduction of pendant sulfophenoxy groups in the imide rings.

3.3 Conductivity enhancement of conducting polymers

Conventional transparent electrode materials are metal oxides, such as indium tin oxide (ITO). But these metal oxides have some problems in the optoelectronic application. One problem is the limitation of indium in earth. Hence, there is a strong demand for cheap and transparent thin films with high conductivity and high mechanical flexibility. Conducting polymers emerged as a promising material to replace ITO. Though conducting polymers have remarkably lower conductivity than ITO. This low conductivity badly affects their applications. Much effort has been made to improve the conductivity of conducting polymers. Here were some descriptions the literature reviews of the previous works related to ways to enhance the conductivity of conducting polymers.

Hoshina et al. [68] prepared nanosized conductive polypyrrole (PPy) powders using emulsion polymerization with aid of high-speed agitation. Different agitation speeds from 650 to 24,000 rpm were used with different anionic, cationic, and non-ionic surfactants. The chemical structures of surfactants were used in this work are shown in Figure 3.10. The effects of the agitation speed and surfactant species were examined in terms of their physical and electrical properties of conductivity and powder size. They have found that the combination of the anionic surfactants and high agitation in the emulsion polymerization could produce nanosized PPy powders with high conductivity.

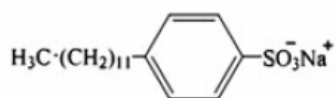
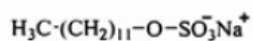
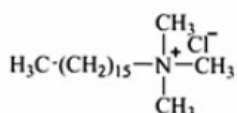
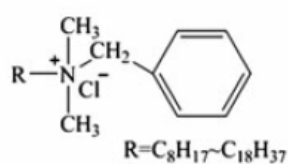
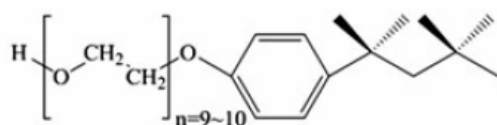
a. Anionic Surfactant**Sodium Dodecyl Benzene Sulfonate (SDBS)****Sodium Dodecyl Sulfate (SDS)****b. Cationic Surfactant****Cetyl Trimethyl Ammonium Chloride (CTAC)****Benzalkonium Chloride (BAC)****c. Non-ionic Surfactant****Polyethylene Glycol Mono-*p*-isooctylphenyl Ether (Triton X-100)****Figure 3.10 Chemical structures of surfactants [68]**

Table 3.3 presented some results obtained from the surfactants in the polymerization of PPy. A different surfactant was used in the polymerization with stirring at 650 rpm. It showed values of conductivity (S/cm) for the PPy pellet and the powder size distribution observed in water. The anionic surfactant systems showed a tendency to have higher conductivity relative to those of the reference. Regarding the increase in the concentrations in the SDBS and SDS systems, the observed conductivity was in range of about 5.9-33 and 4.5-26 S/cm, respectively, from 0.2 to 40 mmol. This phenomenon reflected that extending conjugate chains of the PPy was present and that a high degree of acceptor doping of a form of the DBS⁻ or DS⁻ ion was introduced electrostatically into the polymer powders.

Table 3.3 Polymerization yield, powder size distribution, and conductivity of PPy synthesis with or without each surfactant [68]

Surfactant	Type	Concentration (mmol)	Mole fraction (-)	Yield (%)	Powder size distribution (μm)	Conductivity (S/cm)
SDBS	Anionic	0	0	68	56–210	9.9×10^{-1}
		0.2	0.01	74	23–160	5.9×10^0
		2	0.12	117	12–80	3.0×10^1
		5	0.25	139	5–54	3.1×10^1
		20	0.57	147	1–8	3.3×10^1
SDS	Anionic	40	0.73	150	1–12	3.3×10^1
		0.2	0.01	71	32–167	4.5×10^0
		2	0.12	113	14–83	1.2×10^1
		5	0.25	134	8–50	2.2×10^1
		20	0.57	142	3–19	2.4×10^1
CTAC	Cationic	40	0.73	146	2–13	2.6×10^1
		0.2	0.01	61	45–173	7.9×10^{-1}
		2	0.12	60	36–87	6.3×10^{-1}
		5	0.25	55	30–81	5.1×10^{-1}
		20	0.57	37	5–45	3.3×10^{-1}
BAC	Cationic	40	0.73	35	4–40	2.7×10^{-1}
		0.2	0.01	49	57–187	5.8×10^{-1}
		2	0.12	40	53–155	4.7×10^{-1}
		5	0.25	36	45–135	3.9×10^{-1}
		20	0.57	29	23–76	1.7×10^{-1}
TritonX-100	Non-ionic	40	0.73	21	14–50	1.5×10^{-1}
		0.2	0.01	62	57–192	9.1×10^{-1}
		2	0.12	53	55–174	8.3×10^{-1}
		5	0.25	48	51–167	7.3×10^{-1}
		20	0.57	41	45–159	4.1×10^{-1}
		40	0.73	35	36–113	8.5×10^{-2}

Stirring was carried out at 650 rpm. Pyrrole and oxidant as FeCl_3 amount were 1.0 g (14.9 mmol) and 5.6 g (34.5 mmol) in 200 mL reaction volume. Polymerization was for 2 h and these resultant polymer powders were weighted for calculation of yield

Mole fraction = mole of surfactant/(mole of surfactant + mole of pyrrole)

Yield (%) = (g of PPy/g of pyrrole) \times 100, where g of PPy and g of pyrrole used weights of powder and monomer

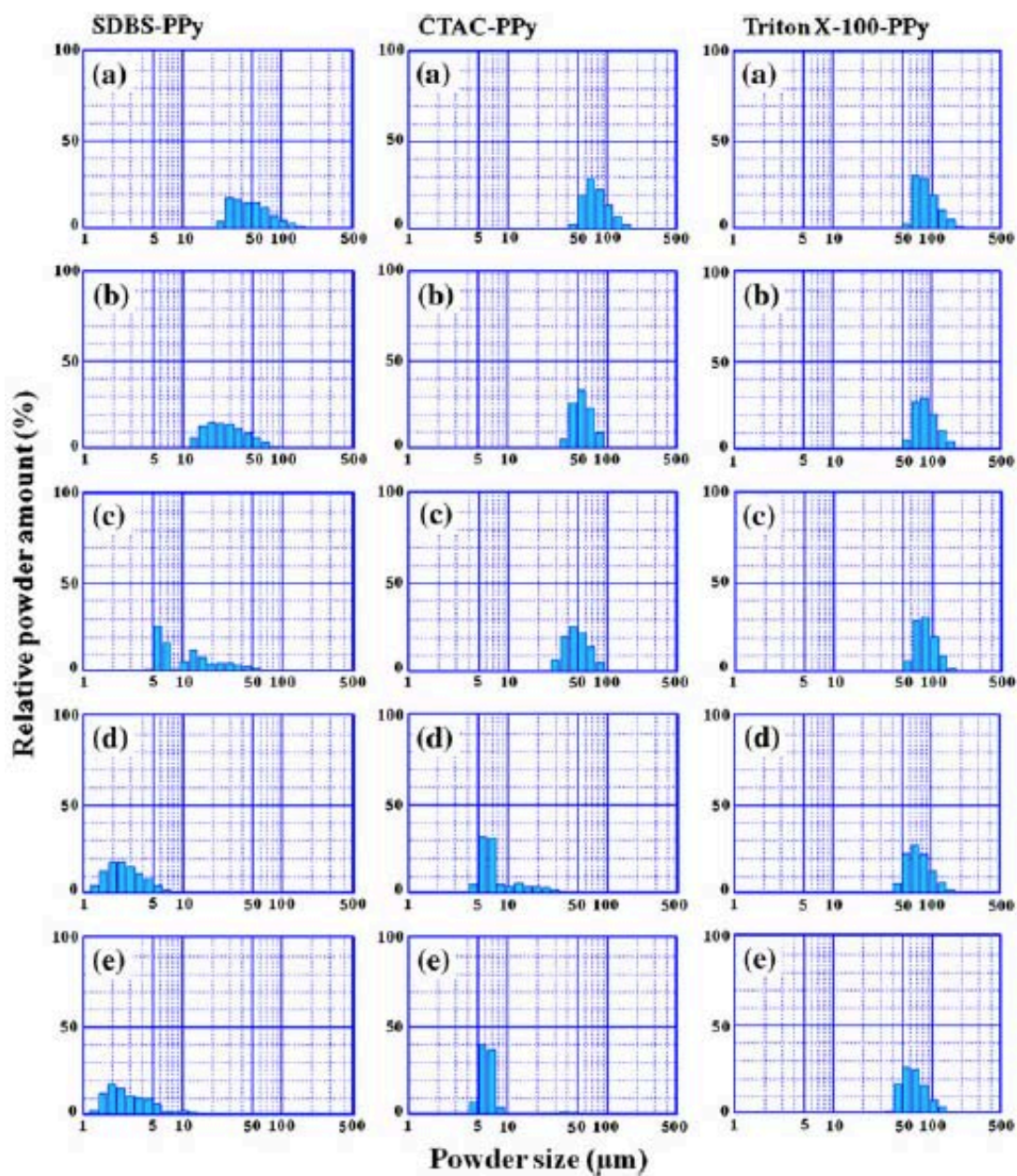


Figure 3.11 Powder size distribution of the PPY with SDBS, CTAC and Triton X-100 of a)

0.2 mmol, b) 2 mmol c) 5 mmol d) 20 mmol, and e) 40 mmol at 650 rpm [68]

Figure 3.11, the powder size distribution of the PPys was shifted to the smaller side when the anionic surfactant concentration increased. Especially, the PPY dispersion was effective

with less than 2 mmol contents. This was mainly because of the dopant of anionic species stabilizing the resultant PPy particles through the formation of the ionic complex.

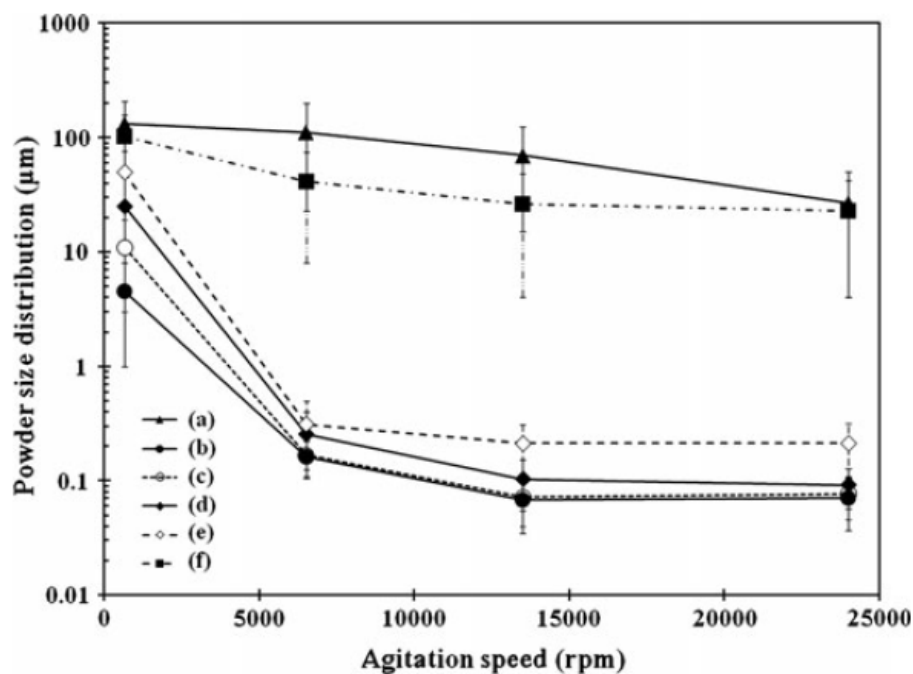


Figure 3.12 Agitation speed of polymerization and powder size distribution of the PPy prepared a) without surfactant and with b) SDBS c) SDS d) CTAC, and f) Triton X-100 by 20 mmol feed [68]

In the anionic surfactant systems, the powder size distribution was shifted to a smaller size of about 40-103 and 46-107 nm, because the respective speeds were 13,500 and 24,000 rpm. In contrast, the cationic system showed the lower effective than in the case of the anionic surfactant systems. The non-ionic surfactant system showed a somewhat larger powder diameter than that obtained using the anionic system. Therefore, these data showed clearly that the agitation speed was effective for the production of PPy nanosize powders (see Figure 3.12).

As shown in Figure 3.13, these results demonstrated that, at high agitation speed, the anionic surfactant could disperse the PPy well. At these conditions, the agitation speed enhanced

the production of nanosized PPy with good dispersion. Relative to cationic and non-ionic surfactants, the anionic surfactants were extremely effective for the dispersion, meaning that the dopant surfactant produced a bipolaron state, which then resulted in the high conductivity.

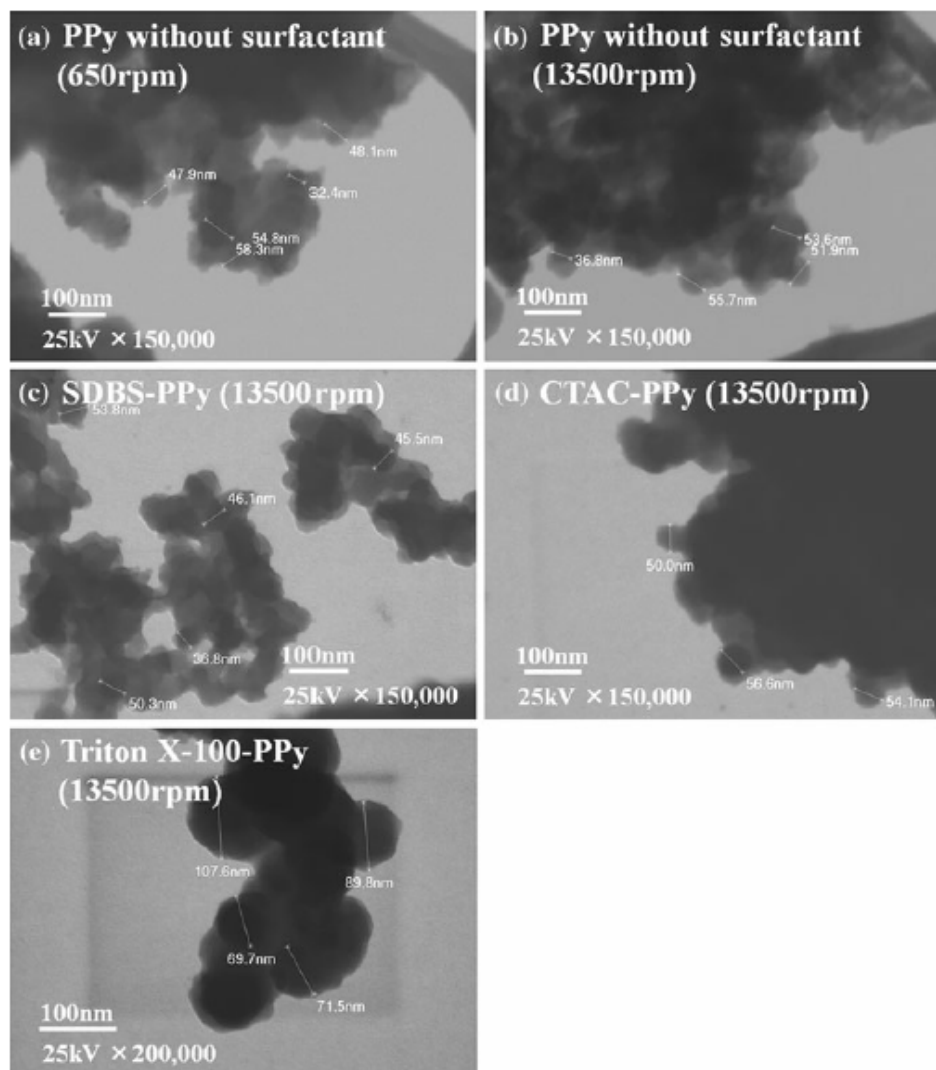


Figure 3.13 TEM images of the PPy without surfactant synthesized at a) 6,500 and b) 13,500 rpm and with c) SDBS, d) CTAC, and e) Triton X-100. Each surfactant was 20 mmol for the emulsion polymerization at 13,500 rpm [68]

Ouyang et al. [69] proposed the conductivity of the PEDOT:PSS film could be significantly enhanced by adding anionic surfactant into the PEDOT:PSS aqueous solution (see Figure 3.14). The conductivity enhancement was attributed to the effect of the anionic surfactant on the conformation of the conductive PEDOT chains. The PEDOT chain had to follow the structure of the PSS chain in water, giving rise to the distortion structure of the PEDOT chain. The anionic surfactant replaced PSS as the counteranions to PEDOT in water, so that the distortion structure of the PEDOT chain disappeared (see Figure 3.15). This conformational change in the PEDOT chain resulted into the significant enhancement in the conductivity of the PEDOT:PSS film. Cationic and non-ionic surfactants were also investigated as the additives into the PEDOT:PSS aqueous solution. It was found that the conductivity almost did not change when cationic and non-ionic surfactants were added.

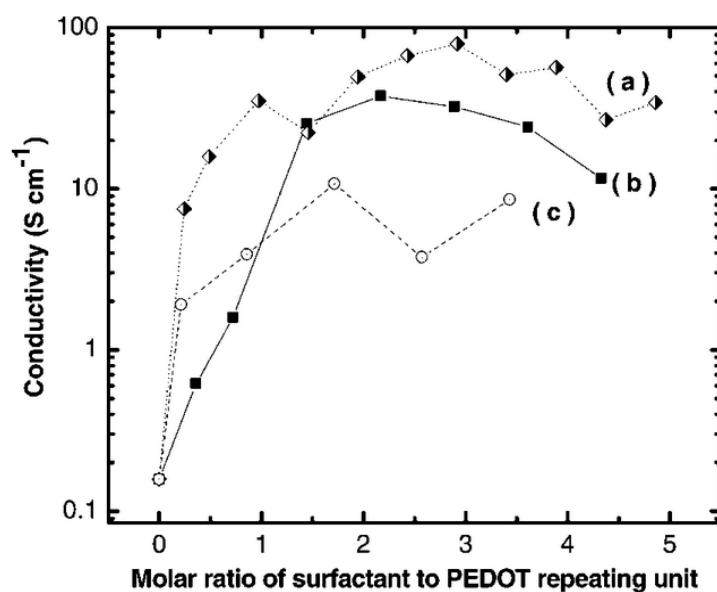


Figure 3.14 Variation of the conductivity of the PEDOT:PSS(surfactant) film. The additives are a) SDS, b) TsONa, and c) dodecylbenzenesulfonic acid sodium salt [69]

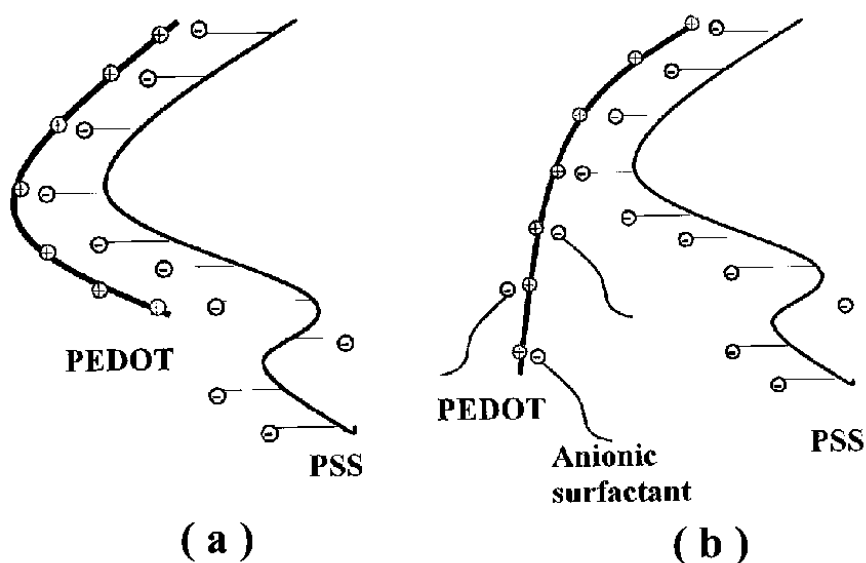


Figure 3.15 Schematic structure of a PEDOT segment and a PSS segment in water a) without and b) with the addition of anionic surfactant [69]

Ouyang et al. [70] developed two novel methods to significantly enhance the conductivity of the PEDOT:PSS films

One was to add anionic surfactant into the PEDOT:PSS aqueous solution. It was found that the conductivity enhancement depended on the concentration and the structure of the anionic surfactants. The used anionic surfactants in this work were shown in Figure 3.16. This method were reported by considering PEDOT:PSS as a polyelectrolyte of conjugated polycations (PEDOT) and non-conjugated polyanions (PSS). Figure 3.17 showed the effect on the conductivity of PEDOT:PSS was dependent on the structure of the surfactant. SDS, an anionic surfactant, could significantly enhance the conductivity of PEDOT:PSS. Significantly conductivity enhancement was also observed when other anionic surfactants, such as TsONa and SDBA, were used. When a non-ionic surfactant, such as POETE, was added, moderate conductivity enhanced was observed. However, the conductivity did not exhibit remarkable change when cationic surfactant, such as TOAB, was added.

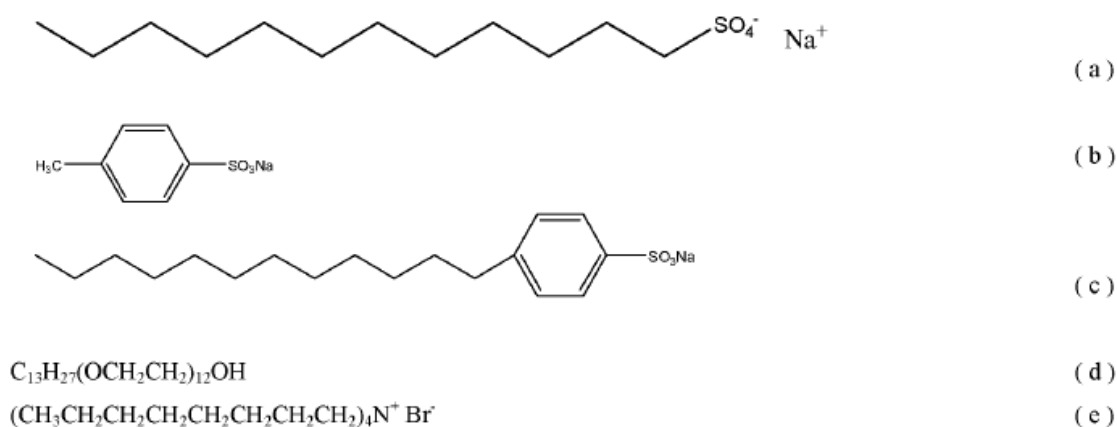


Figure 3.16 Chemical structure of surfactants a) sodium dodecyl sulfate (SDS), b) tosylate sodium (TsONa), c) sodium dodecylbenzenesulfonic acid (SDBA), d) polyoxyethylene(12) tridecyl ether (POETE), and e) (tetra-n-octylammonium bromide)(TOAB) [70]

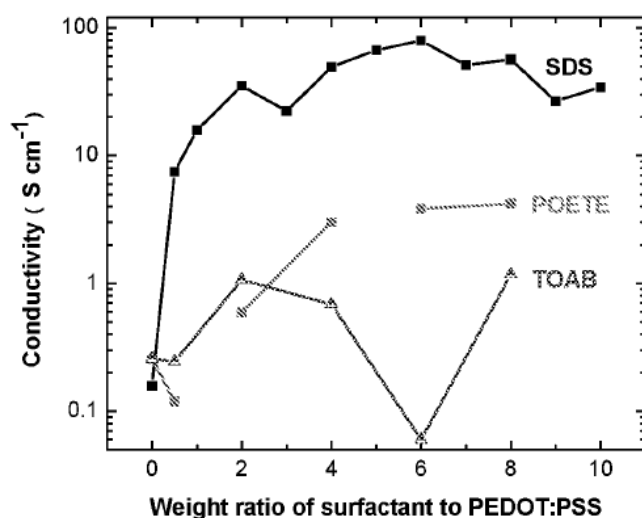


Figure 3.17 Variations of the conductivity of PEDOT:PSS with the weight ratio of added surfactants to PEDOT:PSS [70]

Method 2 was to treat the PEDOT:PSS films with solution of a certain salt, such as $CuCl_2$, $InCl_3$ and $NaCl$. It was well understood that salts could affect the Coulombic interaction between polycations and polyanions of polyelectrolytes. The change of of the Coulombic interaction would give rise to the conformational change of the polymer chains. Thus, it expected that salts can affect the PEDOT conformation as well, since PEDOT:PSS was also a

polyelectrolyte. Significant conductivity enhancement was observed for the PEDOT:PSS films treated with CuCl_2 or InCl_3 solution, and the conductivity was strongly dependent on the concentration of the salt. The salt-induced conductivity enhancement was attributed to the PSS loss from the PEDOT:PSS film and the conformation change of PEDOT. In contrast, the conductivity enhancement was negligible for the PEDOT:PSS film after treated with NaCl solution (see Figure 3.18).

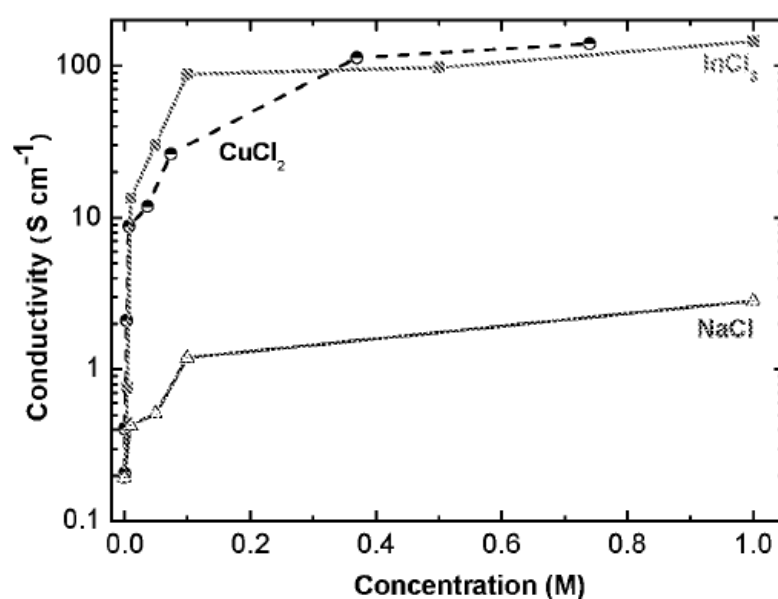


Figure 3.18 Variations of the conductivity of treated PEDOT:PSS films with InCl_3 , CuCl_2 , and NaCl concentrations in aqueous solutions [70]

Omastová et al. [71] synthesized conducting and stable polypyrrole (PPy) by chemical oxidation polymerization of Py in aqueous solution containing an oxidant, ferric sulfate, and a surfactant. Anionic surfactant, sodium dodecylbenzenesulfonate, was added into the solution during chemical oxidation polymerization of Py (see the chemical structure in Figure 3.19).

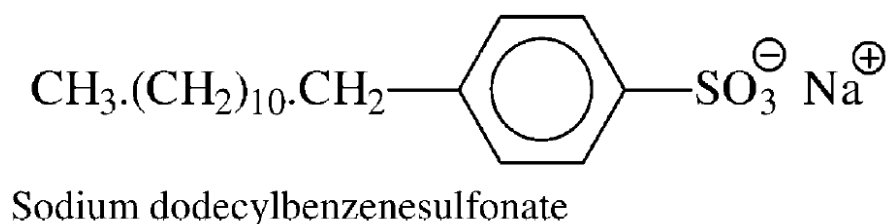


Figure 3.19 Chemical structure of sodium dodecylbenzenesulfonate (DBSNa) [71]

They found that the potential incorporation of a surfactant into a conducting polymer was likely to improve the electrical, thermooxidative, and hydrolytic stability due to the introduction of bulky hydrophobic component (see table 3.4 and Figure 3.20). The conductivity of all PPy samples prepared in the presence of anionic surfactants was higher than PPy-SO₄. PPy chains contain various types of structural disorders which considerable influenced the charge-carrier transport and finally the conductivity of the polymer. There was possibility to modify the parameters of the conducting network created from PPy chains, and chains regularity by the presence of anionic surfactants during polymerization. SEM micrograph of PPy-DBSNa (Figure 3.21) showed significantly smaller globules. It showed that the presence of the anionic surfactant in polymerization mixture strongly influenced the morphology of chemically prepared PPy.

Table 3.4 Conductivity of original PPy-sulfate and PPy-DBSNa samples [71]

Sample	σ (S cm ⁻¹)
PPy-SO ₄	0.24
PPy-DBSNa	3.13

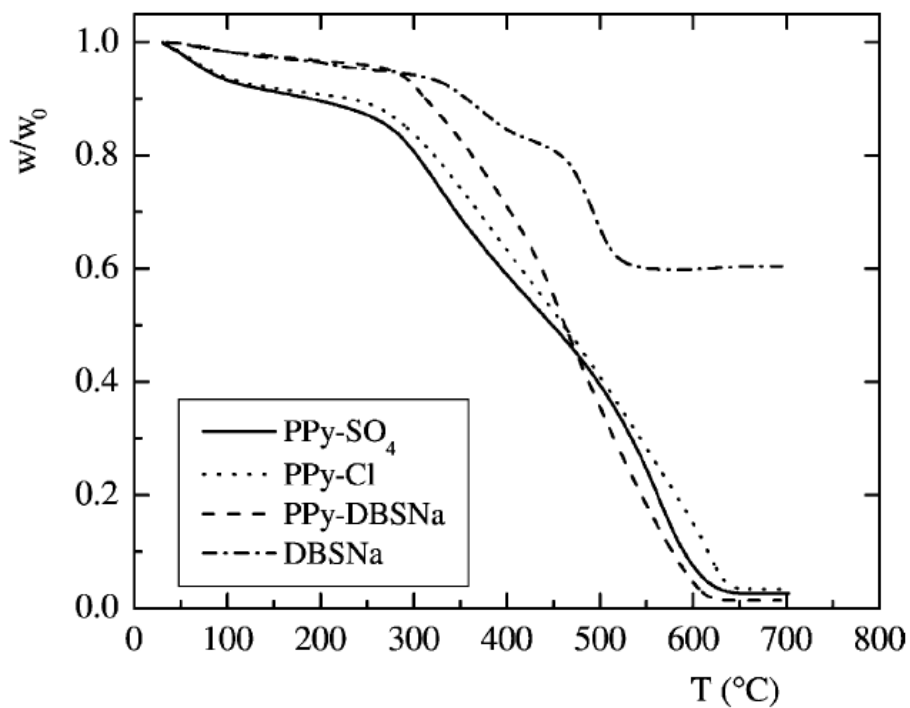


Figure 3.20 TGA curves of PPy-sulfate, PPy-chloride, PPy-DBSNa and curve of neat anionic surfactant DBSNa [71]

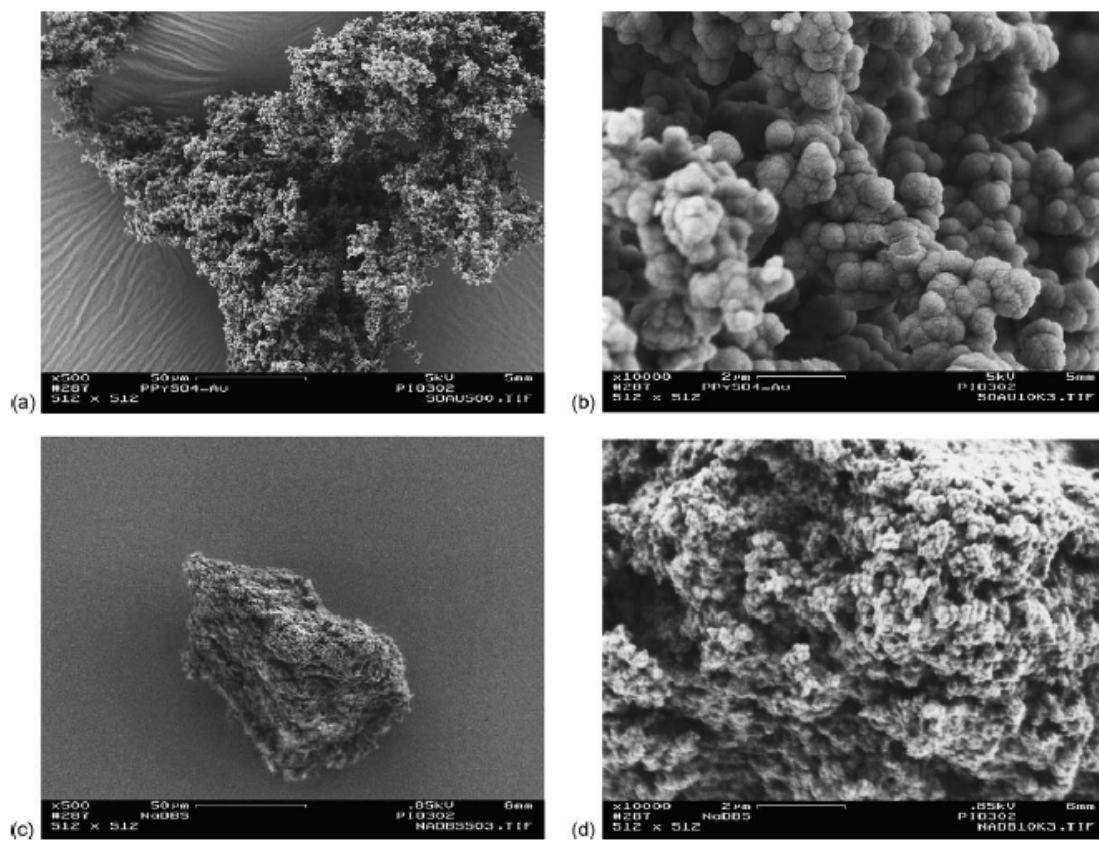


Figure 3.21 SEM micrograph of PPy-sulfate (a and b) and PPy prepared in the presence of anionic surfactant, DBSNa (c and d) [71]

CHAPTER IV

EXPERIMENT

Summarized here are the lists of materials, experimental procedure, techniques and instrumentation that were generally utilized in the subsequent parts, which are divided into three parts as follows:

- (i) Experimental observation on the mixing systems and ways to significantly enhance the conductivity of PEDOT:SPI aqueous dispersion;
- (ii) Effects of the addition of anionic surfactant during template polymerization of conducting polymers containing PEDOT with SPI and PSS as a template for nano-thin film applications;
- (iii) Synthesis and characterization of PEDOT/multi-sulfonated polyimide via template polymerization.

Furthermore, this chapter will provide the detail of characterization techniques such as FT-IR, TGA, NMR, TEM, GPC, Elemental analysis, Four-point probe method, Current generator and nanovoltmeter etc.

4.1 Materials and Chemicals

4.1.1 Experimental observation on the mixing systems and ways to significantly enhance the conductivity of PEDOT:SPI aqueous dispersion

1. 4,4'-diaminodiphenyl ether (4,4'-ODA) was purchased from Sigma-Aldrich.
2. 4,4'-oxydiphthalic anhydride (O-DPDA) was purchased from Sigma-Aldrich.
3. Triethylamine (Et₃N) was purchased from Sigma-Aldrich.
4. m-cresol was purchased from Sigma-Aldrich.

5. Fuming sulfuric acid (SO₃, 20%) was purchased from Sigma-Aldrich.
6. Poly(styrene sulfonic acid) (18 wt.% in water) was purchased from Sigma-Aldrich.
7. Iron (III) p-toluene sulfonate hexahydrate was purchased from Sigma- Aldrich.
8. 3,4-ethylenedioxythiophene (EDOT) was purchased from Sigma-Aldrich.
9. Lithium trifluoromethanesulfonate was purchased from Sigma-Aldrich.
10. 4,4'-Hexafluoroisopropylideneoxydiphthalic anhydride (6FDA) was purchased from TCI America.
11. Concentrated sulfuric acid (95%) was purchased from Fisher Scientific and was used as received.
12. Sodium hydroxide (NaOH) was purchased from Fisher Scientific and was used as received.
13. Hydrochloric acid (HCl) was purchased from Fisher Scientific and was used as received.
14. Acetone was purchased from Fisher Scientific and was used as received.
15. Ion-exchange resin DOWEX 50WX8 50-100 mesh was purchased from Acros Organics.
16. Dialysis tubes (Molecular weight cut off [MWCO] = 3.5 to 5 kDa) was purchased from Spectrum Laboratories Inc.
17. p-toluene sulfonate hexahydrate was purchased from Sigma-Aldrich.
18. Sodium dodecyl sulfate (SDS) was purchased from Sigma-Aldrich.
19. Glass beads (50-100 μm) were purchased from Polysciences, Inc.

4.1.2 Effects of the addition of anionic surfactant during template polymerization of conducting polymers containing PEDOT with SPI and PSS as a template for nano-thin film applications

1. 4,4'-diaminodiphenyl ether (4,4'-ODA) was purchased from Sigma-Aldrich.
2. 4,4'-oxydiphthalic anhydride (O-DPDA) was purchased from Sigma-Aldrich.
3. Triethylamine (Et₃N) was purchased from Sigma-Aldrich.
4. m-cresol was purchased from Sigma-Aldrich.
5. Fuming sulfuric acid (SO₃, 20%) was purchased from Sigma-Aldrich.
6. Poly (styrene sulfonic acid) (18 wt.% in water) was purchased from Sigma-Aldrich.
7. Iron (III) p-toluene sulfonate hexahydrate was purchased from Sigma-Aldrich.
8. 3,4-ethylenedioxythiophene (EDOT) was purchased from Sigma-Aldrich and distilled before using.
9. Lithium trifluoromethanesulfonate was purchased from Sigma-Aldrich.
10. 4,4'-Hexafluoroisopropylideneoxydiphthalic anhydride (6FDA) was purchased from TCI America.
11. Concentrated sulfuric acid (95%) was purchased from Fisher Scientific and was used as received.
12. Sodium hydroxide (NaOH) was purchased from Fisher Scientific and was used as received.
13. Hydrochloric acid (HCl) was purchased from Fisher Scientific and was used as received.
14. Acetone was purchased from Fisher Scientific and was used as received.
15. Ion-exchange resin DOWEX 50WX8 50-100 mesh was purchased from Acros Organics.
16. Dialysis tubes (Molecular weight cut off [MWCO] = 3.5 to 5 kDa) was purchased from Spectrum Laboratories Inc.

17. p-toluene sulfonate hexahydrate was purchased from Sigma-Aldrich.
18. Sodium dodecyl sulfate (SDS) was purchased from Sigma-Aldrich.
19. Glass beads (50-100 μm) were purchased from Polysciences, Inc.

4.1.3 Synthesis and characterization of PEDOT/multi-sulfonated polyimide via template polymerization

1. 4,4'-diaminooctafluorobiphenyl was purchased from TCI America.
2. 4,4'-hexafluoroisopropylideneoxydiphthalic anhydride (6FDA) was purchased from TCI America.
3. 2-phenylphenol was purchased from Sigma-Aldrich.
4. Potassium carbonate (K_2CO_3) was purchased from Sigma-Aldrich and dried before using.
5. 1,3-dimethyl-2-imidazolidinone (DMI) was purchased from Sigma-Aldrich.
6. 4,4'-oxydiphthalic anhydride (O-DPDA) was purchased from Sigma-Aldrich.
7. Toluene was purchased from Merck KGaA Germany.
8. Sodium hydroxide (NaOH) purchased from Merck KGaA Germany
9. Concentrated sulfuric acid (95%) purchased from Aldrich chemical Company, Inc.
10. Hydrochloric acid (HCl) purchased from Aldrich chemical Company, Inc.
11. N-Methyl-2-pyrrolidinone (NMP) purchased from Aldrich chemical Company, Inc.
12. Iron (III) p-toluene sulfonate hexahydrate purchased from Aldrich chemical Company, Inc
13. 3,4-ethylenedioxythiophene (EDOT) purchased from Aldrich chemical Company, Inc

14. Triethylamine (Et_3N) was purchased from Sigma-Aldrich.
15. Fuming sulfuric acid (SO_3 , 20%) was purchased from Sigma-Aldrich.
16. Lithium trifluoromethanesulfonate was purchased from Sigma-Aldrich.
17. Acetone was purchased from Fisher Scientific.
18. Ion-exchange resin DOWEX 50WX8 50-100 mesh was purchased from Acros Organics.

4.2 Equipment

4.2.1 Experimental observation on the mixing systems and ways to significantly enhance the conductivity of PEDOT:SPI aqueous dispersion

1. **Schlenk line** included of vacuum line connected to vacuum pump and argon line for purging when reagents are transferred. The schlenk line was shown in Figure 4.1.

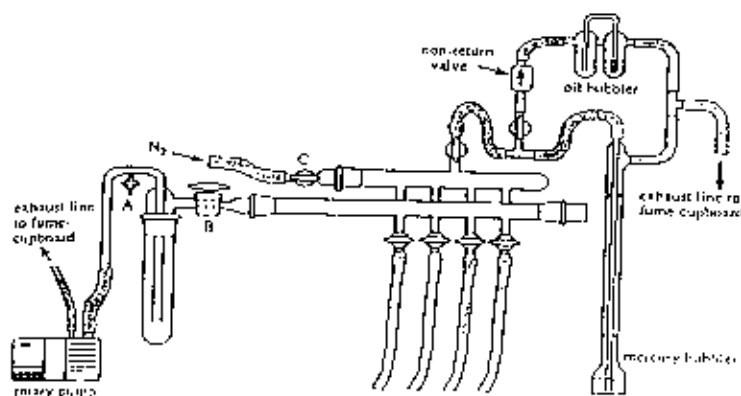


Figure 4.1 Schlenk line.

2. **The inert gas** (argon) from the cylinders was passed through columns of oxygen trap (BASF catalyst, R3-11G), moisture trap (molecular sieve), sodium hydroxide (NaOH) and phosphorus pentaoxide (P_2O_5) in order to purifying the argon gas to obtain ultra high purity argon

which was used in Schlenk line and solvent distillation column. The inert gas supply system can be shown in Figure 4.2.

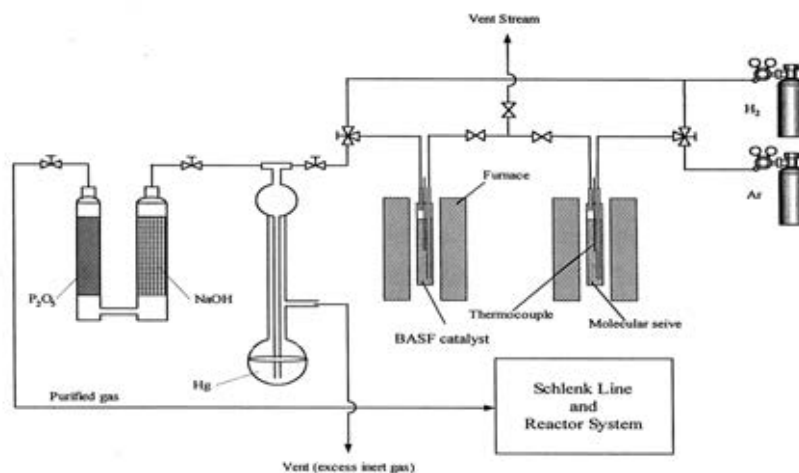


Figure 4.2 Inert gas supply system

3. **The vacuum pump** model 195 from Labconco Corporation was used. The produced low pressure of 10^{-1} to 10^{-3} mmHg was adequate for utilizing as the vacuum supply to the vacuum line of the Schlenk line. The vacuum pump is shown in Figure 4.3.

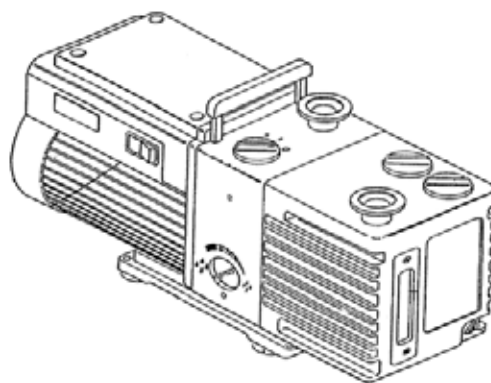


Figure 4.3 Vacuum pump.

4. Magnetic Stirrer and Hot Plate

The magnetic stirrer and hot plate model RCT basic from IKA Labortechnik were used.



Figure 4.4 Magnetic stirrers and Hot Plate

5. Cooling System

The cooling system in the solvent distillation is needed in order to prevent the freshly evaporated solvent from the reactor during the synthesis.

6. Temperature controlled oven

A Carbolite LHT5/30 (201) Temperature controlled oven was utilized in these experiments. The maximum working temperature of this machine is 500°C. The equipment was used for thermal treated the film polyimide.

7. High-speed mechanical mixer

The colloidal dispersions of conducting polymers in water were obtained using high-speed mechanical mixer with a Constant-Torque Digital Brushless mixers with a speed range of 40-6000 rpm manufactured by Cole-Parmer. A picture of the mixer and the stir shaft are shown in Figure 4.5 and 4.6, respectively.



Figure 4.5 A high-speed mechanical mixer

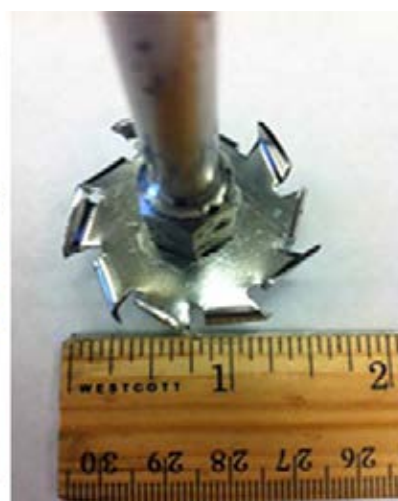


Figure 4.6 A stir shaft used with the mechanical stirrer

4.2.2 Effects of the addition of anionic surfactant during template polymerization of conducting polymers containing PEDOT with SPI and PSS a template for nano-thin film applications

(All equipment using in this part of work are the same as those of section 4.2.1)

4.2.3 Synthesis and characterization of PEDOT/multi-sulfonated polyimide via template polymerization

1. Synthesized reactor

The polymerization reactor was a 100 ml. three-neck flask. The reactor was equipped with several fittings for injecting the chemicals and purging with argon gas. A three-necked, round bottom flask equipped with an argon inlet, a thermometer, a magnetic stir bar and a condenser with a Dean-stark trap, was used as the reaction vessel which can be shown in Figure 4.6.

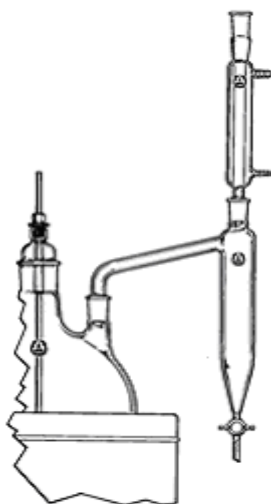


Figure 4.7 Reactor

2. Rotary Evaporator

Rotary Evaporator is used for the efficient and gently removal of solvents from samples by evaporation.



Figure 4.8 Rotary evaporator

4.3 Experiment Procedures

4.3.1 Experimental observation on the mixing systems and ways to

significantly enhance the conductivity of PEDOT:SPI aqueous dispersion

4.3.1.1 Synthesis of 4,4'-diaminodiphenyl ether-2, 2'-disulfonic acid (4,4'-ODADS)

[51]

To a 100 mL three-neck flask with a stirring device was added 5.00 g (25.0 mmol) of 4,4'-diaminodiphenyl ether (4,4'-ODA). The flask was cooled in an ice bath, and then 5 mL of concentrated (95%) sulfuric acid was slowly added with stirring. After 4,4'-ODA was completely dissolved, 27 mL of fuming (SO₃ 20%) sulfuric acid was slowly added to the flask. The reaction mixture was stirred at 0°C for 2 h and then slowly heated to 80°C and kept at this temperature for an additional 4 h. After cooling to room temperature, the slurry solution mixture was carefully poured onto 20 g of crushed ice. The resulting white precipitate was filtered off and then re-dissolved in a sodium hydroxide solution. The basic solution was filtered, and the filtrate was acidified with concentrated hydrochloric acid. The solid was filtered off, washed with water and methanol successively, and dried at 80°C in vacuum oven overnight.

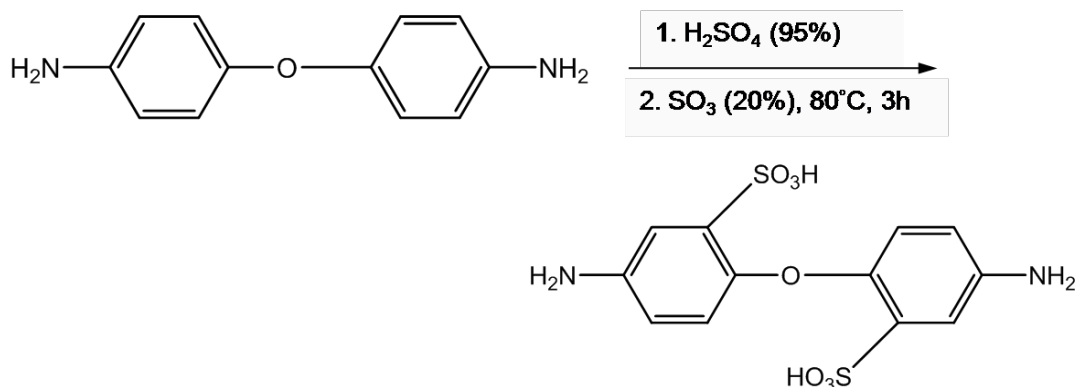


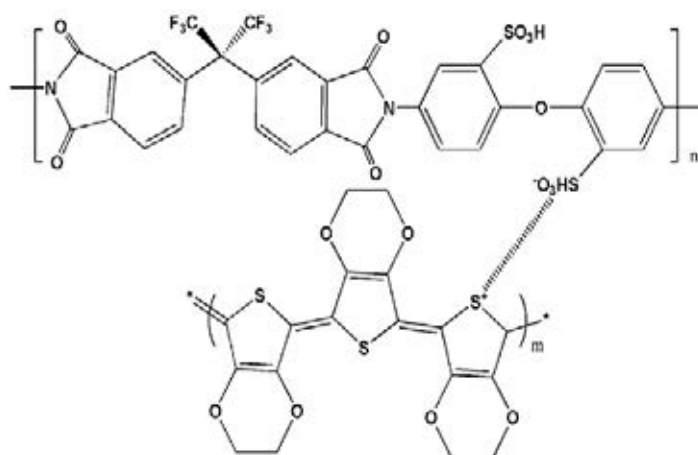
Figure 4.9 Scheme for the 4,4'-ODADS reaction

4.3.1.2 Synthesis of sulfonated poly(imide)s (SPI-6FDA), (SPI-O-DPDA)

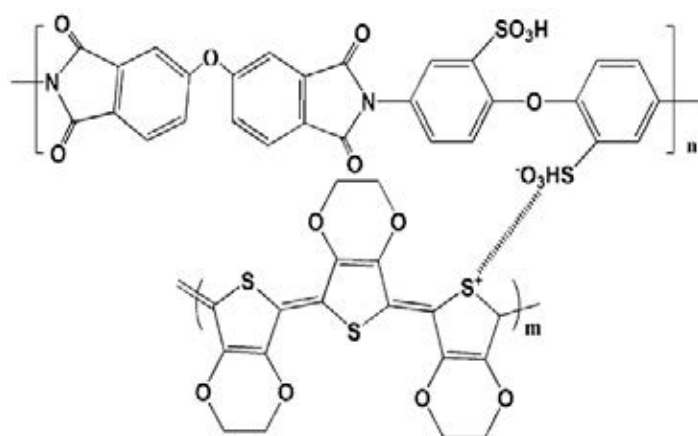
To a 100 mL three-neck flask with an argon inlet and outlet was added 3.5 g (9.71 mmol) of 4,4'-ODADS, 50 mL of m-cresol, and 2.359 g (9.71 mmol) of triethylamine. After 4,4'-ODADS was completely dissolved, 3.013 g (9.71 mmol) of O-DPDA/4.315 g (9.71 mmol) of 6FDA) was added and then the solution was stirred under an argon atmosphere at room temperature for 24 h. When the reactions were complete, the poly(amic acid) solution was cast onto glass dishes and was thermally treated at 70 °C, 150 °C for 1 h each, and 250 °C for another 1 h in a temperature controlled oven.

Ion Exchange

The SPI film in salt form dissolved in DI water was changed to the acid form by reaction with an ion exchange resin of strong acid type DOWEX 50WX8 (cation exchange) in case of utilizing for polymerization with 3,4-ethylenedioxythiophene and pyrrole. The SPIs salt form was stirred in DI water with the selective ion exchange resin for 1 h to convert them to the free acid form (H^+). They were then centrifuged to separate ion exchange resin off from the poly(imide) solution and then evaporated at 100 °C to obtain the poly(imide) acid form as templates for conducting polymer polymerizations.



(a) PEDOT-SPI (6FDA)



(b) PEDOT-SPI (O-DPDA)

Figure 4.10 Chemical structures of PEDOT:SPI [52]

4.3.1.3 Template polymerization of EDOT and sulfonated poly(imide):PEDOT-SPI (6FDA), PEDOT-SPI (O-DPDA)

1. Magnetic stirring system

After an ion exchange and adjusting the mass to 150 g by adding the appropriate amount of DI water, the obtained SPI acid forms were added to a 500 mL Pyrex bottle with a magnetic stirrer bar and stirring device. 0.3195 g (2.25 mmol) of EDOT was then added to the solution. The ratio of EDOT to SPI is 1:2.5 by weight. To this suspension 1.626 g (2.4 mmol) of iron (III) p-toluene sulfonate hexahydrate was added for polymerization. Finally, 10 g of glass beads were added, and the mixture was stirred vigorously at about 1000 rpm for 3 days at room temperature for both of PEDOT-SPI (6-FDA) and PEDOT-SPI (O-DPDA) leading to dark blue dispersions, which were then purified according to literature procedure [51].

2. High-speed mechanical stirring system

After an ion exchange and adjusting the mass to 150 g by adding the appropriate amount of DI water, the obtained SPI acid forms were added to a 1000 mL LDPE bottle equipped with a high speed mechanical stirrer (Fig. 1). 0.3195 g (2.25 mmol) of EDOT was then added to the solution. The ratio of EDOT to SPI is 1:2.5 by weight. To this suspension 1.626 g (2.4 mmol) of iron (III) p-toluene sulfonate hexahydrate was added for polymerization. Finally, 10 g of glass beads were added, and the mixture was stirred vigorously at 1000/4000 rpm at room temperature for both of PEDOT-SPI (6-FDA) and PEDOT-SPI (O-DPDA) leading to dark blue dispersion, which were then purified according to literature procedure [51].

4.3.1.4 Addition of anionic surfactants to improve the conductivity of PEDOT-SPI films

The anionic surfactant, sodium dodecyl sulfonate (SDS), was added at various amounts (0.1, 0.5, 1, 3 and 5 %wt) to the PEDOT-SPI (6-FDA) and PEDOT-SPI (O-DPDA) aqueous solutions, and the solutions were vigorously stirred overnight.

4.3.1.5 Preparation of PEDOT with SPI (6FDA) and SPI (O-DPDA) films

Films were prepared by drop coating onto glass substrates, which had been sonicated in soapy water, DI water, acetone and IPA for 15 min each before use as substrates. The films were left at room temperature over a period of 24 h for slow evaporation then annealed at 110 °C for 30 min to improve conductivities with thermal treatment. Separate films of each material were evaluated for conductivity at room temperature after annealing.

4.3.2 Effects of the addition of anionic surfactant during template polymerization of conducting polymers containing PEDOT with SPI and PSS a template for nano-thin film applications

4.3.2.1 Synthesis of sulfonated poly (imide) (SPI)

(Details in 4.3.1.2)

4.3.2.2 Preparation of PEDOT-PSS and PEDOT-SPI nanoparticle containing anionic surfactant (SDS)

1. Method 1: addition of SDS during template polymerization system

- (a) Template polymerization of EDOT with poly(styrenesulfonic acid) template (PEDOT-PSS):**

To a 1000 mL LDPE bottle equipped with a mechanical shear stirrer, 0.3195 g (2.25 mmol) of EDOT and 4.346 g of 18 wt% PSSA aqueous solutions were added. During polymerization step, 5 wt% of SDS was then slowly added. To this suspension 1.626 g (2.4 mmol) of iron (III) p-toluene sulfonate hexahydrate was added. The total mass of all the reactants was adjusted to 150 g by adding an appropriate amount of de-ionized water. The reaction was added with glass beads 10 g and stirred vigorously at 4000 rpm at room temperature leading to a dark blue dispersion.

(b) Template polymerization of EDOT with sulfonated polyimide template (PEDOT-SPI):

After an ion exchanging and the mass adjusting to 150 g by adding appropriate amount of DI water, the obtained SPI acid forms were added to a 1000 mL LDPE bottle equipped with a mechanical shear stirrer. 0.3195 g (2.25 mmol) of EDOT was then added to the solution. The ratio of EDOT to SPI was 1:2.5 by weight. To this suspension 5 wt% of SDS was added during polymerization step. 1.626 g (2.4 mmol) of iron (III) p-toluene sulfonate hexahydrate was then added into the solution. Finally, 10 g of glass beads were added and the mixture was stirred vigorously at 4000 rpm at room temperature leading to dark blue dispersion.

2. Method 2: addition of SDS after template polymerization system

5 wt% of SDS was added into the PEDOT-PSS and PEDOT-SPI aqueous solution, and the solution was vigorously stirred overnight.

3. Method 3: addition of SDS both during and after template polymerization system

In this method, 5 wt% of SDS was separately added during polymerization (the same way as the method 1) and was then added after template polymerization was finished (the same way as the method 2).

4.3.2.3 Preparation of PEDOT-PSS and PEDOT-SPI films

Films were prepared by drop coating onto glass substrates, which had been sonicated in soapy water, DI water, acetone and IPA for 15 min each before use as substrates. The films were left at room temperature over a period of 24 h for slow evaporation then annealed at 110 °C for 30 min to improve conductivities with thermal treatment. Separate films of each material were evaluated for conductivity at room temperature after annealing.

4.3.3 Synthesis and characterization of PEDOT/multi-sulfonated polyimide via template polymerization

4.3.3.1 Synthesis of diamine

4,4'-diaminooctafluorobiphenyl (1.456 g, 4 mmol), 2-phenylphenol (8.170 g, 48 mmol), and potassium carbonate (6.638 g, 48 mmole) were charged to a round bottomed flask equipped with a Dean-Stark trap. 30 mL of 1,3-dimethyl-2-imidazolidinone and 15 mL of toluene were then added into the flask under argon. The reaction mixture was stirred at 150 °C for about 6 h until about 5 mL of water had distilled off azeotropically via a Dean-Stark trap. After complete removal of water, the residual toluene was distilled off under reduced pressure, next, the reaction temperature was increased to 220 °C, and the reaction was continued for 72 h. The resulting solid was collected by filtration and purified by column chromatography on a silica gel (dichloromethane) to yield a brown powder. The yield was 4.1364 g (67.59%).

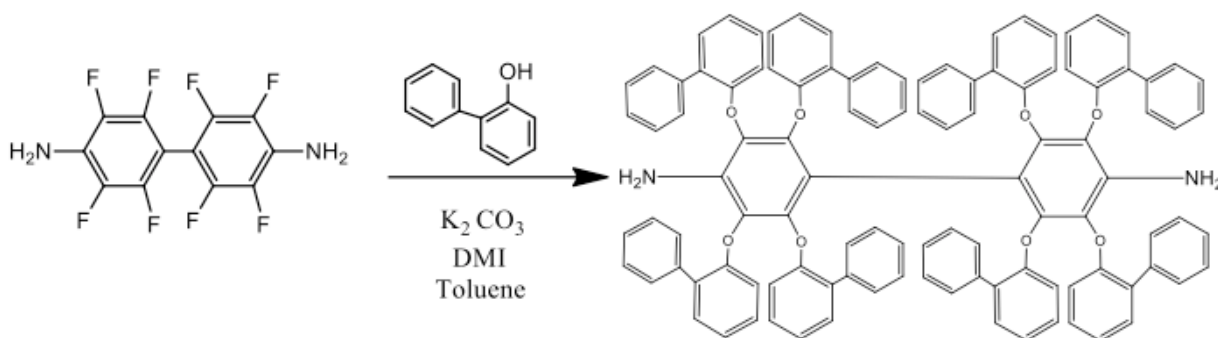


Figure 4.11 Synthesis of diamine

4.3.3.2 Synthesis of multi-sulfonated diamine

To a three-neck flask with stirring device was added synthesized diamine (1.5 g, 0.98 mmol), and concentrated sulfuric acid (95%) (6 mL) was slowly added to the flask. 32.4 mL of fuming (SO_3 20%) sulfuric acid was slowly added to the flask. The reaction mixture was stirred at $0^\circ C$ for 4 h and then slowly heated to $80^\circ C$ and kept at this temperature for an additional 8 h. After that, the solution mixture was carefully poured into crush ice for stop reaction of sulfonation. Then, sodium hydroxide solution dropped into solution mixture in order to adjust pH of solution mixture at $pH \sim 3$. The solution mixture was dried at $80^\circ C$ in oven overnight. The resulting sulfonated diamine was obtained.

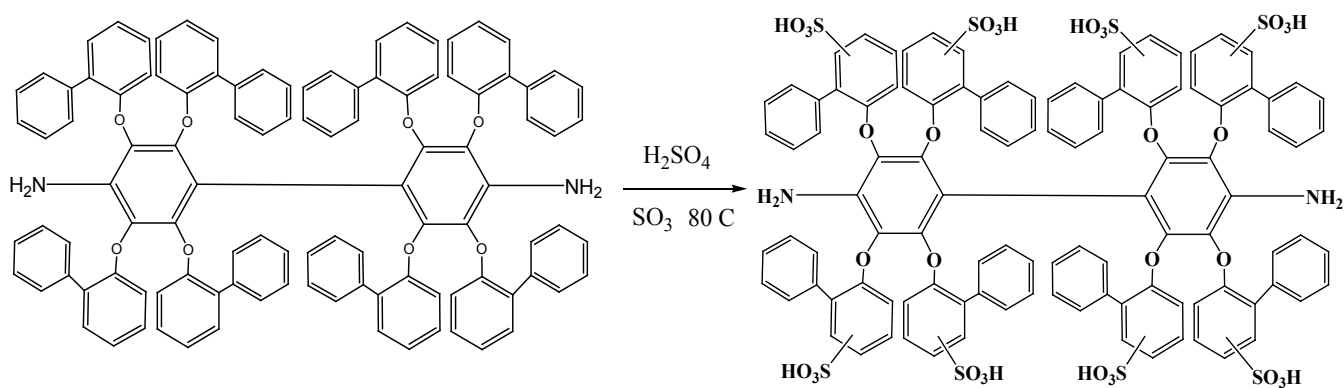


Figure 4.12 Synthesis of multi-sulfonated diamine

4.3.3.3 Preparation of polyimide films

To a 100 mL three-neck flask with argon inlet and outlet were added 1 g (0.348 mmol) of synthesized diamine, 6 mL of m-cresol, and 0.36 g (0.348 mmol) of triethylamine. After synthesized diamine was completely dissolved, 0.1546 g (0.348 mmol) of ODPDA was added and then the solution was stirred under an argon atmosphere at room temperature for 24 h. When the reaction was complete, the poly(amic acid) solution was cast onto glass dishes and was thermally treated at 70 °C, and 150 °C for 1 h each, and 250 °C for an additional hour.

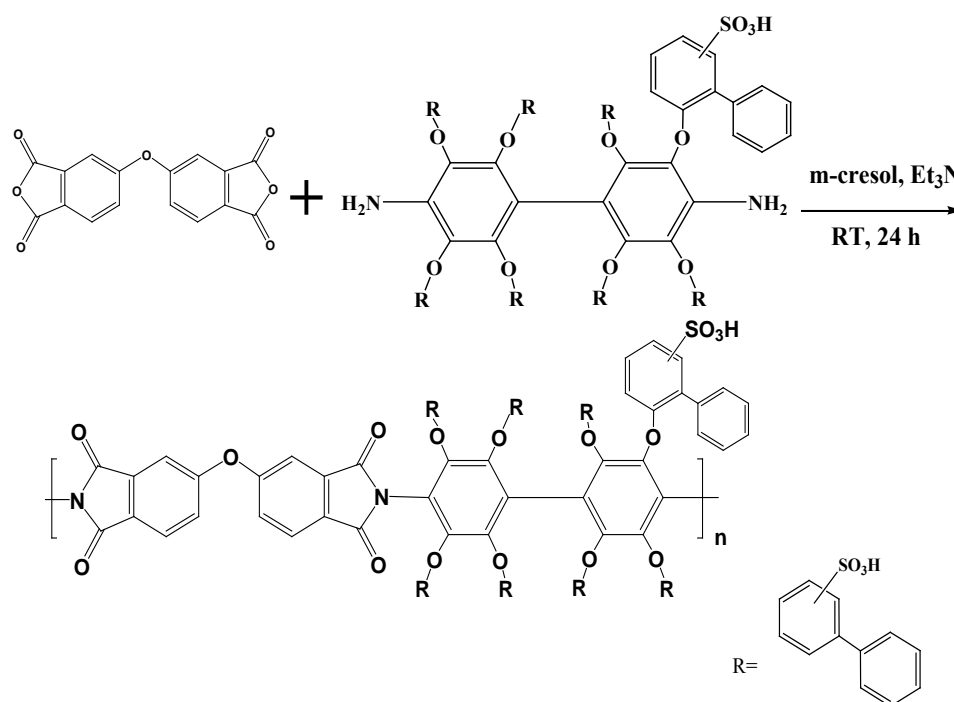


Figure 4.13 Synthesis of sulfonated polyimide using a novel synthesized diamine

4.3.3.4 Template polymerization of EDOT and synthesized sulfonated polyimide (PEDOT-SPI)

To a one-neck flask, 1.98 g (0.6 mmol) of SPI was dissolved with de-ionized water. Then 0.0426 g (0.3 mmol) of EDOT and 0.203 g (0.3 mmol) of iron(III) p-toluene

sulfonate hexahydrate were added. The reaction mixture was stirred vigorously for 5 days at room temperature leading to a dark blue dispersion.

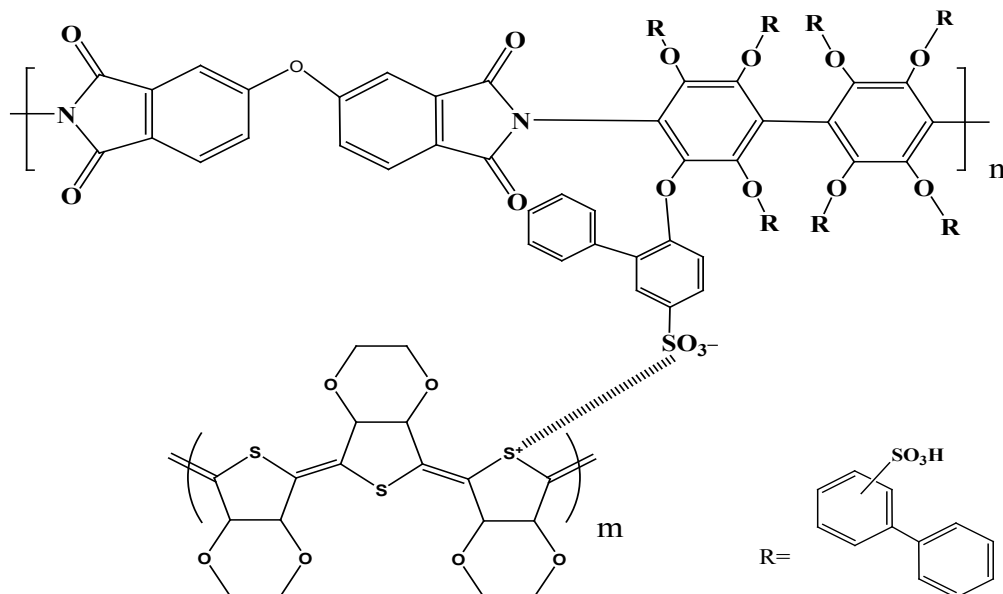


Figure 4.14 Chemical structure of PEDOT-SPI

4.4 Characterization Instrument

4.4.1 Infrared Spectroscopy (FTIR)

- Institute of Materials Science and the Polymer Program at the University of Connecticut, USA.

Fourier transform infrared spectroscopy (FTIR) was performed using a MAGNA-IR560. Spectra was taken on ground powder in a KBr matrix with a scanning range of $500 - 4000 \text{ cm}^{-1}$, 64 scans at a resolution of 4 cm^{-1} .

- Center of Excellence on Catalysis and Catalytic Reaction Engineering.

Infrared survey spectra were recorded with Nicolet 6700 FTIR spectrometer. The scanning ranged from 400 to 4000 cm^{-1} with scanning 64 times.



Figure 4.15 Fourier transform infrared spectroscopy (FT-IR) Equipment.

4.4.2 Thermogravimetric analysis (TGA)

- Institute of Materials Science and the Polymer Program at the University of Connecticut, USA.

Thermogravimetric Analysis (TGA) was performed by a Perkin-Elmer TGA 7 series analysis system at a heating rate of $20^{\circ}\text{C}/\text{min}$ under air at a flow rate of 60 mL/min.

- Center of Excellence on Catalysis and Catalytic Reaction Engineering.

Thermogravimetric analysis (TGA) was performed by a SDT Analyzer Model Q600 from TA Instruments, USA. The sample weights were 3-10 mg. and the temperature range of $30-700^{\circ}\text{C}$ at a heating rate of $20^{\circ}\text{C}/\text{min}$ under air at a flow rate of 400 mL/min.



Figure 4.16 Thermogravimetric analysis (TGA) Equipment

4.4.3 Gel Permeation Chromatography (GPC)

- Institute of Materials Science and the Polymer Program at the University of Connecticut, USA.

Gel Permeation Chromatography (GPC) was done using a millipore model 150-C GPC system; DMAC was used as the mobile phase. The results were calibrated by standards of poly(methyl methacrylate).

4.4.4 Nuclear Magnetic Resonance (NMR)

- Institute of Materials Science and the Polymer Program at the University of Connecticut, USA.

Nuclear Magnetic Resonance (NMR) ^1H NMR spectra were recorded on a Bruker DMX-500 NMR Spectrometer.

- Center of Excellence on Catalysis and Catalytic Reaction Engineering.

Nuclear Magnetic Resonance (NMR) ^1H NMR spectra were recorded by Bruker Biospin DPX400 NMR spectrometer (Switzerland) operating at 400 MHz with deuterated dimethyl sulfoxide ($\text{DMSO-}d_6$).



Figure 4.17 Nuclear Magnetic Resonance Spectrometers

4.4.5 Conductivity

- Institute of Materials Science and the Polymer Program at the University of Connecticut, USA.

Conductivities were measured using a four-line collinear array utilizing a Keithley Instruments 224 constant current source and a 2700 Multimeter. The polymer was coated on the glass substrate having four gold-coated leads on the surface across the entire width of the polymer and 0.25 cm apart from each other. The current was applied across the outer leads and voltage was measured across the inner leads.

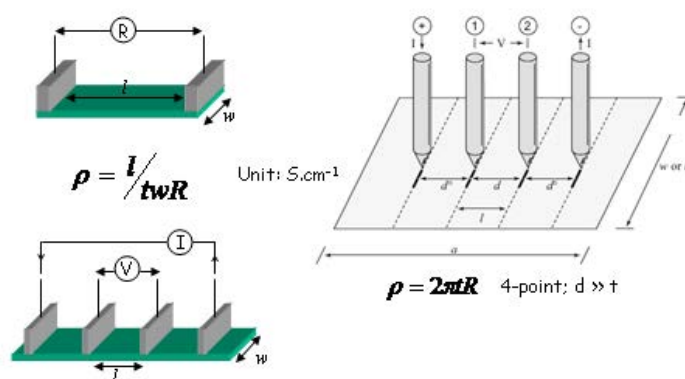


Figure 4.18 a four-point-probe conductivity cell.

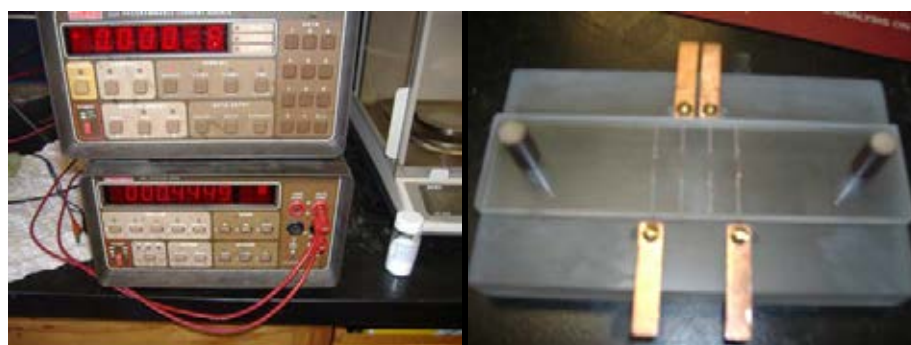


Figure 4.19 Current generator and Multimeter (left), Four-point probe (Gold wires) (right).

- Center of Excellence on Catalysis and Catalytic Reaction Engineering.

Conductivities were measured using a four-line collinear array utilizing a Keithley Instruments 6221 DC and AC current source and a Keithley 2182A Nanovoltmeter. Conductivity is calculated from $\sigma = l/twR$ (S/cm) where l is the distance between platinum wires, w is the width of the film, and t is the thickness of the film.

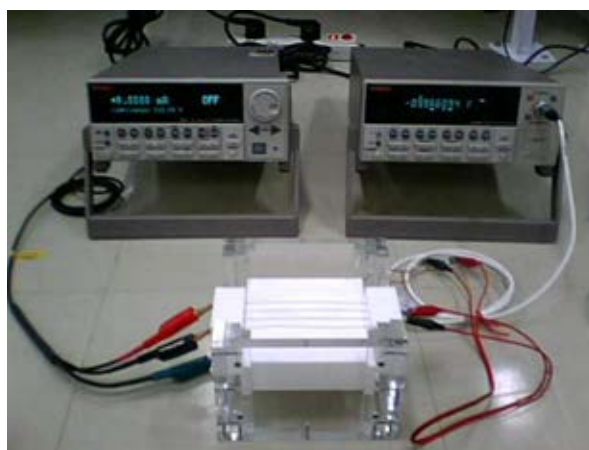


Figure 4.20 Current generator and Nanovoltmeter equipped with Four-point probe (Platinum wires).

4.4.6 Transmission electron microscope (TEM)

- Institute of Materials Science and the Polymer Program at the University of Connecticut, USA.

The PEDOT-PSS and PEDOT-SPAA particles were imaged using JEOL 2010 Fas and Philips EM420 transmission electron microscope.



Figure 4.21 Transmission Electron Microscope (TEM)

4.4.7 Elemental analysis

- Institute of Materials Science and the Polymer Program at the University of Connecticut, USA.

Elemental analysis was performed using a Vario Micro Elementar CHNS system.



Figure 4.22 Elemental analysis

CHAPTER V

RESULTS AND DISCUSSION

The results and discussion in this chapter are basically divided into 3 parts:

The first part (section 5.1) shows the accomplishment of experimental observation on the mixing systems and ways to significantly enhance the conductivity of PEDOT:SPI aqueous dispersion, which is published in *Microelectronic Engineering* volume 111 (2013), page 7-13.

The second part (section 5.2) will be the studying of effects of the addition of anionic surfactant during template polymerization of conducting polymers containing PEDOT with SPI or PSS templates for nano-thin film applications, which is published in *Synthetic Metals* volume xxx (2013), page xx-xx.

The last part (section 5.3) explains the synthesis and characterization of PEDOT/multi-sulfonated polyimide via template polymerization, which will be published.

5.1 Experimental observation on the mixing systems and ways to significantly enhance the conductivity of PEDOT:SPI aqueous dispersion

This part aims to study comparative synthesized PEDOT:SPI aqueous dispersions using mechanical stirring to a conventional magnetic stirring system. The mechanical stirring system was subjected to improve particle size, thermal stability, and dispersion stability due to the shear force from the stirrer. In addition, an anionic surfactant, sodium dodecyl sulfonate (SDS), was utilized as an additive to improve the dispersion stability, conductivity and thermal stability. Due to the combination of those concepts, superior dispersion stability, high conductivity and good thermal stability PEDOT:SPI films were achieved. The effects of different polyimide structures in PEDOT:SPI on the film properties were also investigated.

5.1.1 Synthesis of sulfonated diamine (4,4'-ODADS) and sulfonated poly(imide)

The sulfonated diamine monomer, 4,4'-Diaminodiphenyl ether-2,2'-disulfonic acid (4,4'-ODADS), was synthesized by direct sulfonation of the 4,4'-diaminodiphenyl ether (4,4'-ODA). Fuming sulfuric acid was used as a sulfonating agent. Firstly, 4,4'-ODA was reacted with concentrated sulfuric acid (H_2SO_4) to form the sulfuric acid salt of 4,4'-ODA. Secondly, SO_3 in fuming sulfuric acid reacted with 4,4'-ODA at 80°C . The monomer structure was confirmed by FTIR and ^1H NMR.

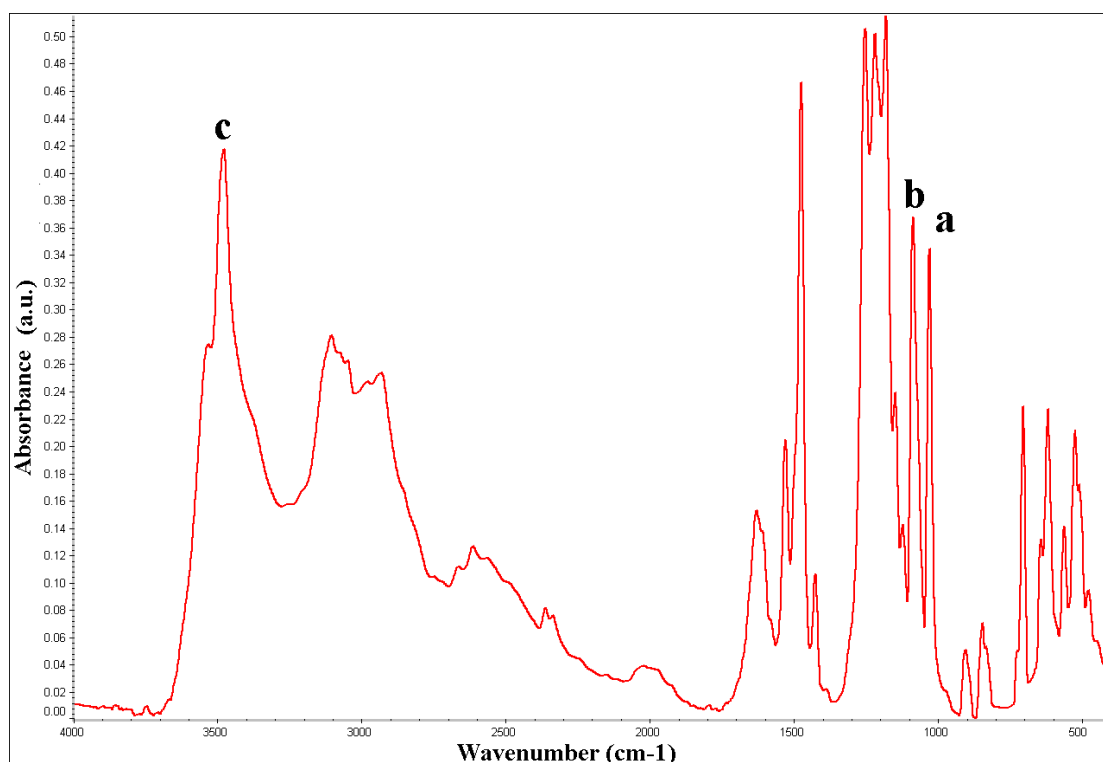


Figure 5.1 FTIR spectrum of 4,4'-ODADS

The FTIR spectrum in Figure 5.1 shows absorptions at a) 1028.4 and b) 1085.6 cm^{-1} assigned to the sulfonic acid group, and at c) 3479.0 cm^{-1} assigned to NH_2 of the diamine. The sulfonation primarily occurred at the meta position as shown in ^1H NMR spectrum of Figure 5.2.

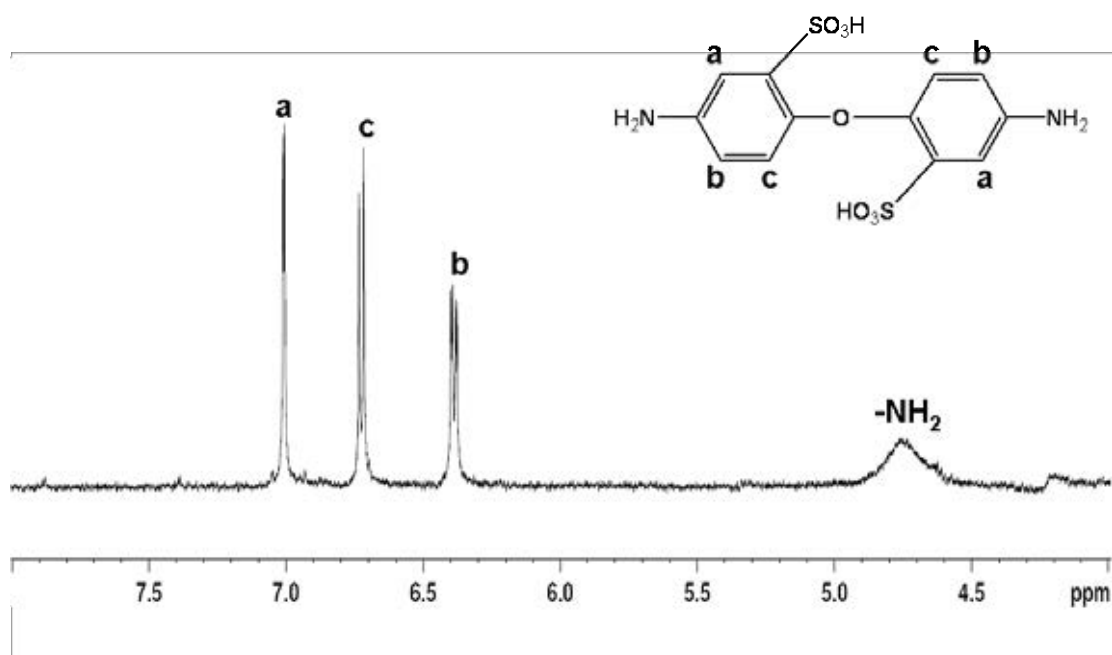
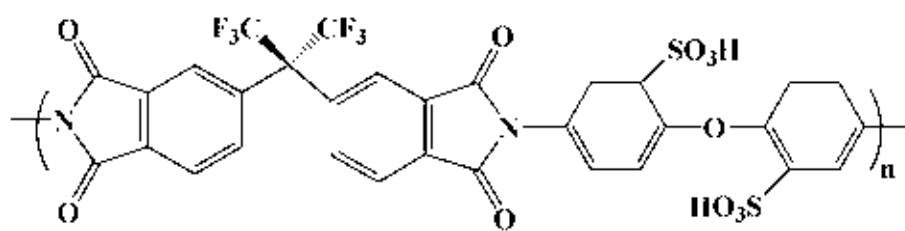
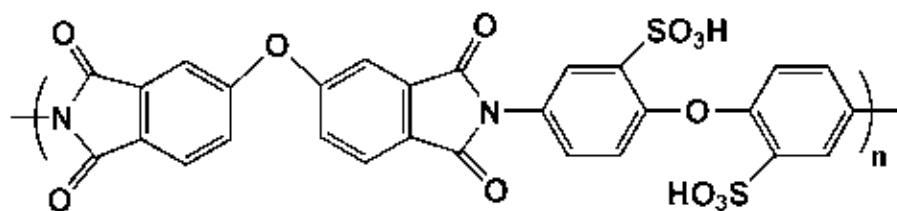


Figure 5.2 ¹H NMR spectrum of 4,4'-ODADS

Sulfonated poly(imide) polymerization of 4,4'-ODADS and O-DPDA/6FDA was synthesized by using *m*-cresol as a solvent in presence of triethylamine (Et₃N) for improving the solubility of 4,4'-ODADS. The solution was carried out at room temperature for 3 days to form poly(amic acid). The poly(amic acid) polymerization is an exothermic reaction; if the reaction was carried out at a higher temperature, hydrolysis would have occurred, producing lower molecular weight and unstable polymers. When the reactions were complete, the poly(amic acid) solution was thermally imidized at 70 °C, 150 °C for 1 h each, and 250 °C for another 1 h to get the sulfonated poly(imide). The chemical structure of SPI(O-DPDA) and SPI(6FDA) are shown in Figure 5.3 (a) and (b), respectively.



(a) SPI (6FDA)



(b) SPI (O-DPDA)

Figure 5.3 Chemical structures of SPI

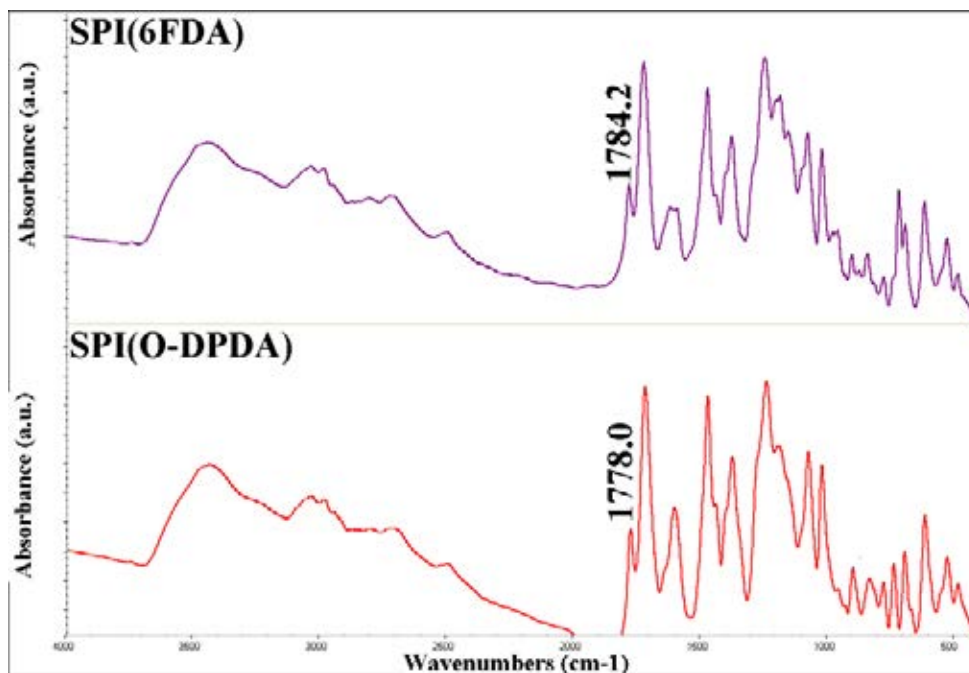


Figure 5.4 FT-IR spectrum of SPI(6FDA) and SPI(O-DPDA)

The imidization was confirmed by FTIR measurements, as shown in Figure 5.4. It shows the complete conversion of the sulfonated poly(amic acid) (SPAA) to sulfonated poly(imide). The peak at 1784.2 and 1778.0 cm^{-1} corresponds to the imide form of SPI(6FDA) and SPI(O-DPDA), respectively. This confirmed that the imidization takes place during the relatively short curing process.

5.1.2 Template polymerization of EDOT and sulfonated poly(imide): PEDOT-SPI(6FDA) and PEDOT-SPI(O-DPDA)

FTIR spectrums of PEDOT-SPI(6FDA) and PEDOT-SPI(O-DPDA) are shown in Figure 5.5. The stretching of ethylenedioxy group was indicated at 1189.7 and 1191.3 cm^{-1} while the stretching of C=C and C-C bonds in thiophene were represented at 1515, 1473, 1388, 1311 cm^{-1}

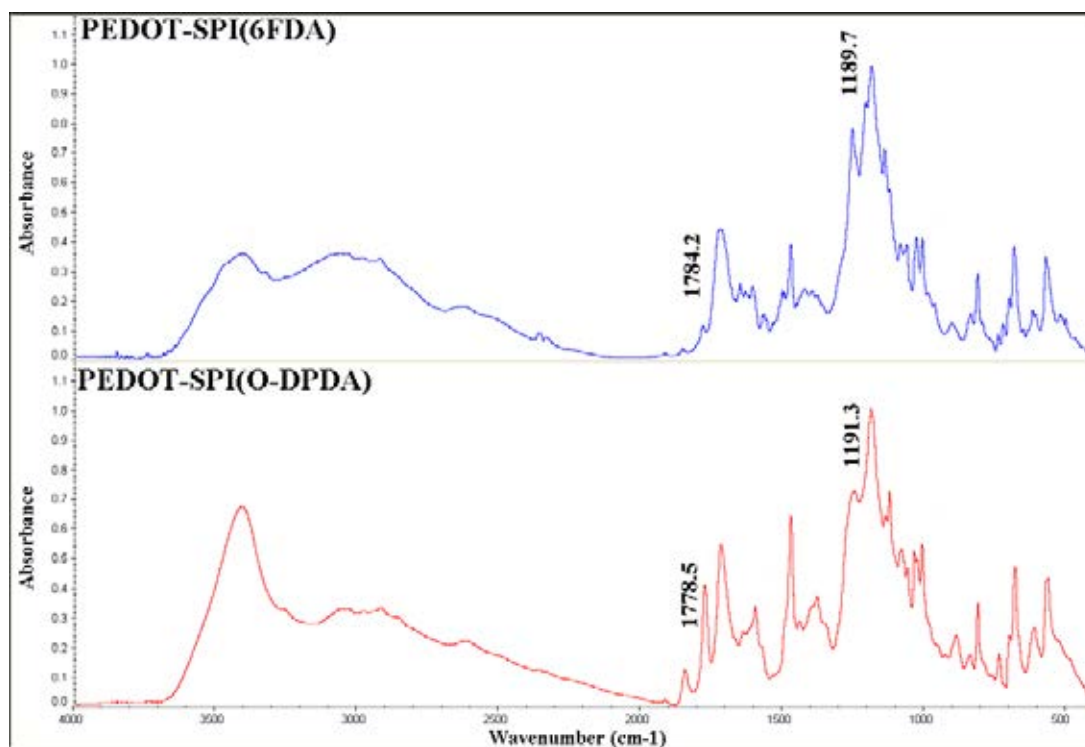


Figure 5.5 FT-IR spectrum of PEDOT-SPI

5.1.3 Conductivity

Conductivity for all PEDOT-SPI films was measured via the four-point probe technique. Significant enhancement in the conductivity was observed, when the mechanical mixing system was used. The data is shown in Table 5.1. Conductivity enhancement of PEDOT-SPI (6-FDA) and PEDOT-SPI (O-DPDA) were obtained by using mechanical mixing systems at 1000 and 4000 rpm. The maximum conductivities of 2.04 and 1.15 S cm⁻¹ were observed for PEDOT-SPI(6-FDA) and PEDOT-SPI (O-DPDA) films respectively in the 4000-rpm mechanical mixing system. In comparison of the mechanical mixing system to the same magnetic stirrer rotation frequency (1000 rpm), we found that the conductivities of the 1000-rpm mechanical mixing system are higher than those of magnetic stirring. The increase is attributed to the smaller particle size of PEDOT-SPI when the mechanical mixing system was used. The effect of morphology and particle size of conducting polymers on conductivity is related to the passing of charge carriers.

The smaller particle sizes of PEDOT:SPI leads to a smaller void between particle in the final film, which allows for an easier transfer of charge between particles. Compared to magnetic bar mixing system, a mechanical mixing system provides a very different mechanism in delivering the shear stress for dispersing particle suspension. The shear stress effect when using paddle stirrer are higher comparing to that of cylindrical magnetic bar. The stirring effect of the mixing system is not the only factors, but the size and shape of the stirrer is also important. When being mixed in a solution, PEDOT-SPI was subjected to shear stress imparted from the medium (e.g., solvent). Therefore, the flow of the medium was response to an external force through the rotation of a stir shaft and delivery of a mechanical energy into the solution to separate the aggregate generates the shear stresses that were ultimately responsible for dispersion. Thus, an appropriate stirrer together with a higher rotation speed (rpm) could cause a smaller particle, resulting in better conductivities. Furthermore, under stronger rotation frequency (4000 rpm), the suspension from the mechanical mixing shows better conductivities and its maximum value is higher than those of a magnetic bar and a 1000 rpm-mechanical mixing system by a factor of 346 and 3.1 for PEDOT-SPI (6-FDA) and 325 and 3.4 for PEDOT-SPI (ODPDA) respectively. This increase is attributed to the particle size of PEDOT-SPI, which can be decreased by using a high-speed mechanical stirring system. The particle sizes of PEDOT-SPI in aqueous suspensions were investigated by transmission electron microscopy (TEM).

Table 5.1 Conductivities of PEDOT-SPI systems from each mechanical and magnetic stirring process.

Mixing systems		PEDOT-SPI (6-FDA)	PEDOT-SPI (O-DPDA)
Magnetic bar	Conductivity (S/cm)	5.9×10^{-3}	3.54×10^{-3}
	Std. Dev.	2.84×10^{-3}	1.16×10^{-3}
Mechanical (1000 rpm)	Conductivity (S/cm)	6.57×10^{-1}	3.43×10^{-1}
	Std. Dev.	3.04×10^{-2}	6.79×10^{-2}
Mechanical (4000 rpm)	Conductivity (S/cm)	2.04	1.15
	Std. Dev.	3.36×10^{-3}	1.29×10^{-3}

The effect of adding the anionic surfactant, sodium dodecyl sulfonate (SDS), into the polymer solution was also investigated. Much effort has been made to improve the conductivity of PEDOT-PSS and PEDOT-SPI. One method recently developed is to add high-boiling-point polar organic compounds into the PEDOT-PSS and PEDOT-SPI aqueous solution or to treat the PEDOT-PSS and PEDOT-SPI film with a polar solvent, such as ethylene glycol, DMF or DMSO [47,49,50-53]. Here, we report a method to significantly enhance in conductivity of the PEDOT-SPI film by adding sodium dodecyl sulfonate (SDS). The data is shown in Table 5.2 and Figure 5.6.

Table 5.2 Conductivities of PEDOT-SPI(SDS) systems from mechanical stirring process

SDS contents (%wt)		PEDOT-SPI (6-FDA)	PEDOT-SPI (O-DPDA)
0	Conductivity (S/cm)	2.04	1.15
	Std. Dev.	3.36×10^{-3}	1.29×10^{-3}
0.1	Conductivity (S/cm)	2.88	1.99
	Std. Dev.	6.88×10^{-1}	3.77×10^{-1}
0.5	Conductivity (S/cm)	4.26	2.86
	Std. Dev.	1.87×10^{-1}	1.06
1	Conductivity (S/cm)	9.50	5.16
	Std. Dev.	3.61	1.16
3	Conductivity (S/cm)	6.61	3.90
	Std. Dev.	2.74	8.46×10^{-1}
5	Conductivity (S/cm)	7.74	4.36
	Std. Dev.	2.76	4.77×10^{-1}

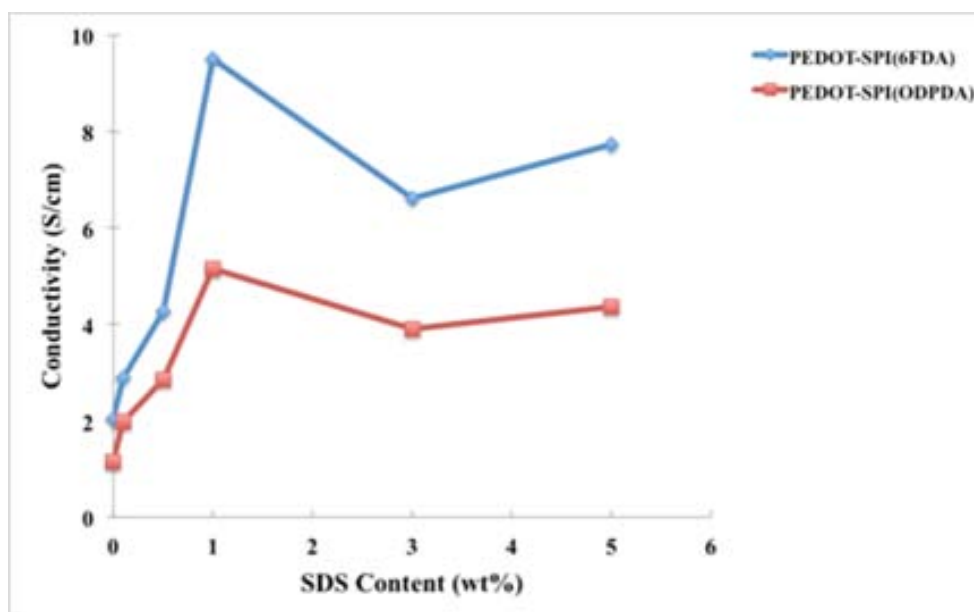


Figure 5.6 Variation of the conductivity of the PEDOT-SPI (SDS) film mechanical (4000 rpm) stirring system with the weight fraction of the anionic surfactant.

In fact, the highest conductivities of PEDOT-SPI (6-FDA)-SDS and PEDOT-SPI(ODPDA)-SDS films obtained were 9.5 and 5.16 S cm⁻¹ at a SDS weight fraction of 1, respectively. These maximum conductivities were higher than those of the PEDOT-SPI films without SDS by a factor of ~5. In this system, the SDS plays a dual function; dopant and surfactant, leading to the incorporation of the dopant anions in the PEDOT-SPI backbone. The conductivity enhancement mechanism due to the anionic surfactant was different from that due to the secondary dopants such as ethylene glycol, DMSO or DMF, since this anionic surfactant has a remarkably different structure from those secondary dopants. The conductivity enhancement due to the anionic surfactant was observed even for the PEDOT-SPI films dried at room temperature. Subsequently, heating these dried PEDOT-SPI films with anionic surfactant at high temperature did not further increase the conductivity. This was different from the conductivity enhancement of the films due to the high-boiling point polar compound, which requires a heating process at a high temperature. The PEDOT segment, which has positive charges, was bound to the SPI

segment, which has negative charges, by cooperatively interacting oppositely charged attraction between chain units. In fact, the length of the PEDOT repeating unit, 3,4-ethylenedioxythiophene, was longer than that of SPI repeating unit. Thus we needed to use an excess amount of SPI to form a water-soluble polyelectrolyte complex. However, some PEDOT chains match with SPI perfectly. It exhibits an enhanced rigidity, relatively weak hydrophilic properties and low conductivity. This is the reason why after the anionic surfactant was introduced into the PEDOT-SPI aqueous solution, the anionic surfactants acted as counterions for conducting-polymer polycations and the hydrophobic part of the SDS molecules adsorbed onto the produced conducting polymer, a surfactant thus becoming a part of the PEDOT-SPI so they can make the conversion of hydrophobic blocks of PEDOT-SPI into hydrophilic blocks. This conformational change may be the key reason to significantly enhance the conductivity of the polymer films with an anionic surfactant. Nevertheless, the conductivity of the film also depended on the molar ratio of SDS to the PEDOT-SPI repeating unit. At first, the conductivity of the PEDOT-SPI film rapidly increased with the increasing SDS additive. Then, the conductivity enhancement became less remarkable with the large amount of SDS. This can be attributed to the presence of large amount of insulator SDS in PEDOT:SPI. The intrinsic conductivity of PEDOT:SPI(SDS) should be higher than the apparent conductivity.

5.1.4 Thermal stability of PEDOT-SPI(6FDA) and PEDOT-SPI(O-DPDA)

The effect of the mixing system on the thermal stability of the conducting polymers was also investigated. Figure 5.7 shows that thermal stability of PEDOT-SPI could be improved by using a mechanical mixing system. The thermal behavior of the PEDOT-SPI prepared from the high-speed mechanical mixing system was compared to the PEDOT-SPI prepared from the magnetic bar mixing system. Clearly, the high-speed (4000-rpm) mechanically-mixed PEDOTSPI essentially showed a higher onset temperature (T_o) than the 1000 rpm-mechanically-mixed and magnetic-bar-mixed PEDOT-SPI. The onset temperatures of PEDOT-SPI prepared

from the high-speed mechanical (4000-rpm), mechanical (1000-rpm) and magnetic bar mixing system are 236, 221 and 208 °C, respectively.

We ascribed the thermal stability changed to the decrease in particle size of PEDOT-SPI because the specific surface area of the particles varied inversely with the particle diameter squared. Therefore, an enhancement in thermal stability was expected because a reduction in particle size could result in a large surface area. The enhanced thermal stability of the nanoparticle appeared highly dependent on the morphology of the particles. Therefore, the particle size of PEDOT-SPI was confirmed with TEM as shown in Figure 5.9. Furthermore, Figure 5.7 shows the same trend in thermal behavior of the three films. There were three decomposition steps. The first step (<200 °C) was due to water, the second (~280 °C) and third step (>400 °C) indicated the weight loss due to PEDOT and SPI, respectively. The TGA curve clearly shows that the 4000-rpm mixed film demonstrated much better thermal stability because of a higher fraction of SPI relative to 1000 rpm and magnetic-bar-mixed films.

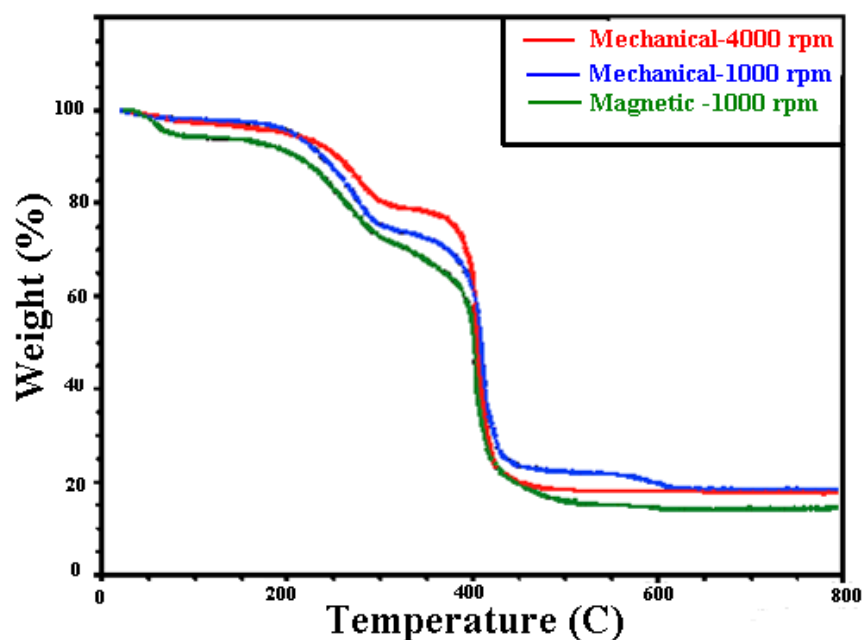


Figure 5.7 TGA of PEDOT-SPI with varied mixing system

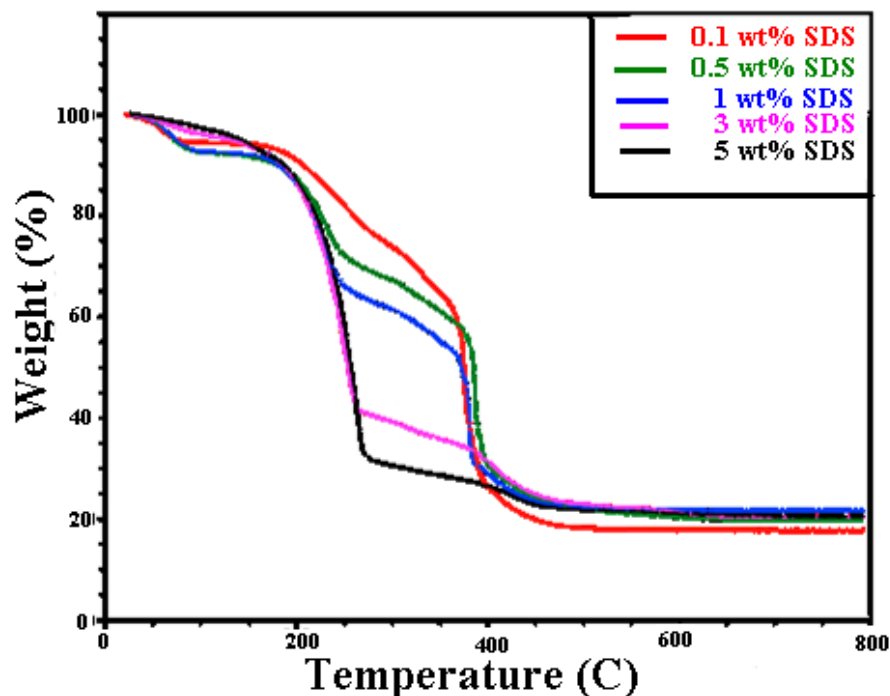


Figure 5.8 TGA of PEDOT-SPI with various %wt of SDS

The effect of anionic surfactant (SDS) on thermal stability of the conducting polymer was also investigated as shown in Figure 5.8. The surfactant, if incorporated into the conducting polymer, was likely to affect the thermal stability of the film's conductivity. The first significant weight loss had occurred already at a temperature between 30–100 °C. It is known, that PEDOT-SPI is hygroscopic, and during the heating to 100 °C the residual water evaporates. At a temperature higher than 300 °C, the thermal stability of PEDOT:SPI-SDS can be respectively rearranged as follow; PEDOT:SPI-0.1% SDS > PEDOT:SPI-0.5% SDS > PEDOT:SPI-1% SDS > PEDOT:SPI-3% SDS > PEDOT:SPI-5%SDS. Therefore, the curves presented for various weight fractions of SDS in PEDOT:SPI had the same shape, and they seem to be slightly less stable when having more SDS contents if we compared their TGA curves with pure PEDOT-SPI in the whole temperature range due to the decomposition of SDS related to its thermal stability.

5.1.5 Morphological and dispersion stability

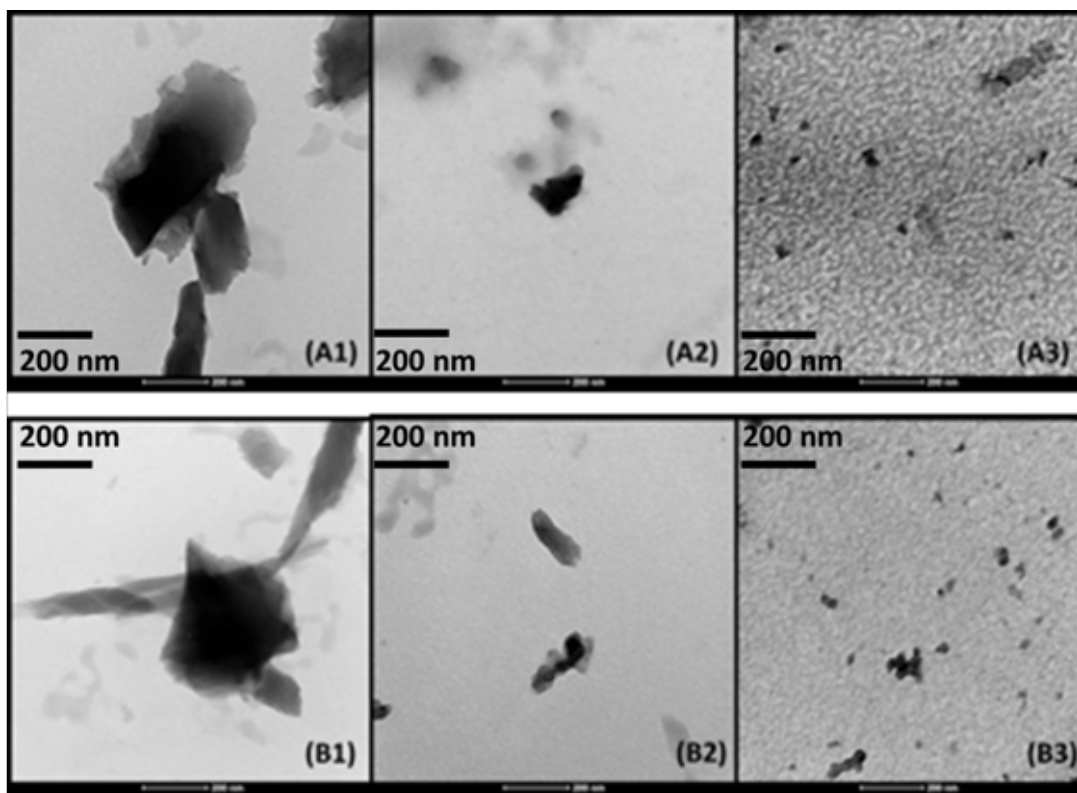


Figure 5.9 TEM of various mixing systems (A-B1= magnetic bar, A-B2= mechanical at 1000 rpm, and A-B3= mechanical at 4000 rpm)

The TEM images of the PEDOT-SPI samples dispersed in water are shown in Figure 5.9. The magnetic stirring system was not capable of dispersing clusters of particles. With the mechanical stirring system, the dimensions of the PEDOT-SPI particles became smaller and their dispersibility in water consequently improved. Compared to magnetic bar mixing system, a mechanical mixing system uses a very different mechanism in delivering the shear stress for dispersing particle suspension. The shear stress effect when using a paddle stirrer was higher compared to that of cylindrical magnetic bar. The stirring effect of the mixing system was not the only factors, but the size and shape of the stirrer are also important. When being mixed in a solution, PEDOT-SPIs were subjected to shear stress imparted from the medium (e.g., solvent). Therefore, the flow of the medium in response to an external force through the rotation of a stir

shaft and delivery of a mechanical energy into the solution to separated the aggregate generated the shear stresses that were ultimately responsible for dispersion. TEM images of the samples clearly indicated that the materials had uniform solid nanoparticles and their diameters are about 43 nm on average, which are much smaller than particle sizes of PEDOT:SPI in the previous work (in the range of 500–550 nm.) [57].

Additionally, the dispersing stability of the PEDOT-SPI samples in water (Figure 5.10) was also found to be improved with the addition of the anionic surfactant (SDS). Sedimentation was only found at a weight fraction of <0.1 wt% SDS after a week.

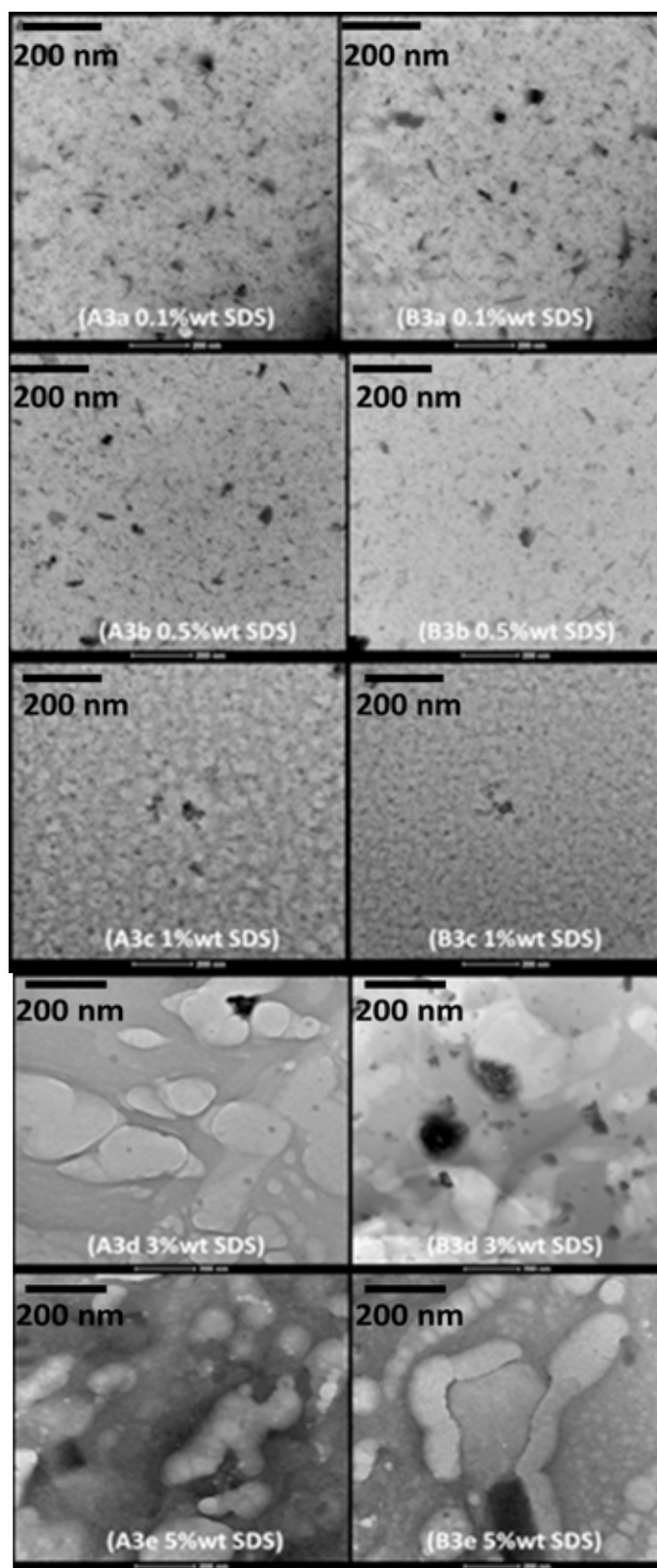


Figure 5.10 TEM of PEDOT-SPI with various wt% of SDS

5.2 Effects of the addition of anionic surfactant during template polymerization of conducting polymers containing PEDOT with SPI or PSS templates for nano-thin film applications

5.2.1 Synthesis of sulfonated diamine (*4,4'*-ODADS) and sulfonated poly(imide)

(See details in 5.1.1)

5.2.2 Method of addition of anionic surfactant, SDS, to the synthesis of nanoparticle suspension

Generally, the surfactant was added to the aqueous solution of conducting polymer in the last step before films formation or after completion of polymerization of PEDOT-PSS. The solution was then vigorously stirred overnight before further film formation or other process steps. Most spherical particles, however, were connected, agglomerated, to each other at this point, indicating that the addition of surfactant after polymerization was not as effective enough for particle separation. We have also found that the addition of surfactant after polymerization causes lower thermal stability of the obtained polymers because SDS can only insert between conducting polymer chains. To overcome this problem, the addition of surfactant during polymerization may be worth investigation.

In this work, we proposed a novel approach to synthesize nanoparticle suspensions (PEDOT-PSS, PEDOT-SPI) through addition of the anionic surfactant, SDS, during template polymerization while using a mechanical shear stirrer to disperse the particles. The surfactant could be incorporated into synthesized particles during polymerization as well as effectively function as a dopant, resulting in an increasing dispersion of nanoparticles, improving thermal stability, and inducing smaller nanoparticles dimensions. Chemical structures of all components can be shown in Figure 5.11. We have divided our studies into three systems based on when the SDS was added to the dispersion:

(1) Surfactant added during template polymerization of nanoparticle suspensions (PEDOT-PSS, PEDOT-SPI);

(2) Surfactant added after template polymerization of nanoparticle suspensions;

(3) Surfactant added both during and after polymerization.

Also, we have evaluated the effect of SDS on the chemical structure of the colloid particles, their thermal stability, morphological dispersion, and their conductivity.

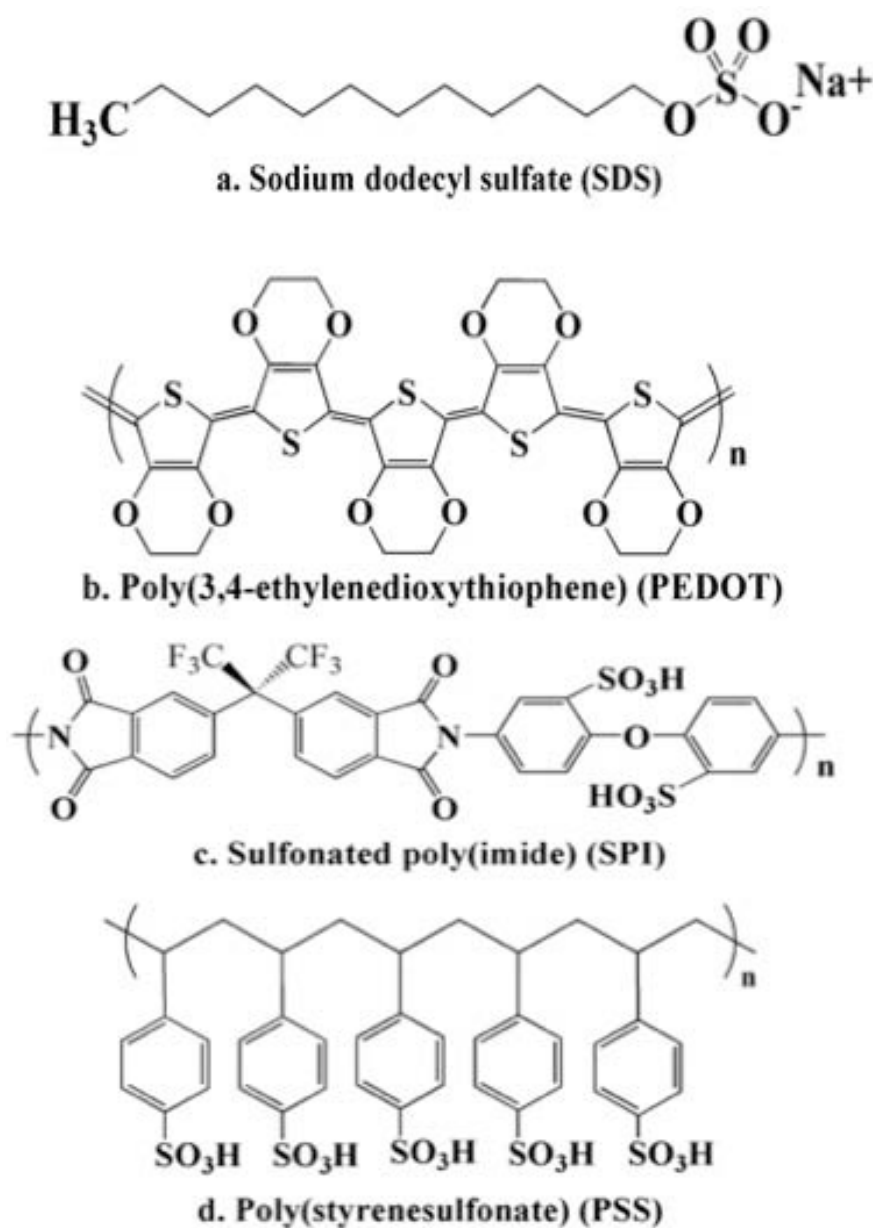


Figure 5.11 Chemical structure of SDS, PEDOT, sulfonated polyimide (SPI) and PSS

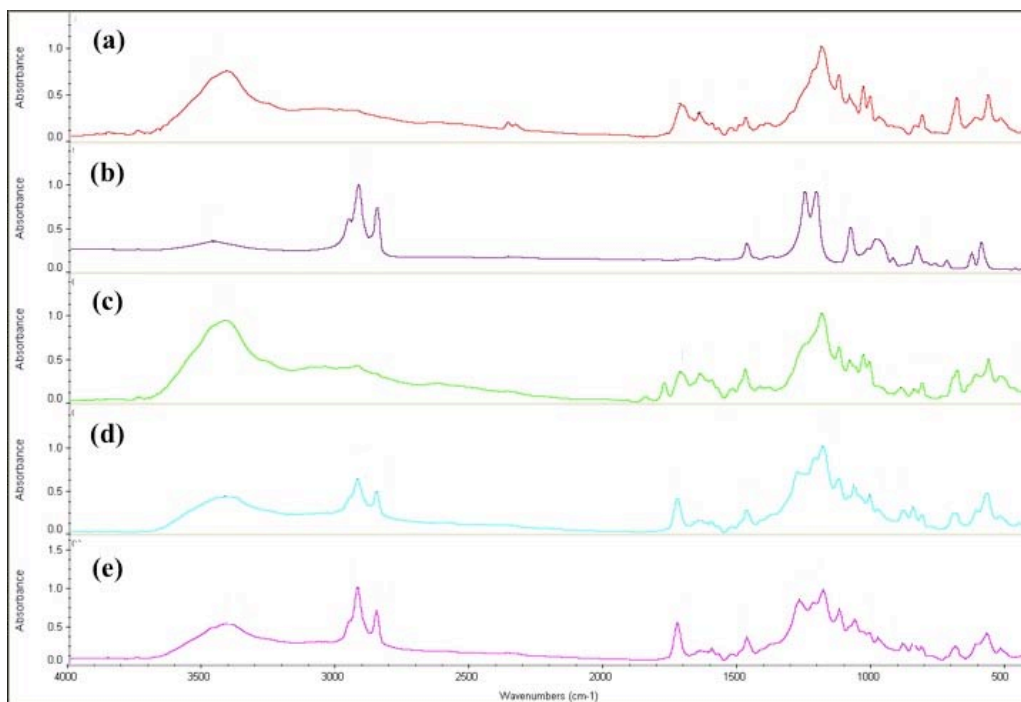


Figure 5.12 FTIR results of PEDOT-SPI system

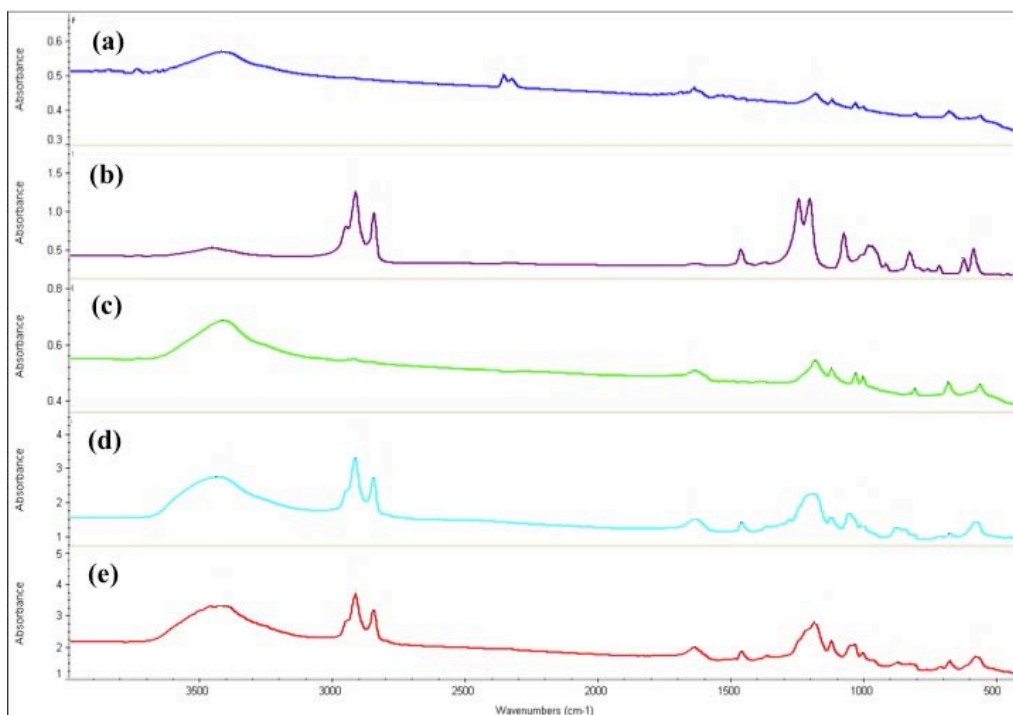


Figure 5.13 FTIR results of PEDOT-PSS system

The effects of the anionic surfactants, SDS, on the chemical structure of synthesized nanoparticles were studied by FTIR spectroscopy. To well understand the FTIR spectra, FTIR spectra of SDS, pristine synthesized conductive polymers, and synthesized conductive polymers with different methods of addition of SDS were presented and compared as well. The structure of pristine PEDOT-SPI and PEDOT-PSS were shown in Figure 5.12a and 5.13a. The S=O stretching for SO_3H appeared at 1034.9, 1038.6 cm^{-1} , confirming the formation of the sulfonated poly(imide) and polystyrene sulfonate, respectively. The absorption band at 1645.9 cm^{-1} was assigned to the symmetric imide C=O stretching, and the peak at 1715.8 cm^{-1} indicates the asymmetric imide C=O stretching. The characteristic peak of PEDOT could be seen at 1474.2 cm^{-1} ; C=C stretching of quinoid structure of thiophene, 1085.8, 1126.3, 1189.1 cm^{-1} ; C-O-C bond stretching in ethylenedioxy group, and 1009.4, 815, 685.1 cm^{-1} ; C-S bond in thiophene ring. Figure 5.12b and 5.13b showed the FTIR spectra of anionic surfactant, SDS, The bands at 1252.5 and 1210.6 cm^{-1} corresponded to S=O stretching from sulfonate group. The peaks at 833.7, 923.8, and 1081.1 cm^{-1} were typical characteristic peaks of the S-O stretching. The bands at 2851.9 and 2923.5 cm^{-1} , which belonged to C-H stretching of SDS were observed for method of addition of 5 wt% SDS after and both during and after polymerization of PEDOT-SPI and PEDOT-PSS. However, for both systems, the peaks at 2851.9 and 2923.5 cm^{-1} were shifted toward higher wave number with the addition of SDS after polymerization system and addition of SDS both during and after polymerization into conducting polymer suspensions (see Figure 5.12d and 5.13d and e). This result was distinctly different from that of surfactant addition during polymerization into conducting polymer suspension. In this system, those peaks were become broader and shifted to lower wavelengths in the presence of surfactant during polymerization of conducting polymers (see Figure 5.12c and 5.13c). These broad peaks and shifting had confirmed strong interactions between PEDOT and surfactant molecules as doping materials. Combine with

the result of conductivity, the obtained conducting polymers, when anionic surfactant was added during polymerization, showed higher conductivity beside lower nano-particles produced. On the basis of these experimental results, a mechanism was proposed for the conductivity enhancement by adding surfactant during polymerization of PEDOT:SPI and PEDOT:PSS aqueous solution. The PEDOT segment, which has positive charges, was bound to both SPI(PSS) and anionic surfactant (SDS) which had negative charges. Upon anionic surfactant adding during polymerization, the anionic surfactant could be interacted to the PEDOT chain more than those of the addition of anionic surfactant after and the addition in both during and after polymerization. Ouyang et al. proposed that PSS chain adopts a coiled conformation in water, and the PEDOT chain has to follow the coiled conformation of PSS chain. Thus the PEDOT segment must distort, and the distortion results into the localization of the positive charges in the PEDOT chain. The distortion of the PEDOT chain may be the reason for lower conductivity of PEDOT:PSS [58]. After the anionic surfactant was introduced during the PEDOT:PSS (PEDOT:SPI) polymerization in our study, the anionic could replace PSS^- (SPI^-) more than those of addition of SDS after and both during and after systems polymerization. Hence, the distortion structures of the PEDOT chain disappeared, so the conductivity was improved. For the addition of anionic surfactant after polymerization, it could not replace PSS^- (SPI^-) or only small amount of anionic surfactant molecules could replace PSS^- (SPI^-), so less conductivity would occur. To add SDS after the polymerization, the SDS mostly located at outer surface of conducting particles, resulting in the strong absorption bands FTIR and the clear perimeter around conducting particles (black dots) in TEM images, thus the lower conductivity due to insulating behavior of SDS hydrophobic tails for this system had dominated.

5.2.3 Thermal properties

The thermal stability of synthesized particles is crucial for their potential application in industrial. TGA is an important dynamic method to detect the degradation behavior of the

synthesized nanoparticles. The thermal stability of PEDOT-PSS, PEDOT-SPI was measured by TGA. From TGA study, the degradation characteristic could be seen at 100°C; the degradation temperature of pure SDS took place from 200 °C – 250 °C. Meanwhile, the fragment of PSS sulfonate group degradation occurred after approximately at 230 °C [36]. At higher temperatures above 420 °C, the other fragments due to carbon oxidation degradation were observed. Figure 5.14 and 5.15 show the weight loss of PEDOT-SPI and PEDOT-PSS with various systems (without SDS, 5 wt% SDS added during polymerization, 5 wt% added after polymerization, and 5 wt% added both during and after polymerization, respectively), as a function of temperature. The nanoparticles of PEDOT-SPI (and PEDOT-PSS) synthesized with addition of SDS during polymerization showed significant improvement in the degradation temperature. In combination with the result from FTIR and TEM measurement, the improvement in the thermal stability was likely attributed to the higher molecular weight of PEDOT chains synthesized due to an intermolecular interaction between SDS molecules with the corresponding PEDOT- SPI and PEDOT-PSS. With 5 wt% SDS added after polymerization method and 5 wt% SDS added both during and after polymerization method of PEDOT-SPI, the synthesized particles showed relatively poor thermal stability due to the presence of SDS on the outer surface of particles and the results of breaking apart of particles, respectively. The effects of different methods of addition of SDS on thermal property were also consistent with the TEM measurement.

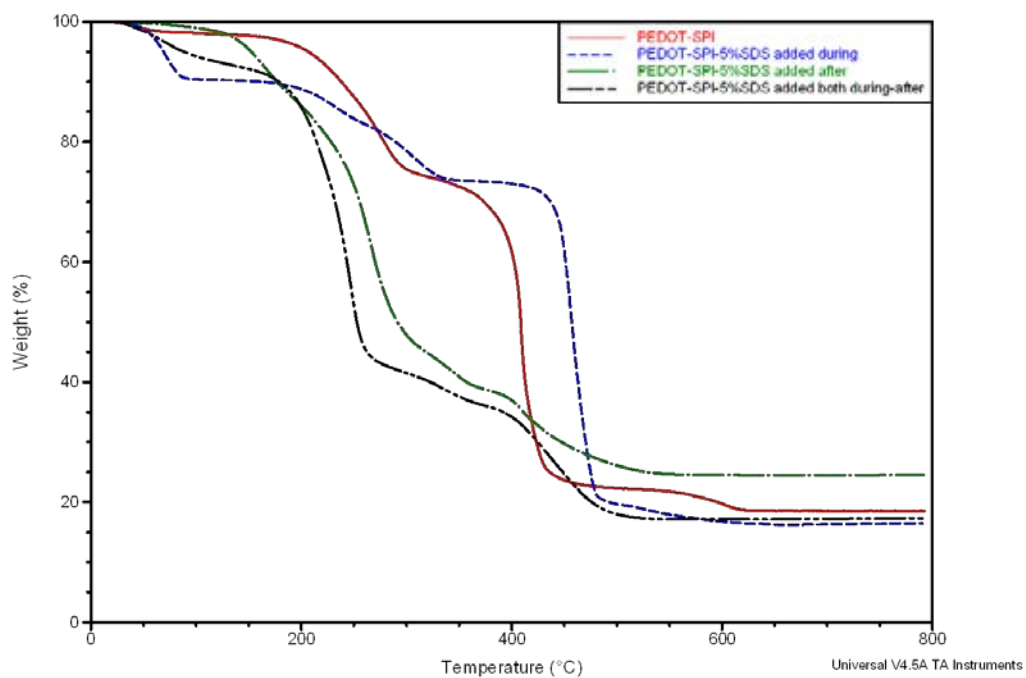


Figure 5.14 TGA results of PEDOT-SPI system

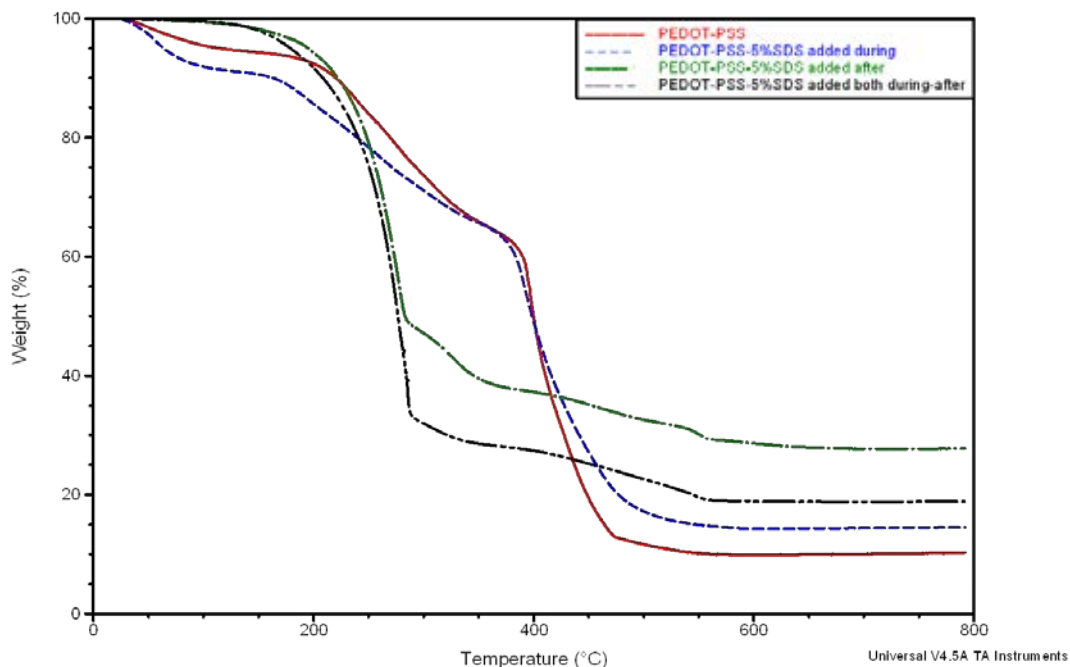


Figure 5.15 TGA results of PEDOT-PSS system

5.2.4 Morphological and dispersion stabilities

The effect of surfactant, SDS, on the morphology of the synthesized nanoparticles is shown in Figure 5.16(a–d) and 5.17(a–d). TEM studies showed that the PEDOT-PSS or PEDOT-SPI particles synthesized without addition of SDS were larger with irregular shapes, and most particles were connected to each other (see (Figure 5.16a and 5.17a)). Figure 5.16b shows that with addition of SDS during polymerization, the morphology of the synthesized nanoparticles of PEDOT-SPI (also PEDOT-PSS) changed from irregular-shape to perfectly spherical nanoparticle at 5 wt% of SDS. In addition, each of the nanoparticle was separated from each other, so this would induce higher conductivity. For the polymerization with addition of SDS during polymerization, stabilized particles could grow in size by the absorption of more SDS. Because of the increase in the hydrophilicity inside growing particles, the formations of spherical particles

were occurred. The effects of addition of SDS after polymerization step on the synthesized nanoparticle morphology can be shown in Figure 5.16c and 5.17c. They showed that the particles were trapped into the white area. Combine with the result from TGA measurements; the white areas were most likely attributed to the presence of SDS hydrophobic tail on the outer surface of already synthesized particles, resulting in the diminishing of thermal property. With 5 wt% addition of SDS both during and after polymerization step, the particles were broken apart when SDS was added which was consistent with TGA measurement (see (Figure 5.16d and 5.17d)) and the SDS that added after polymerization would coated the surface of the particles, so induced lower conductivity. Therefore, the addition of SDS during polymerization step only was more effective in stabilizing particles against coagulation than addition after polymerization, especially with PEDOT-PSS and PEDOT-SPI systems. Moreover, the addition of SDS in both after and during polymerization could not improve the conductivity and dispersion of PEDOT particles as much as the addition during polymerization.

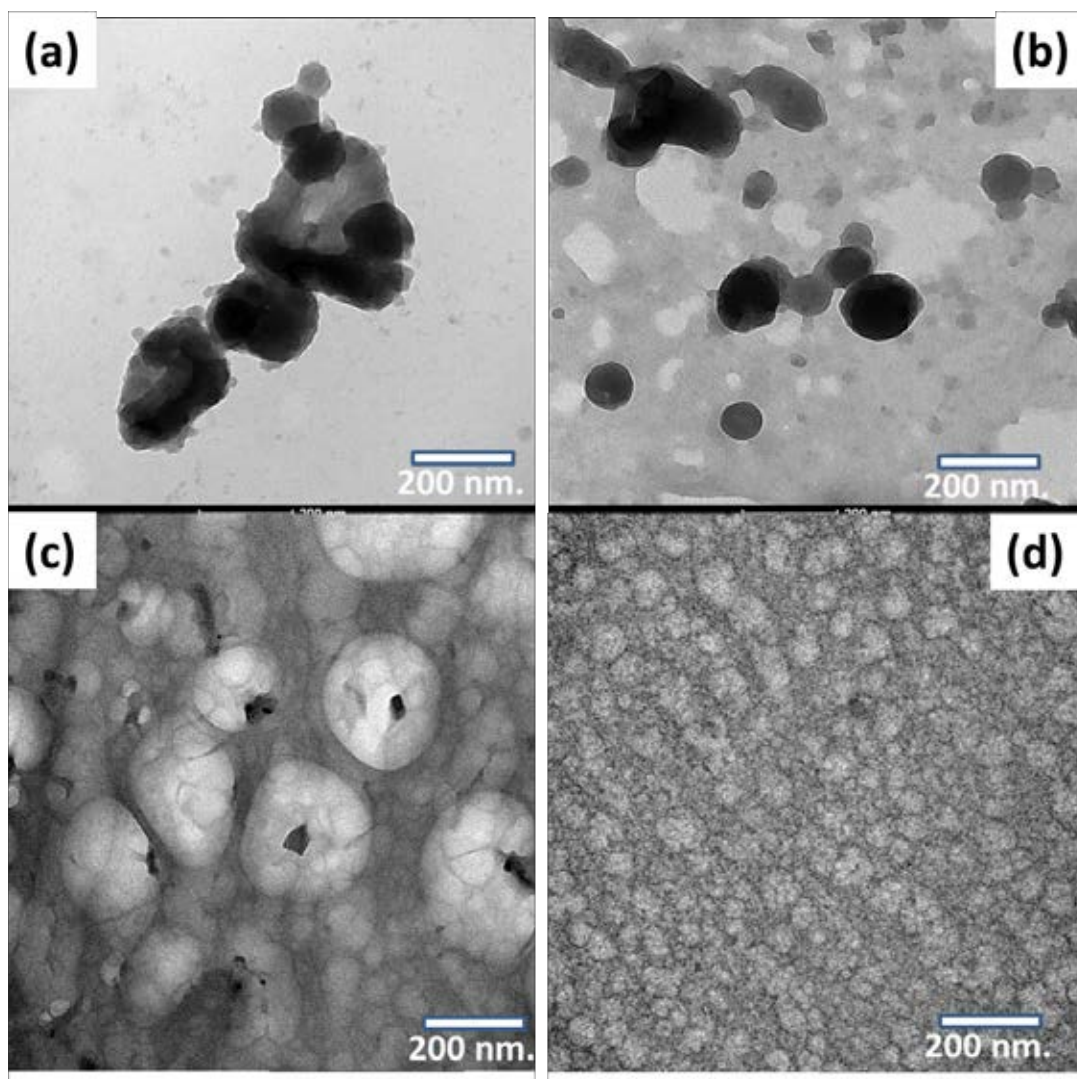


Figure 5.16 TEM of PEDOT-SPI system

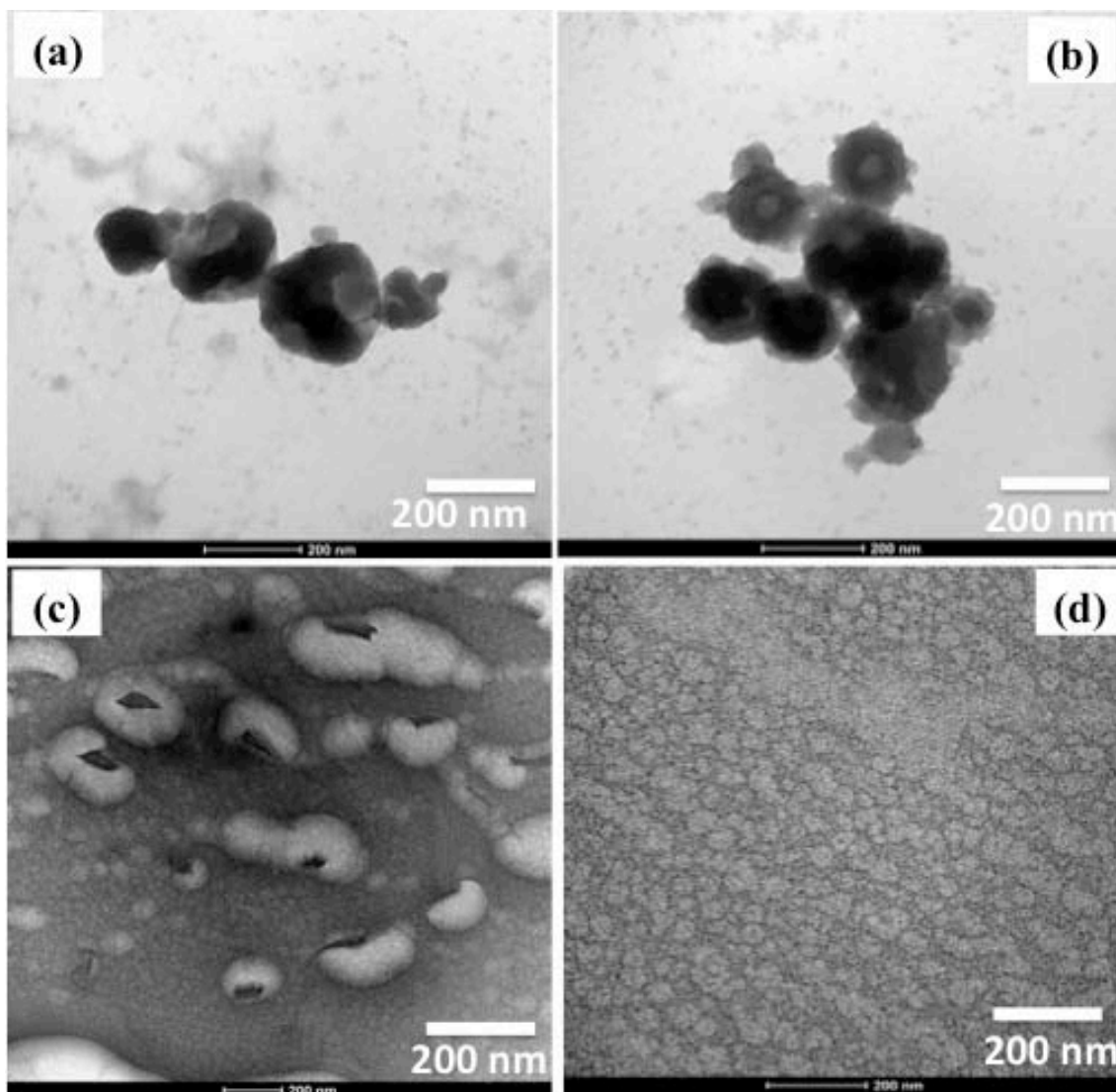


Figure 5.17 TEM of PEDOT-PSS system

5.2.5 Conductivity

As can be seen in the Table 5.3, the effects of different ways of SDS addition to the suspension on the conductivity of the PEDOT-SPI (or PEDOT-PSS) coated films could be compared. Without any SDS, the conductivity of PEDOT-SPI and PEDOT-PSS films were found to be around 1.89 and 1.46 S/cm, respectively. With the addition of anionic surfactant during polymerization, PEDOT-SPI and PEDOT-PSS films showed the higher conductivity (8.69 S/cm; PEDOT-SPI, 6.47 S/cm; PEDOT-PSS) than those of other films, when anionic surfactant was

added after polymerization (3.62 S/cm; PEDOT-SPI, 2.51 S/cm; PEDOT-PSS) or added both during and after polymerization (6.04 S/cm; PEDOT-SPI, 4.83 S/cm; PEDOT-PSS). The improvement of conductivity of conducting polymer films with addition of anionic surfactant during polymerization might be the presence of SDS molecule caused by the decrease in the distortion of PEDOT chains from the interacting of SDS with PEDOT molecules more than when it was added after polymerization, interacting with already made PEDOT particles. Moreover, the comparison of the conductivity stability between PEDOT-SPI and PEDOT-PSS was reported in our previous work [51]. The conductivity of the films was studied by annealing the films at 180 °C for 90 min, and 300 °C for 10 min. The PEDOT -SPI polymer exhibited 10–1000 times increase in conductivities compared to PEDOT-PSS after processing at room temperature and annealing at elevated temperatures at 180 °C and 300 °C respectively. However, the conductivity was lost considerably if annealing process performed above 300C. The addition of surfactants into PEDOT-PSS could affect the conductivity of the PEDOT-PSS films prepared from the solution. The effect of addition of SDS could significantly enhance the conductivity of PEDOT-PSS. The conductivity increased with the increase of the weight ratio of SDS to PEDOT-PSS at first, then it decreased when the weight ratio of SDS to PEDOT-PSS is higher than a certain value [39,37]. In our work, we have also found the same trend of PEDOT-PSS-SDS system. However, the optimum amount of SDS to provide the highest conductivity for PEDOT-SPI system is 5 wt% of SDS. Therefore, this value is the most appropriate amount of SDS for our work. In addition, the addition of SDS at 5 wt% also provided the small spherical particles as shown by TEM.

Table 5.3 Conductivities of PEDOT-SPI and PEDOT-PSS (in house) with various different method of addition of anionic surfactant

Method of addition of SDS		PEDOT-SPI	PEDOT-PSS
No SDS	Conductivity (S/cm)	1.89	1.46
	Std.Dev.	4.80×10^{-1}	3.90×10^{-1}
SDS added during polymerization	Conductivity (S/cm)	8.69	6.47
	Std.Dev.	1.16	3.73×10^{-1}
SDS added after polymerization	Conductivity (S/cm)	3.62	2.51
	Std.Dev.	8.46×10^{-1}	1.18×10^{-1}
SDS added both during and after polymerization	Conductivity (S/cm)	6.04	4.83
	Std.Dev.	4.17×10^{-1}	1.27×10^{-1}

5.3 Synthesis and characterization of PEDOT/multi-sulfonated polyimide via template polymerization

In this study, the novel multi-sulfonated group in a single molecule of sulfonated polyimides, which obtained from 2 symmetrical aromatic synthesized sulfonated bulky diamines, was proposed. The new symmetrical aromatic diamines were synthesized by the aromatic nucleophilic substitution reaction. The chemical structure of the novel multi-sulfonated polyimide is shown in Figure 5.18. Furthermore, the comparison effects of conductivity of PEDOT using the different sulfonated polyimide templates were investigated. The sulfonated polyimides were characterized by Nuclear magnetic resonance (NMR), Fourier transform infrared spectroscopy (FT-IR), Thermal gravimetric analysis (TGA) and conductivity measurement.

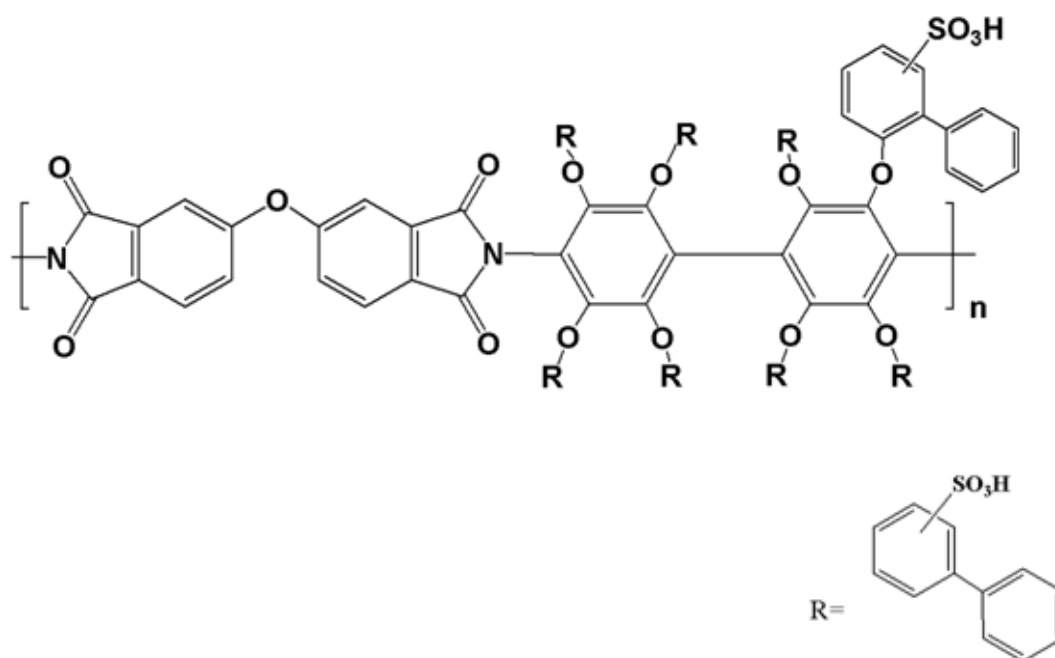


Figure 5.18 Chemical structure of a novel multi-sulfonated polyimide

5.3.1 Synthesis of diamine monomer

The diamine monomer (see figure 5.19) was prepared by the reaction of 2-phenylphenol with 4,4'-diaminooctafluorobiphenyl, which required a high temperature (220 °C) and a long reaction time (72 h) due to the steric hindrance of 2-phenylphenol. FTIR and NMR spectroscopy confirmed the structure of a new synthesized diamine monomer.

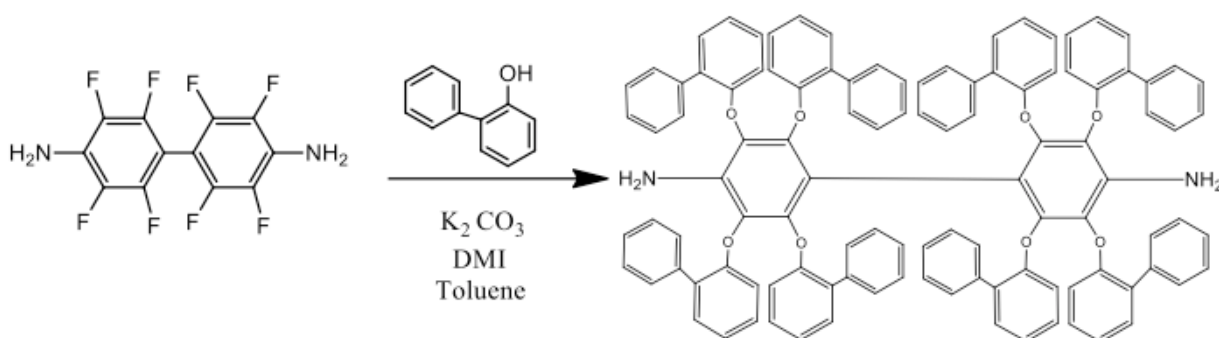


Figure 5.19 Scheme of synthesis of diamine monomer

The FTIR spectrum of synthesized diamine monomer showed characteristic absorptions corresponding to C-O-C and N-H of diamine at 1252.1 and 3366.9 cm^{-1} , respectively. Figure 5.21 showed the ^1H NMR spectrum of synthesized diamine, consisting of a peak at 4 ppm and multiplets 6.52-7.72 ppm that are assigned to NH and aromatic protons, respectively.

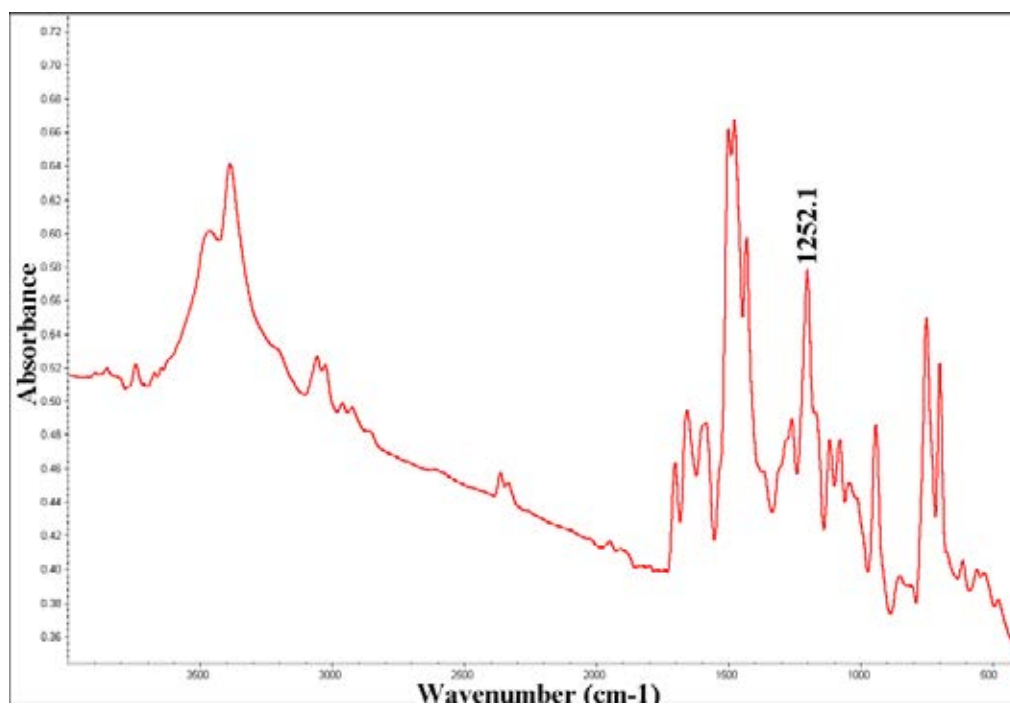


Figure 5.20 FTIR spectrum of synthesized diamine.

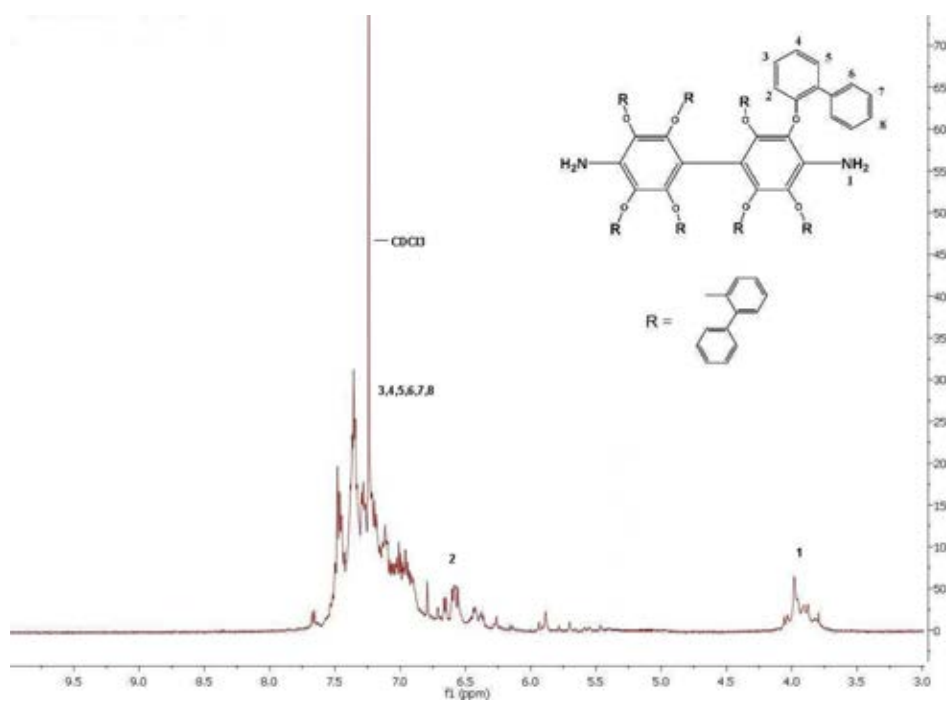


Figure 5.21 ¹H NMR spectrum of synthesized diamine.

5.3.2 Synthesis of multi-sulfonated diamine monomer

The multi-sulfonated diamine was synthesized by direct sulfonation of synthesized diamine with concentrated sulfuric acid (95%) at 80°C for 8 h. The scheme of the synthesized diamine monomer is shown in figure 5.22. The structure of multi-sulfonated diamine was verified by FTIR and NMR spectroscopy.

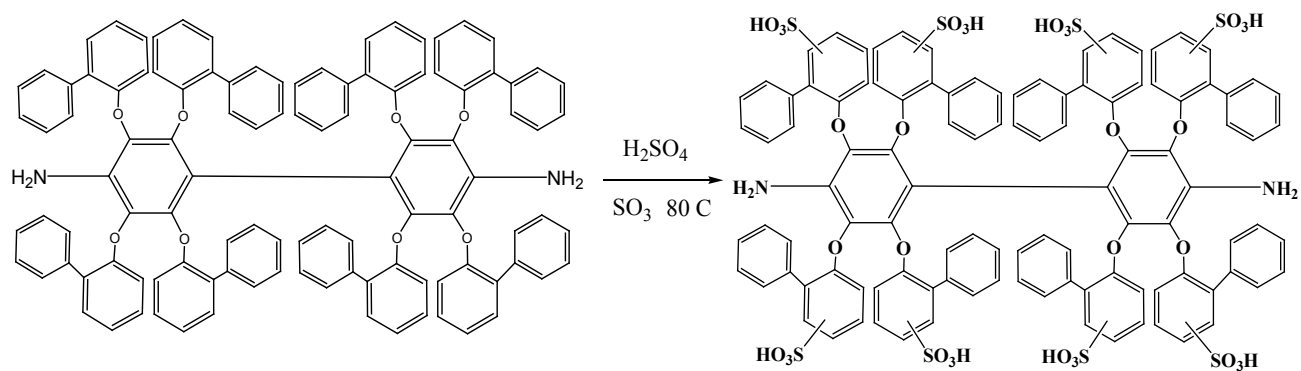


Figure 5.22 Scheme of synthesis of multi-sulfonated diamine monomer

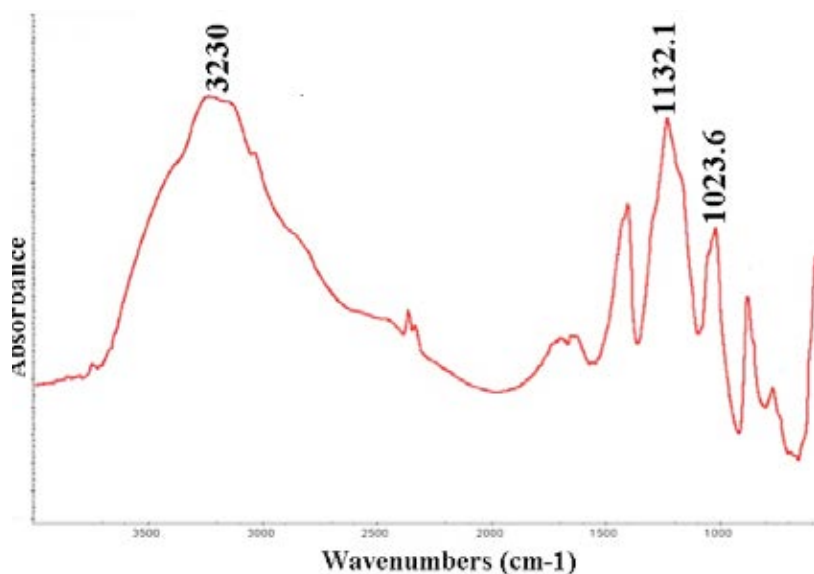


Figure 5.23 FTIR spectrum of multi-sulfonated diamine

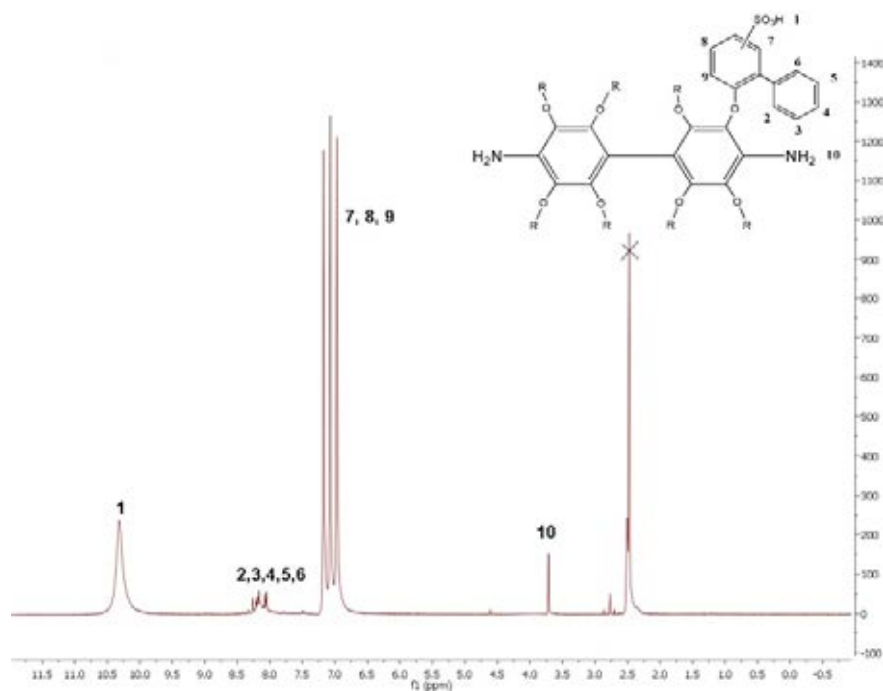


Figure 5.24 ^1H NMR spectrum of multi-sulfonated diamine

FT-IR spectrum of multi-sulfonated diamine showed the absorption of sulfuric acid group at 1023.6 and 1132.1 cm^{-1} (shown in Figure 5.23). The broad absorption band at 3230 cm^{-1} was assigned to the absorbed water in the sample due to the sulfonic acid groups were highly

hydrophilic, which confirmed the formation of the multi-synthesized sulfonated diamine. Furthermore, the structure of multi-sulfonated diamine was confirmed by elemental analysis as shown in Table 5.4.

Figure 5.24 shows the ^1H NMR spectrum of multi-sulfonated diamine consist of a singlet peak at 3.73 ppm and multiplets at 6.75-8.5 ppm that are assigned to NH_2 and aromatic protons, respectively. The single peak at 10.25 ppm is relative to sulfuric acid group.

Table 5.4 Elemental analysis of multi-sulfonated diamine

Elements	Theoretical (%)	Found (%)
C	46.79	43.64
H	0.97	1.06
N	3.23	3.62
S	17.85	20.76

5.3.3 Synthesis of multi-sulfonated polyimide

The multi-sulfonated diamine monomer was used as a starting material for multi-sulfonated poly(imide) polymerization. Sulfonated poly(imide) polymerization of O-DPDA and a multi-sulfonated polyimide was carried out in m-cresol medium in the presence of triethylamine (Et_3N). The poor solubility of multi-sulfonated polyimide was improved by the addition of Et_3N . The reaction was carried out at room temperature to prevent any imidization from occurring at this stage. The poly(amic acid) polymerization is an exothermic reaction; if the reaction was carried out at a higher temperature, hydrolysis would have occurred, producing lower molecular

weight and unstable polymers. The structure was confirmed by FTIR, NMR spectroscopy and elemental analysis as shown in Figure 5.26, 5.27 and Table 5.5, respectively.

The FTIR spectrum of multi-sulfonated poly(imide) is shown in Figure 5.26. The broad absorption band at 3476.6 cm^{-1} was assigned to the absorbed water in the sample (the sulfonic acid groups are highly hydrophilic). The strong absorption bands at 1723.6 cm^{-1} was assigned to the symmetric imide $\text{C}=\text{O}$ stretching. The peak at 1605.2 cm^{-1} indicated the absorption band of carbonyl group (CONH) and peak at 1366 cm^{-1} indicated the absorption bands of $\text{C}-\text{N}-\text{C}$ stretching vibration. The absorption bands at 1031.3 and 1090.3 cm^{-1} corresponded to of sulfuric acid groups (SO_3H).

Furthermore, the overlaid FTIR spectrum of synthesized diamine, multi-sulfonated diamine and multi-sulfonated poly(imide) is shown in Figure 5.27.

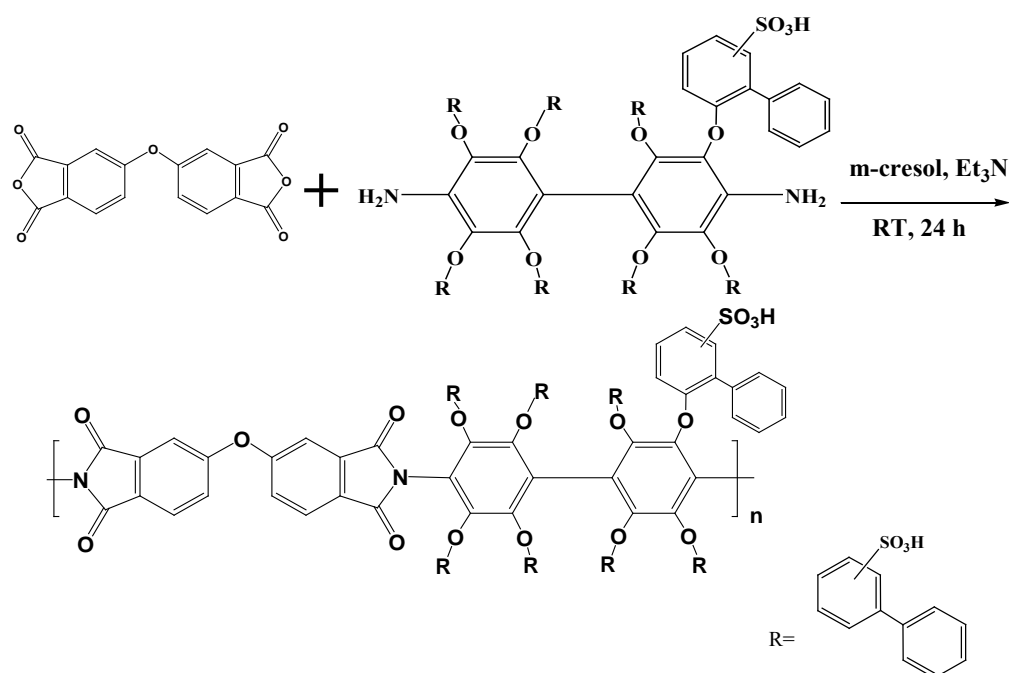


Figure 5.25 Scheme of synthesis of multi-sulfonated poly(imide)

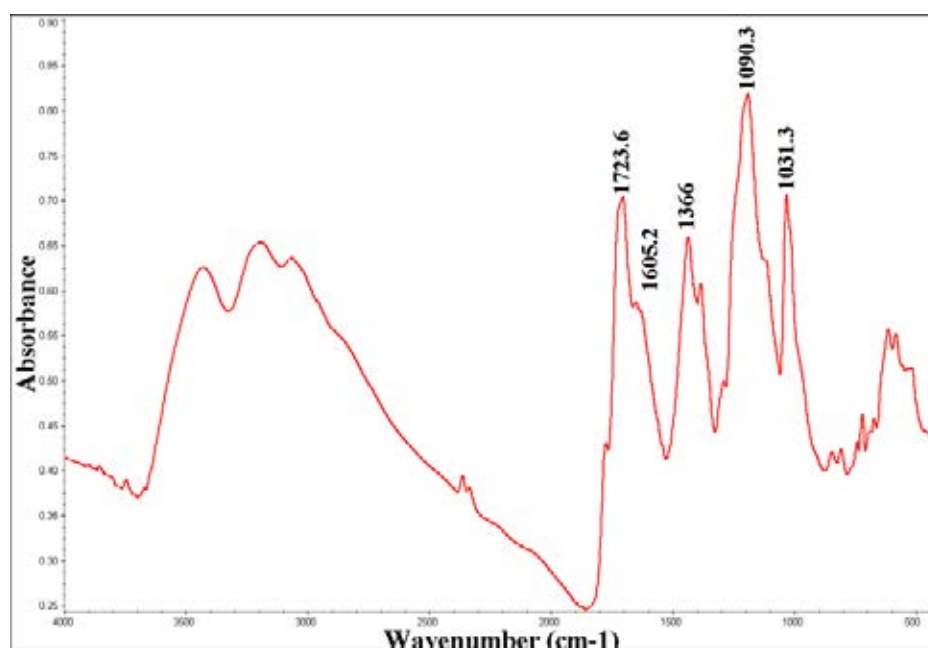


Figure 5.26 FTIR spectrum of sulfonated poly(imide)

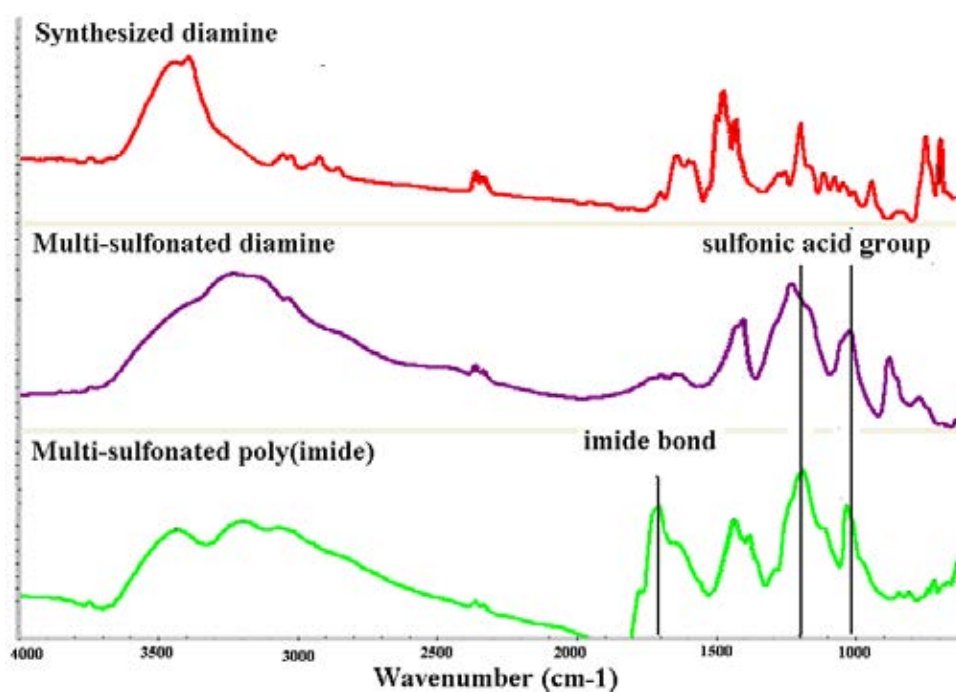


Figure 5.27 Overlaid FTIR spectrum of synthesized diamine, multi-sulfonated diamine and sulfonated poly(imide)

Table 5.5 Elemental analysis of multi-sulfonated poly(imide)

Elements	Theoretical (%)	Found (%)
C	59.90	58.02
H	4.10	5.55
N	1.03	1.08
S	9.48	8.30

5.3.4 Preparation of PEDOT/multi-sulfonated poly(imide) (PEDOT-SPI)

The PEDOT/multi-sulfonated poly(imide) was prepared by template polymerization of EDOT and the new synthesized multi-sulfonated poly(imide) in DI water. The peak at 1723.6 cm^{-1} in Figure 5.28 corresponded to the imide bond. The peaks at 1125.4 cm^{-1} indicated C-O-C bond stretching in ethylenedioxy group and the other peaks at 1025.7, 1008.6, 814.3 cm^{-1} indicated the C-S bonds in thiophene.

For further understanding, the overlaid FTIR spectrum of multi-sulfonated diamine, sulfonated poly(imide) and PEDOT-SPI is shown in Figure 5.29.

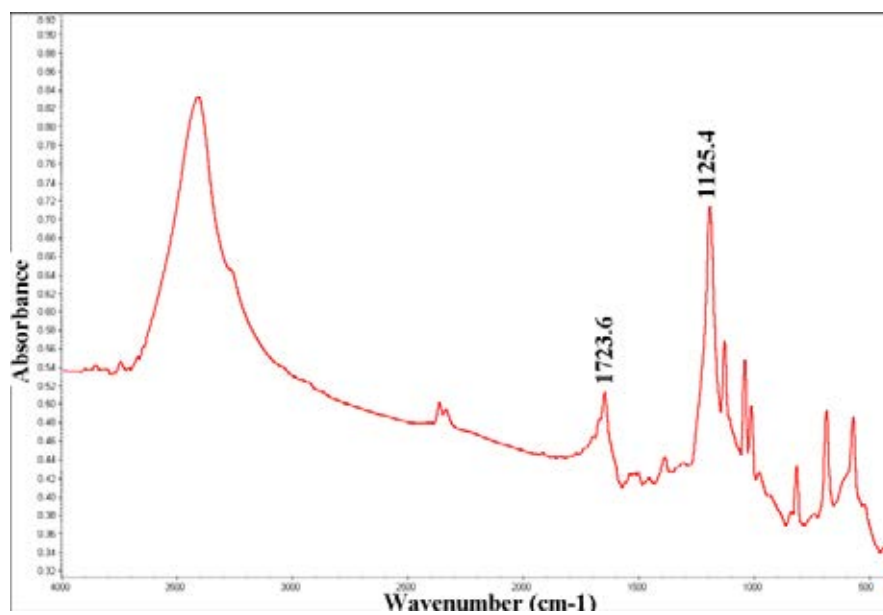


Figure 5.28 FTIR spectrum of PEDOT/multi-sulfonated poly(imide)

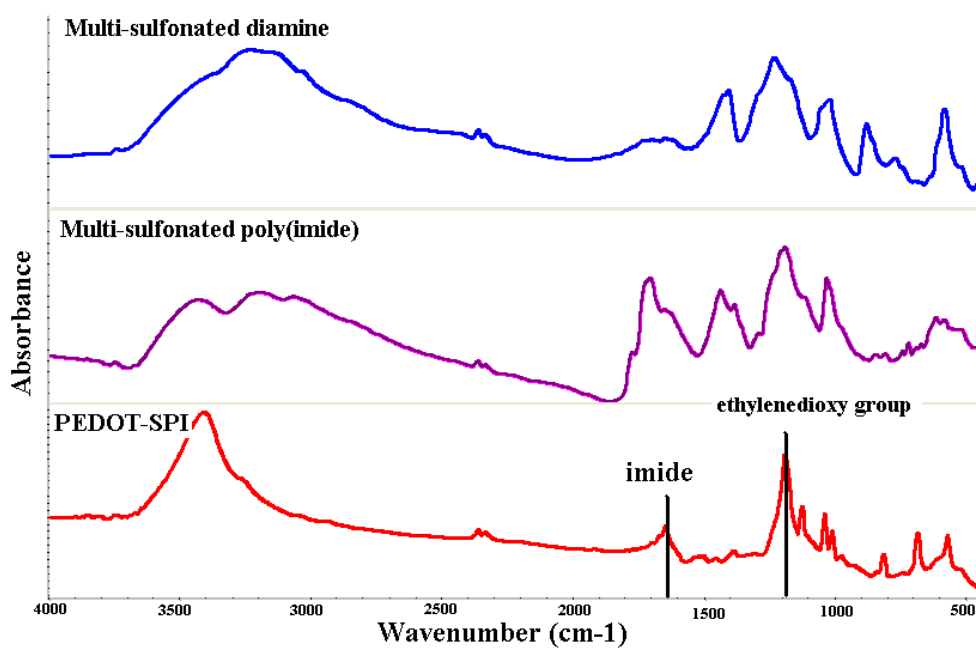


Figure 5.29 Overlaid FTIR spectrum of multi-sulfonated diamine, sulfonated poly(imide) and PEDOT-SPI

5.3.5 Conductivity

Conductivity of PEDOT/multi-sulfonated poly(imide) (PEDOT/multi-SPI) films was measured by the four-point probes technique. The conductivity of PEDOT/multi-SPI films showed high conductivity of 5.63×10^{-1} S/cm at room temperature. After annealing at 180 °C for 10 mins, the conductivity of PEDOT/multi-SPI films was slightly increased to 7.90×10^{-1} S/cm. PEDOT/multi-SPI films showed the highest conductivity (9.60×10^{-1} S/cm) after annealing at 300 °C for 10 mins. After heat treatment, the chain alignment in thin polymer films changes with temperature, leading to modified morphologies. These conductivities are summarized in Table 5.6.

To compare PEDOT-SPI between the SPI; 4,4'-ODAS:O-DPDA [52] with multi-SPI in this work, the multi-SPI showed higher conductivity than SPI (4,4'-ODADS:O-DPDA) because the multi-SPI had multi-sulfonated groups in a single molecule. The conductivity of PEDOT/SPI (4,4'-ODADS:O-DPDA) in the previous work showed the conductivity of 3.54×10^{-3} S/cm. For the conductivity of PEDOT/PSS, prepared in laboratory, showed conductivity of 5.93×10^{-4} S/cm. Hence, the PEDOT/multi-SPI films were observed to have increased 159 times and 949 times, respectively, to the conductivity of PEDOT/SPI (4,4'-ODADS:O-DPDA) and PEDOT/PSS.

Table 5.6 Conductivities of PEDOT/multi-sulfonated poly(imide) at various processing temperature

Processing Temperature		PEDOT-SPI
25 °C	Conductivity (S/cm)	5.63×10^{-1}
	Std.Dev.	8.45×10^{-3}
180 °C (10 mins)	Conductivity (S/cm)	7.90×10^{-1}
	Std.Dev.	3.81×10^{-3}
300 °C (10 mins)	Conductivity (S/cm)	9.60×10^{-1}
	Std.Dev.	4.60×10^{-2}

5.3.6 Thermal property

The thermal stability of synthesized diamine, multi-sulfonated poly(imide) and PEDOT/multi-SPI were evaluated by TG analysis. TGA of synthesized diamine was run under air atmosphere at a heating rate of 20 °C/min. Figure 5.30 shows the thermal stability of the synthesized diamine. The onset temperature of the synthesized diamine is 504 °C. The thermal property of multi-sulfonated poly(imide), in an air atmosphere, was investigated and shown in Figure 5.31. A three-step weight loss was observed from 50-150 °C, from 370-550 °C and above

550 °C. The first weight loss was due to the evaporation of hydrated water, and the second and third ones were attributed to the decomposition of the sulfonic acid groups and the polymer main chains, respectively. Generally, the decomposition of sulfonic acid groups attached to electron-rich benzene rings starts at around 250 °C. Although the sulfonic acid groups were attached to the electron-rich benzene rings, their decomposition temperature was higher than 300 °C. This decomposition behavior may be explained as follows: the electron-donating effect of the phenoxy group is weakened by resonance with the pendant phenyl group and the electron-withdrawing effect of the sulfonic acid group attached to the pendant phenyl group.

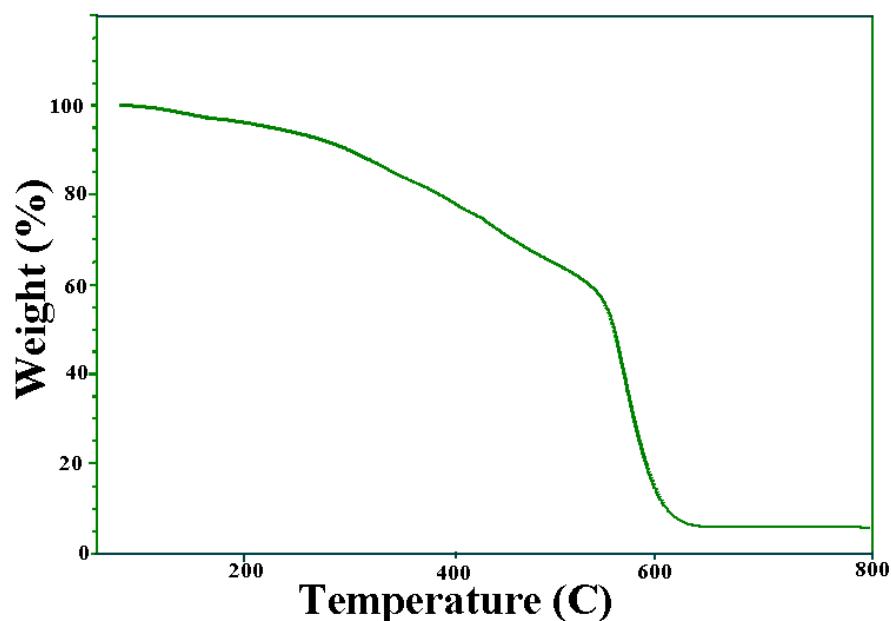


Figure 5. 30 TGA of synthesized diamine

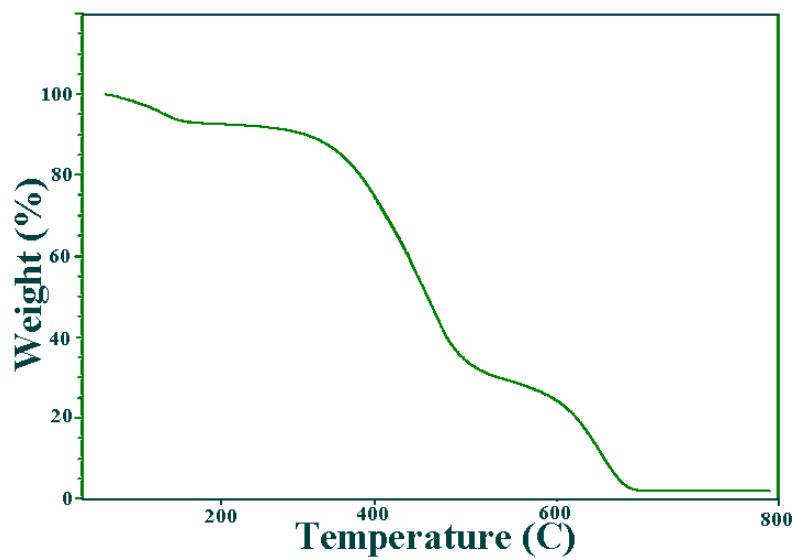


Figure 5.31 TGA of multi-sulfonated poly(imide)

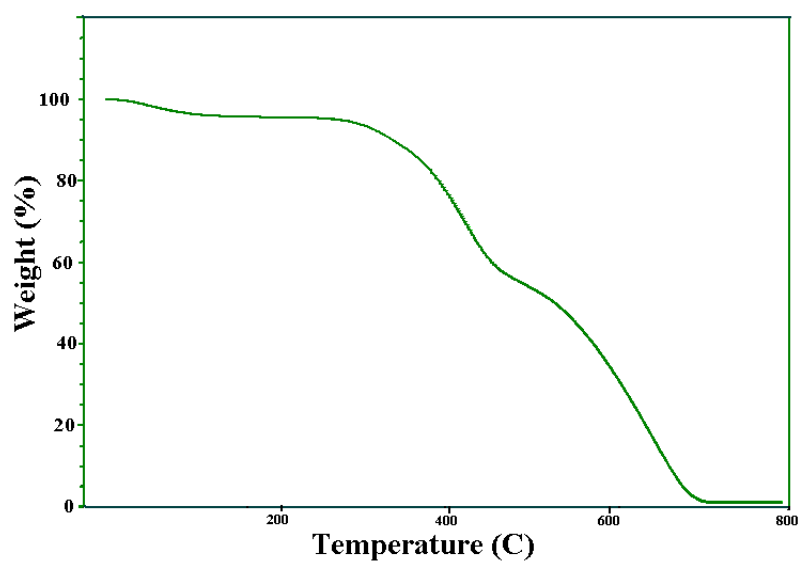


Figure 5.32 TGA of PEDOT/multi-sulfonated poly(imide)

For PEDOT/multi-SPI, in an air atmosphere was investigated and shown in Figure 5.32. We can see that the thermal stability of PEDOT/multi-SPI exhibited a typical three-steps degradation pattern. It can be seen that the weight loss was observed up to 110 °C for the first step, from 280°C- 400°C for the second step and from 400°C- 700°C for the last step. The first weight loss was due to the loss of water molecules, which absorbed by the highly hygroscopic –SO₃H groups. The second weight loss period was due to the decomposition of sulfonic acid groups or desulfonation reactions. The third stage weight loss was assigned to the decomposition of polymer aromatic main chain. The degradation of the polymer backbone at 700 °C shows that this polymer possesses high thermal stability.

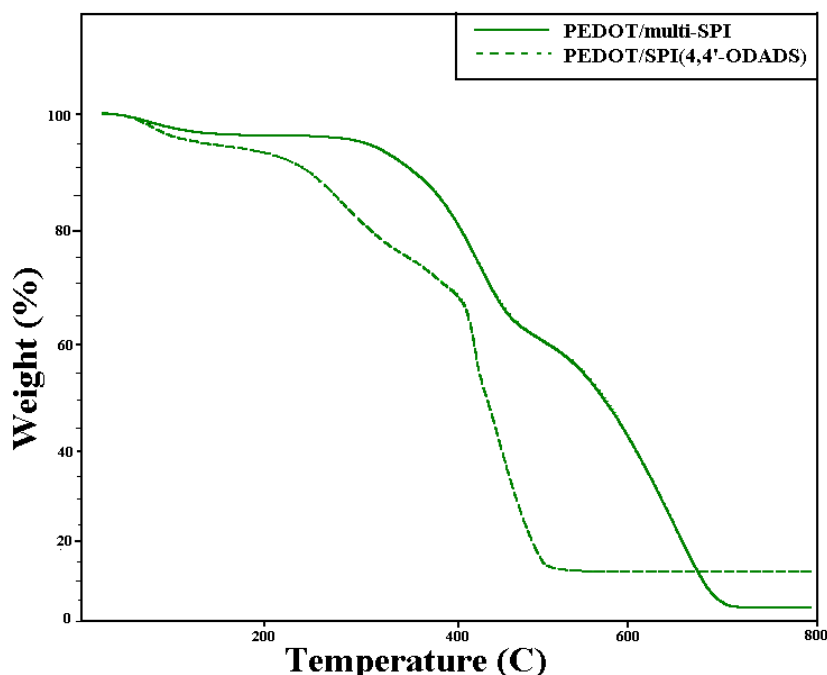


Figure 5.33 TGA of PEDOT/multi-SPI and PEDOT/SPI(4,4'-ODADS)

Figure 5.33 shows the thermal properties of PEDOT/multi-SPI and PEDOT/SPI(4,4'-ODADS) in an air atmosphere. We can see that the thermal stability of PEDOT containing the new template, multi-sulfonated poly(imide), is higher than that of PEDOT containing the template in the previous work [52].

5.3.7 Morphological property

The particle size of the colloidal dispersion PEDOT/multi-SPI was investigated by TEM, as shown in Figure 5.33. Figure 5.33 shows the particle sizes of a sample of PEDOT/multi-SPI, averaging ca. 78 nm. It is seen that the particle of conducting polymer was agglomeration as increasing size.

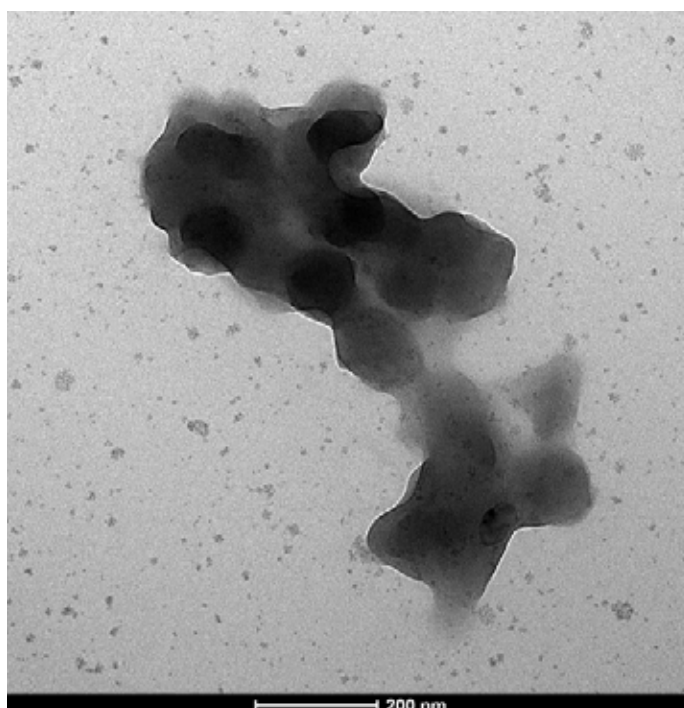


Figure 5.34 TEM of PEDOT/multi-sulfonated poly(imide)

CHAPTER VI

CONCLUSIONS & RECOMMENDATIONS

6.1 Conclusions

6.1.1 Experimental observation on the mixing systems and ways to significantly enhance the conductivity of PEDOT-SPI aqueous dispersion

1. Significant conductivity and thermal stability enhancement of the obtained PEDOT-SPI films by using designed stir shaft with high-speed mechanical mixing systems allowing for smaller particles sizes of PEDOT-SPI about 43 nm averaging were discovered in this research.
2. The maximum conductivities of 2.04 and 1.15 S/cm were respectively observed for PEDOT-SPI(6-FDA) and PEDOT-SPI(O-DPDA) films using the 4000-rpm mechanical mixing system.
3. These maximum conductivities (4000 rpm-mechanical mixing system) were higher than those of magnetic and 1000 rpm-mechanical mixing systems by a factor of 346 and 3.1 for PEDOT-SPI(6-FDA) and 325 and 3.4 for PEDOT-SPI(O-DPDA), respectively.
4. The further conductivity enhancement and thermal stability of PEDOT-SPI were achieved by adding various amounts of anionic surfactant into the aqueous polymer suspension because of the resulting conformation changes and decreasing in the distortion of polymer chains.
5. The highest conductivity, 9.5 S/cm, was achieved at 1 wt% SDS in PEDOT-SPI(6-FDA) film which increased by a factor of 5 from the PEDOT-SPI without addition of SDS.
6. The combination of using high-speed mechanical mixing and adding of anionic surfactant, superior dispersion stability, high conductivity and good thermal stability of PEDOT-SPI films were achieved.

6.1.2 Effects of the addition of anionic surfactant during template polymerization of conducting polymers containing PEDOT with SPI or PSS templates for nano-thin film applications

1. The improvement of PEDOT-SPI and PEDOT-PSS films were successfully improved by adding anionic surfactant during template polymerization of PEDOT-SPI and PEDOT-PSS.
2. The maximum conductivities were found at 8.69 S/cm and 6.47 S/cm for PEDOT-SPI and PEDOT-PSS films, respectively, which showed higher than those of other films, when anionic surfactant was added after polymerization.
3. The conductivity improvement of conducting polymer films with addition of anionic surfactant during polymerization could be the presence of SDS molecule caused by the decrease in the distortion of PEDOT chains from interacting of SDS with PEDOT molecules.
4. Molecular interactions between SDS and PEDOT chains resulted in the decrease in distortion of the structures and in the effectiveness of doping of the PEDOT chains.
5. Smaller and spherical conducting nanoparticles with diameter <100 nm successfully synthesized by addition of SDS during polymerization.
6. The addition of SDS during polymerization of both PEDOT-SPI and PEDOT-PSS was more effective in stabilizing particles against coagulation, significantly reducing the sizes of conducting particles, forming stable spherical particles, and enhancing thermal stability and conductivity.

6.1.3 Synthesis and characterization of PEDOT/multi-sulfonated polyimide via template polymerization

1. The new symmetrical aromatic diamine monomer was successfully synthesized by aromatic nucleophilic substitution reaction at high temperature and long reaction time.
2. The multi-sulfonated diamine monomer was successfully synthesized by direct sulfonation reaction using concentrated sulfuric acid (95%) as a sulfonating agent.

3. The sulfonated polyimide was prepared from O-DPDA and sulfonated diamine, which displayed high thermal stability.
4. The conducting polymer/sulfonated polyimide, PEDOT/multi-sulfonated polyimide, was successfully prepared by template polymerization resulting in higher conductivity and thermal stability than PEDOT/SPI and PEDOT/PSS from the previous work [52].
5. After heat treatment, the conductivity of PEDOT/multi-sulfonated polyimide showed enhancement in observed conductivity.

6.2 Recommendations

6.2.1 Smaller particle sizes improvement could be prepared by using a homogenizer, which has very high speed of mixing and its speed could be adjusted, resulting in better colloidal dispersion.

6.2.2 Electrochemical characterization of conducting polymers would be interesting to carry out to study the effect of surfactant and morphological modifications onto the electrochemical behavior.

6.2.3 The modification of conductivity, electronic delocalization and the band gap of the materials could be deeply studied by other technic of characterization such as UV-Visible spectroscopy.

6.2.4 The film formation method should be modified by spin-coating to obtain a thinner and more transparency film.

6.2.5 The modification of conductivity, thermal stability and morphological properties of new conducting polymer, PEDOT/multi-sulfonated polyimide, could be investigated by using a homogenizer.

6.2.6 The conductivity of the new conducting polymer, PEDOT/multi-sulfonated polyimide could be further improved by addition of surfactants or other secondary dopants.

6.2.7 Using DT-TGA could identify the degradation of each composition of conducting polymer.

VITA

Miss Kulthida Sukchol was born on May 13, 1984 in Nakhon Si Thammarat, Thailand. After graduating from Benjamarachutit School in 2003, she spent 4 years at Thammasat University and eventually earned Bachelor's Degree of Chemical Engineering, graduating in May 2007. She received the Degree of Master of Engineering in Chemical Engineering at the Department of Chemical Engineering, Chulalongkorn University in 2009. After the M.Eng graduation, she has received the Royal Golden Jubilee Ph.D. program, Thailand Research Fund to study the Doctoral Degree of Engineering in Chemical Engineering at Chulalongkorn University in July, 2009. She had spent one-year research at Institute of Materials Science and the Polymer program, University of Connecticut, USA during her Ph.D. Program and six months at University of Michigan during her Master.